CHAPTER ONE

INTRODUCTION

1.0 Background

Many radionuclides have been in existence since the formation of the earth about four billion years ago and they constituted part of the earth formation. Most of these radionuclides have however gone extinct because of their decay processes. They are short lived isotopes whose half-lives are below 100 million years. Examples of extinct radionuclides include iodine – 129, aluminium – 26 and neptunium - 237. Only those nuclides of long half-lives such as 100 million years or more, known as primordial radionuclides, remain with their daughter products.

People are exposed to ionizing radiation arising from both natural and artificial sources which constitute background radiation. Both natural and artificial background radiation varies depending on local geology and altitude. Every day, we inhale nuclides in the air we breathe; we ingest nuclides in the food we eat and in the water we drink. Radioactivity is found in the rocks and soil that make up our planet, in the water and oceans, and even in our building materials and homes indicating its ubiquitousness (Uosif and Abdel-Salam, 2011). All types of building materials such as concrete, cement, brick, sand, aggregate, marble, granite, limestone, gypsum, etc. are sources of direct radiation exposure because of their radium, thorium and potassium content. Granitic rock is widely in use as a building and ornamental material due to its brilliantly polished surface, durability, decorative appearance and availability in a variety of attractive colours (Cetin *et al*., 2012). These rocks contain natural radionuclides in varying degree depending on the composition of the molten rock from which they formed. Geologists provide an explanation of this behavior in the course of partial melting and fractional crystallization of magma, which enables U and Th to be concentrated in the liquid phase and become incorporated into the more silica-rich products. For that reason, igneous rocks of granitic composition are strongly enriched in U and Th (Mason and Moore, 1982).

Nigeria, especially the southwestern part of the country, is blessed with large deposit of the granitic rocks which extrude across the country. The high demand for the products of granitic rock by people for building, road construction, decoration purposes etc. enhanced mass locations of granitic quarry industries in southwestern Nigeria. Statistics revealed that over half a million people are working as miners in the industries across southwestern Nigeria (NBS, 2015). The presence of radionuclides in rock therefore poses exposure of the miners and the users of the facilities to radiation derivable from the naturally occurring radioactive materials present in the granites. Hence, the theory of the radioactivity of these naturally occurring radionuclide particles present in the granitic rocks needed discussion.

1.1 Radioactivity

An atom comprises a nucleus surrounded by a cloud of electrons. The nucleus is the central part of the atom consisting of protons and neutrons. The atom as a whole is electrically neutral because the number of protons (carrying positive charges) and electrons (carrying negative charges) are the same while neutrons are without charges. Though there exists nuclear force binding the nuclear constituents (nucleons) together, the presence of positive protons in the nucleus creates a Columbic force of expulsion within the nucleons. When the Columbic force exceeds the binding nuclear force, the nuclide becomes unstable. Generally, a light nuclide is stable when its number of neutron (N) to number of proton (Z) ratio is about one ($N/Z \approx 1$), and a heavy nuclide is stable when the ratio of $N/Z \approx 1.5$. Unstable nuclides undergo intra-nuclear spontaneous transmutation towards stability, which shifts the N/Z ratio to a more stable configuration for the nuclei. This process is achieved by the emission of sub-atomic particles as well as electromagnetic energy in form of gamma radiation.

The particles that are usually emitted in natural radioactivity are the relatively heavy alpha particles (He^{2+}) and light beta particles (e^{+}, e^{-}); The emission of beta particles is often accompanied by a neutral and much lighter particle known as neutrinos. An atom with atomic mass A and atomic number Z in an alpha decay will transform into a new atom with atomic mass (A-4) and atomic number (Z-2), while in a beta ($ß^{\pm}$) decay the transformation of a similar atom with atomic mass A and atomic number Z would not change A but a change of Z to $Z \pm 1$ will definitely occur. Gamma radiation is a mechanism by which excess energy is emitted from such radionuclides.

Every mode of nuclear decay follows a decay law, which is the basis of the dynamics of radioactivity. The rate of disintegration A of a radioactive material is given by

$$A = A_0 e^{-\lambda t} \qquad (1.1)$$

where, A_0 is the initial activity, and A is the activity at time t and λ is the decay constant, which is the probability of a nucleus decaying per second. The unit of activity is the Becquerel (Bq), which is one disintegration per second. The old unit, the curie (Ci) is the activity of 1g of ^{226}Ra, which is equal to 3.7 x 10^{10} Bq. The S.I unit of activity concentration of a radionuclide in a given sample, such as, soil and granitic rocks is Bq.kg^{-1}.

If the daughter nuclide in a decay series is stable, then after a time t, the number of daughter N_d present is given by:

$$N_d = N_0\left(1 - e^{-\lambda t}\right) \qquad (1.2)$$

But for an unstable daughter, the process of radioactivity continues and the number of daughter nuclide becomes:

$$N_d = N_0 \left[\frac{\lambda}{\lambda' - \lambda}\right]\left(e^{-\lambda t} - e^{-\lambda' t}\right) \qquad (1.3)$$

where, λ' is the decay constant of the daughter.

If the parent has a long half-life such that $\lambda' >> \lambda$ then $\lambda' - \lambda = \lambda'$ and after a long time,

$e^{-\lambda' t} \rightarrow 0$, therefore

$$\lambda N_0 = \lambda' N_d \qquad (1.4)$$

Equation 1.4 implies that at large (t), the activity of the parent becomes the same with that of the daughter. This is called secular equilibrium. Both ^{226}Ra and ^{232}Th series exhibit this condition with their daughter products, such as, ^{214}Bi and ^{208}T1, respectively when confined in an enclosure. This is the basis of their measurement with the gamma activities of their daughters.

1.2 Natural decay series

There are four series of natural radioactive elements, which decay into a number of successive daughter products before stable end products are attained. They are the uranium, thorium, actinium and neptunium series. They were named after the longest-lived member in each series.

Naturally occurring isotopes of uranium are ^{238}U, ^{235}U and ^{234}U with 4.47 x 10^9 y, 7.13 x 10^8 y and 2.5 x $l0^5$ y half-lives respectively. They are all alpha emitters with long decay series. However, ^{238}U isotope is the most significant because it is the most abundant (99.27%). The ^{238}U series includes (^{226}Ra), the most important radium isotope. Most of the members in this series are alpha emitters. The atomic mass (A) of the members of the series can be represented by (4n + 2), starting with ^{238}U and ending with stable ^{206}Pb. These series can be found in soil, and rocks, such as, metamorphic, sedimentary and granitic rocks.

Thorium series starts with ^{232}Th and has a long half-life of 1.39 x 10^{10} yr. It undergoes a number of successive disintegrations before ending with ^{208}Pb stable isotope. The atomic mass (A) of this series is represented by (4n). Its relative abundance in the earth crust is 0.0006% (Paulo, 2015). The actinium series begins with rarer ^{235}U which is the longest lived member of the series. It has a half-life of 7.1 x 10^8 y. The stable end-member is ^{207}Pb and the series can take the form (4n + 3).

Neptunium series has no natural radioactive series because the half-life 2.14 x 10^6 y of the longest lived member (^{237}Np) is far lower than the age of the universe (4.5 x 10^9 y). All the members have been artificially produced and take the form (4n+1). The stable end of the series is ^{209}Bi.

Another important naturally occurring radioactive element with a long half-life of 1.28 x 10^9 is ^{40}K, which does not belong to a decay series. Like ^{238}U and ^{232}Th, ^{40}K is also an important radioactive isotope found in earth crust especially in rocks, which will be examined in this work. Its presence in living tissue enables it to make significant contribution to the radioactivity of the tissue.

1.3 Radioactivity in the rocks

Rocks contain natural radionuclides ^{40}K, ^{232}Th and ^{238}U at different concentrations. They include primordial radioactive nuclides, which originated from the early stages of formation of the solar system (Kerur *et al*., 2010). Igneous rocks, such as granite, are associated with higher level of radionuclides and sedimentary

rocks are with lower level of radionuclides (Florou and Kritidis, 1992). Shale and phosphate rocks have exceptionally high content of radionuclides (UNSCEAR, 2000). Cases abound of different igneous rock types with wide range of radioactivity concentration values (Rodrigo and Carlos, 2009). The variation in radioactivity concentrations in the rocks is due to their disparity in mineral compositions. Granite and granitic rocks exhibit some variation in radioactivity concentration according to their mineral compositions(Shams*et al*., 2012; Uosif *et al*., 2015; El Mezayen *et al*., 2017). The essential minerals in granite are albite, oligoclase, microcline, perthite, quartz, muscovite and biotite. Accessory minerals may include beryl, apatite, zircon, garnet, tourmaline and titanite.

1.4 Health effects of radiation

The effect of radiation on a biological tissue may be due to direct or indirect attack on the living cells, which takes place through ionization and excitation of atoms making up the cells. It is direct when the body cells receive the radiation dose without any agent and damage is caused to the cells. The indirect attack is brought about via the water content in the body. When a water molecule (H_2O) is irradiated, a free electron (e^-) and a positive ion (H_2O^+) are produced. The free electron can be attracted to another water molecule to give rise to a negatively charged molecule (H_2O^-). Dissociation of the positive and negative ions, which is inexorable because of their instability, takes place to generate highly reactive free radicals denoted by HO* and H* respectively. They absorb hydrogen from organic structures (signified by RH) of the body on their interaction to yield organic free radicals represented by R* (Lilley, 2001). The summary of the chemical reactions that take place is as follows:

$$\text{Radiation} + H_2O \rightarrow H_2O^+ + e^-$$

$$H_2O + e^- \rightarrow H_2O^-$$

$$H_2O^+ \rightarrow H^+ + OH^*$$

$$H_2O^- \rightarrow H^* + OH^-$$

$$RH + OH^* \rightarrow R^* + H_2O$$

$$RH + H^* \rightarrow R^* + H_2$$

They are very powerful oxidizing agents that can disrupt complex molecules of the body system. The biologically important molecules usually affected are deoxyribonucleic acid (DNA) and ribonucleic acid (RNA). The damage can be to the autosomal cells or gonadal cells. The resulting effect will be limited to the exposed

individual if only autosomal cell is affected. This effect is known as somatic effect. The gonad or cell attack has genetic effect that is extended to the offspring of the affected individual.

Exposure to radiation occurs in two ways depending on the time and amount of exposure, acute and chronic exposure. Acute exposure is exposure to a large, single dose of radiation, or a series of doses, for a short period of time (UNSCEAR, 2000). Chronic exposure is as a result of exposure to low-level radiation for a long time, example of which could be found in quarry workers. The effect in both cases are categorized into two, namely, stochastic and non-stochastic effects.

Stochastic effects are probabilistic and can occur at any level of dose. The chance of occurrence increases with increase in the level of dose. Stochastic effects can occur among people that are exposed to both low-level and high-level radiation doses (Ademola, 2003). Quarry activities are contributing to exposure of people to low-level gamma radiation that can lead to chronic doses. Examples of stochastic effects are radiation induced cancer and genetic mutation.

Non-stochastic effects are deterministic. It requires a minimum (threshold) dose before a particular effect can occur. The severity of the effect increases with increase in dose above the threshold value. Examples of non-stochastic effects are autoimmune thyroiditis, reproductive dysfunctioning, circulatory diseases, haemopoietic syndrome, gastrointestinal syndrome and visual impairment, such as, lens opacities and cataracts. These effects can only be incurred during accident because the threshold value for the effects are high and beyond 1.5 Gy. Therefore, unlike stochastic effect, quarry workers are not subjected to acute doses, which are not present in quarry sites.

1.5 Justification for the work

Over half a million people work in the quarry industry in southwestern Nigeria (NBS, 2015). Several outcrops of granite and granitic rocks, such as, granodiorite, syenite and pegmatite abound in the area. Other metamorphic rocks that are also quarried include granite gneisses and migmatites. Though they vary in composition, Papadopoulos *et al*. (2012) emphasised that granite or granitic rock is the market term widely used for the varieties of igneous and metamorphic rocks being quarried in the quarry industries. The demand for granite products for building and construction companies necessitated the setting up of quite a number of quarry sites in the region.

The large population in the study area could also be responsible for high demand for building materials, such as, granite chippings and dusts.

Despite the importance of granites as raw materials in the provision of comfortable accommodation, it is noted that the presence of natural radionuclides in the granitic rocks produces, among others, gamma radiation, which can lead to external or internal exposure of people to radiation. Chronic dose of radiation absorption in the quarry workers, from radionuclides in the granitic rocks, is possible due to prolong exposure of these workers to dust generated during mine operation. Exposure to the radiation could be by body contact or inhalation of airborne radioactive laden dust, which could lead to adverse health consequences over a long period of time.

Presently, there is paucity of the essential information on the tripartite approach of the petrology (mineralogy) of the rocks, their radioactivity concentration and the radiological health implications, on quarry workers. The major challenge with the widely used gamma spectrometry is the rigor of measurement, time required to carry out the analysis and the cost effectiveness of the method. The quest to proffer solution to radiation exposure in quarry sites and to provide baseline data on the level of radioactivity from the granites in the study area and their radiation effects on quarry workers informs this research work.

The objective of this study is to determine activity concentrations of radionuclides in individual minerals contained in granitic rocks as against the conventional whole rock concentrations hitherto used. Also, radiological health implication on over half a million quarry workers in the region is to be assessed. The coverage area is limited to southwestern Nigeria for logistic reasons, which include availability of granitic rock outcrops, sufficient number of quarries, access to the quarries and proximity of the region to the needed analytical laboratories.

1.6 Aim and objectives of the study

The aim of this work is to assess the mineralogical influence of granitic rocks on the activity concentrations of the primordial radionuclides in granitic rocks and radiological implications of quarry activities at selected quarry sites in southwestern Nigeria. The objectives are as follows:

1. To use petrographic analysis to identify and determine the percentage composition of major minerals in quarry rock samples collected from selected sites in southwestern Nigeria.

2. To use gamma ray spectrometry to identify and determine naturalradioactivity concentration of the same quarry rock samples.
3. To correlate data on percentage mineral composition with data on radioactivity concentration for any possible relationship that can be useful in determination of radioactivity concentrationvia petrographic data.
4. To determine radiological health risk on quarry workers from the health indices derived from the radioactivity concentration of the quarry rock samples.
5. To evaluate the health risk to the quarry workers against accepted international standard and guidelines.

CHAPTER TWO

LITERATURE REVIEW

2.1 Rock formation and radioactivity

Rocks are naturally occurring aggregates of minerals. According to Read (2004), a mineral is a substance having a definite chemical composition and atomic structure and formed by the inorganic processes of nature. One or more minerals make up a rock and the earth's crust is made up of different types of rocks with variable chemical compositions and physical properties. They were formed at different geological periods (age) (Bolarinwa, 2005). The scientific study of rocks is called petrology. Rocks are composed of essential and accessory minerals, for example granite is made up essentially of quartz, feldspar and mica minerals. Rocks can be divided into three major classes based on their mode of formation, namely:

1. Igneous rocks formed by the cooling and consolidation of magma or lava.
2. Sedimentary rocks formed from lithification of sediments generated through sedimentary processes and deposited in a sedimentary basin.
3. Metamorphic rocks formed through metamorphism of preexisting rocks by high temperature, pressure and chemical activity.

2.1.1 Igneous rocks

Partial melting of the lower crust and the upper mantle results in the generation of molten magma at depths of about 50 to 200 km in the subsurface. Reduction in the temperature of the molten magma leads to solidification or crystallisation, that is, formation of mineral crystals, and hence igneous rock formation (Bolarinwa, 2005). Igneous rocks are therefore formed through the crystallisation of magma as it cools in an exothermic process either in the mantle or on the surface after a volcanic eruption. The components of rock are minerals consisting of various elements including natural radioactive elements. Each mineral crystallises under a certain temperature and pressure. Crystallisation is the process whereby the mineral particles form tight bonds in a well-defined three-dimensional shape. The size of the crystal is determined by the

time that it takes to cool. If cooled slowly, the crystal shapes are large. As magma cools, minerals crystallise and the resulting rock is characterised by interlocking mineral crystalline grains. Magma that cools beneath earth's surface generally cool slowly and produces intrusive igneous rocks which are also called plutonic rocks, while magma that cools at earth's surface are quick in cooling to produce extrusive igneous rocks also called volcanic rocks. Intrusive or plutonic igneous rocks have coarse-grained textures characterised by large mineral crystals, whereas extrusive or volcanic rocks are fine-grained and have small mineral crystals. Common volcanic rocks include tuff, rhyolite, andesite and basalt; and examples of plutonic rocks are granite, diorite and gabbro (Table 2.1). Both plutonic and volcanic rocks are identical in mineralogical and chemical compositions but different in textures due to the disparity in their environment of formation and their rate of crystallization. Some of the common plutonic rocks and their volcanic equivalents are presented in Table 2.1. They can be pink to dark gray or black in color depending on their chemistry and mineralogy and they commonly contain the highest radioactive element content (Bruce, 2009) among the rock types.

The average of Uranium and Thorium contents of the earth's crust has been estimated to be 1.8 and 7.2 ppm (Pourimani e*t al*. 2014). Though U and Th series occur naturally all over the earth's crust in small quantity, their concentrations can be relatively high in some granites (UNSCEAR, 1988). Their high content in igneous rock or granite is due to the partial melting and fractional crystallisation of magma which encourage the concentration of uranium and thorium in liquid phase (Fares *et al*., 2012). The three natural radioisotopes of uranium in the universe are ^{234}U, ^{235}U and ^{238}U. Uranium – 238 is the most abundant with 99.274% relative abundance. Because of its high concentration, the contributions of ^{234}U and ^{235}U in the natural pollution are negligible.

Table 2.1. Plutonic rocks and their volcanic equivalents (after Bolarinwa, 2005)

Classification	Plutonic rock	Volcanic equivalent
Acid igneous rocks	**Granite**	Rhyolite
Intermediate igneous rocks	Diorite	Andesite
Basic igneous rocks	Gabbro	Basalt
Ultrabasic igneous rocks	Picrite	Oceanite
Alkaline rocks	Syenite	Trachyte

2.1.2 Sedimentary rocks

Sedimentary rocks are formed through chemical and physical weathering of rocks, erosion, transport, deposition and compaction of mud. The compacted deposits are cemented and thereby converted into sedimentary rock. The process by which sediment is transformed into sedimentary rock is called lithification. They are in layers of different densities according to the extent of compaction by the top layers over millions of years. Sedimentary rocks may contain fossils of animals and plants trapped in the sediments as the rock is being formed. Most of the minerals in sedimentary rock are clay minerals that are capable of accommodating some nuclides like K, U and Th (Bruce, 2009). Depending on the origin of sediments, sedimentary rocks are divided into clastic or detrital rocks, which are formed from the transportation and deposition of particles of minerals and rocks from outside the depocentre (sandstone, siltstone, claystone and shale) or nonclastic, chemical and organic rocks, which are rocks formed by inorganic precipitation of animal and plant organic remains (fossils), such as, limestone, diatomite and coal.

2.1.3 Metamorphic rocks

Metamorphic rocks are rocks originally igneous, sedimentary or even metamorphic that have been changed by heat, pressure or the chemical action of fluids. Metamorphic rocks result from the transformation of other rocks by metamorphic processes that occur below earth's surface. Metamorphism is the process of mineralogical and structural changes of rocks in their solid state in response to physical and chemical conditions, which differ from the conditions prevailing during the formation of the rocks.

Metamorphic rocks may be formed from rocks which already contain a high content of radioactive elements and tend to retain that content. In the metamorphic process the change in the rock may be minor, where the features of the parent rock are still recognisable. The change may also be a major one that results in the formation of new minerals and probably a change in texture of the rock. In this situation any features of the parent rock may not be recognisable. Examples are schist from shale and marble from limestone. Some common igneous and sedimentary rocks and their metamorphic equivalents are shown in Table 2.2.

Table 2.2: Igneous and sedimentary rocks and their metamorphic equivalents (after Bolarinwa, 2005)

Igneous rocks	**Metamorphic equivalents**
Granite	**Granite gneiss**
Basalt	Amphibolite, amphibole schist
Sedimentary rocks	**Metamorphic equivalents**
Sandstone	Quartzite
Shale	Slate, phyllite, schist, **gneiss, migmatite**
Limestone	Marble, calc-silicate gneiss
Coal (Peat)	Anthracite, graphite

2.2 Geology of the precambrian basement complex of Nigeria

Nigeria is made up of 36 states and bounded by Latitudes 4^{o} and 14^{o} north of the Equator and Longitudes 2^{o} 2' and 14^{o} 30' east of the Greenwich Meridian. Nigeria is located within the Pan-African mobile belt between the West African Craton and the Congo Craton. The Basement Complex of Nigeria is composed of rocks of Precambrian age (Fig. 2.1), ranging from >2500 to about 500 million years. On the basis of age and structural disposition, the basement complex rocks can be broadly classified into three: The migmatite-gneiss-quartzite complex, the schist belt and the Older Granites.

The migmatite-gneiss-quartzite complex vary from augen to banded gneiss. The schist belt consists of slightly migmatized to unmigmatized paraschists with interbeds of meta-igneous rocks. The Older Granite suite comprising different varieties of granitic rocks which include porphyritic granites, muscovite granites, biotite granites, hornblende-biotite granites, granodiorites, quartz diorites, syenites and charnockites, as well as minor pegmatite, aplites and gabbroic rocks. The commonly found intrusions in the Basement Complex are unmetamorphosed dolerite and rhyolite porphyry dykes, pegmatite dykes and numerous veins of quartzo-feldspathic materials (Oyawoye, 1964, 1972; Rahaman, 1976; Makanjuola, 1982; Onyeagocha, 1984; Olarewaju, 1987; Ekwueme, 1987, 1994; Obiora, 2005, 2006).

2.3 Geology of the precambrian basement complex of southwestern Nigeria

The area covered by the southwestern Nigeria falls in the equatorial rain forest region of Africa and bounded by Latitudes 7^{o}N and 10^{o}N, and Longitudes 3^{o}E and 6^{o}E. The geology of the Precambrian basement complex of southwestern region is similar to that of the entire country (Fig. 2.1). The main lithologies include the migmatite gneisses, amphibolites, talc-tremolite schist, biotite schist, muscovite schist, quartzite and quartz schist. The granitic rocks, namely porphyritic granites, muscovite granites, biotite granites, hornblende-biotite granites, granodiorites, quartz diorites, syenites and charnockites, as well as minor pegmatite, aplites and gabbroic rocks intruded into the migmatite gneisses and the schistose rocks.

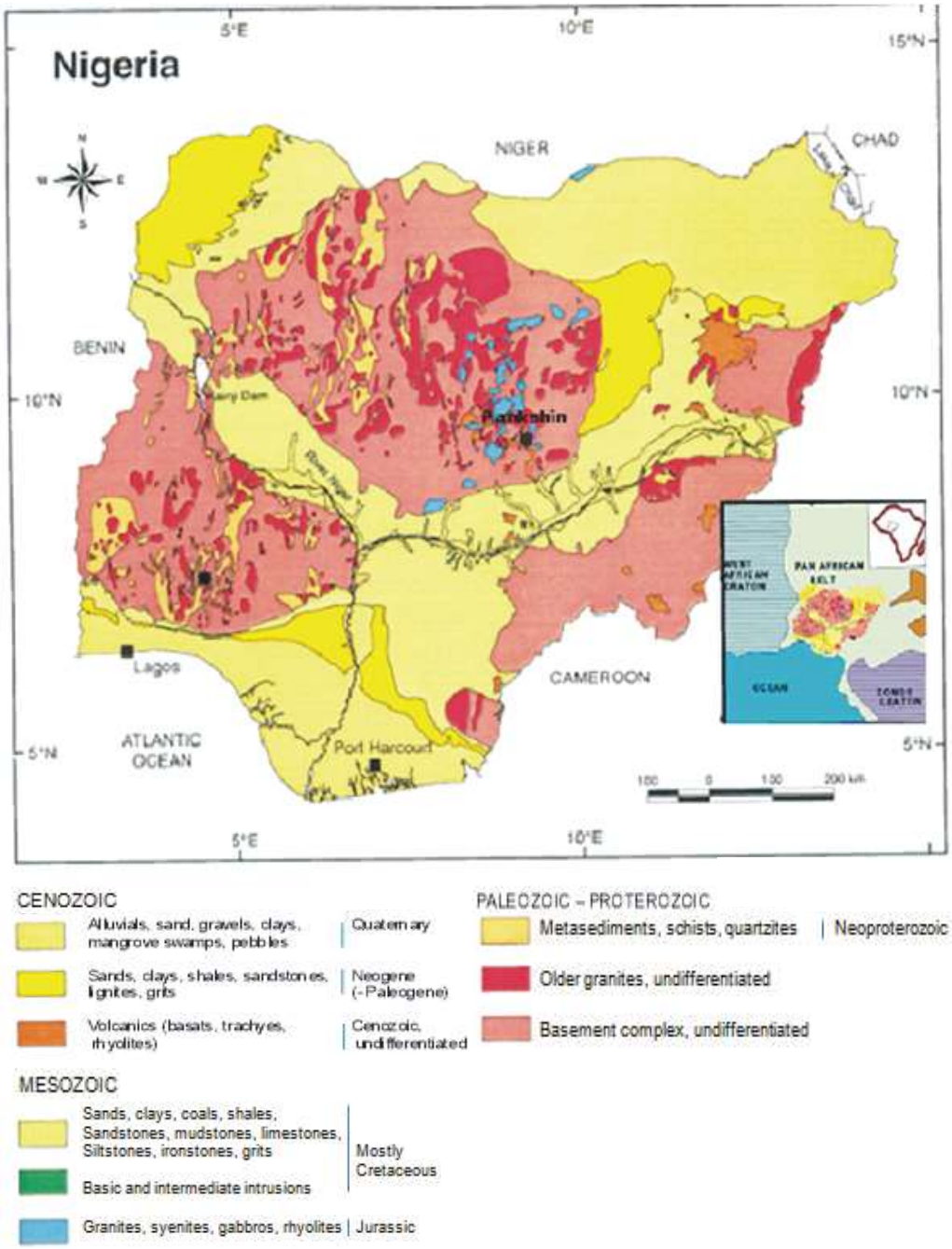

Fig. 2.1. Geological map showing the study area (in shades of red) within the Precambrian basement complex of southwestern Nigeria (Nigeria Geological Survey Agency, 2004)

2.4 Mineral composition of rocks

More than 2000 minerals are known. However, 99.9% of the rocks of the earth's crust are made of about 20 minerals. These minerals are called the rock-forming minerals. They are mainly silicates, as shown in Table 2.3 (Elueze and Bolarinwa, 2004). Accessory minerals in granitic rocks include Apatite, Zircon, Rutile, Ilmenite, Magnetite, Sphene/Titanite, Tourmaline and Monazite,

Granitic rocks of igneous origin (biotite granite, biotite-hornblende granite, muscovite granite, porphyritic granite, granodiorite and syenite), and to some extent gneissic rocks of metamorphic origin (migmatite gneiss, granite gneiss, augen gneiss and porphyroblastic gneiss) are quarried for construction purposes. Microcline ($KAlSi_3O_8$) which is K- feldspar is also commonly found in granite unlike orthoclase of metamorphic rock which crystallises at a higher temperature. Albite ($NaAlSi_3O_8$) and oligoclase are the plagioclase minerals in the granite as documented by Elueze and Bolarinwa (2004). These granitic (with some gneiss-migmatite) rocks constitute the main focus of this study. They are composed of albite, oligoclase, microcline, perthite, quartz, muscovite and biotite. Accessory minerals include apatite, zircon, garnet, tourmaline, titanite and opaques.The physical properties of the minerals are usedfor petrographic identification under the microscope.

According to El-Arabi *et al*. (2007) and Harb *et al*. (2012), mineral compositions are related to the level of natural radionuclides in granites. While ^{232}Th and ^{238}U are linked to minerals such as apatite, sphene zircon, monazite, allanite, uraninite, biotite, thorite and pyrochlore; ^{40}K had been reportedly found in K-feldspars, such as microcline and orthoclase, or in micas, like muscovite (El-Arabi *et al*., 2007; Gbadebo, 2011). Variation in composition of the minerals depends on the origin, evolution and the geotectonic environments of formation.

Table 2.3: Common rock-forming silicate minerals (EluezeandBolarinwa,2004)

Name	Chemical formula	Crystal system
Silica Group *		
Quartz varieties	SiO_2	Trigonal
Feldspar Group *		
Orthoclase	$KAlSi_3O_8$	Monoclinic
Albite	$Na\ Al\ Si_3O_8$	Triclinic
Anorthite	$Ca\ Al_2Si_2O_8$	Triclinic
Feldspathoid Group*		
Leucite	$K\ Al\ Si_2O_6$	Isometric
Nepheline	$Na\ Al\ SiO_4$	Hexagonal
Mica Group *		
Muscovite *	$K\ Al_2\ (Al\ Si_3O_{10})\ (OH)_2$	Monoclinic
Lepidolite *	$K\ Li_2\ Al\ Si_4O_{10}\ (OH)_2$	Monoclinic
Biotite **	$K\ (Mg, Fe)_3\ (Al\ Si_3O_{10})\ (OH)_2$	Monoclinic
Amphibole Group **	$(Mg, Fe)_7\ Si_8O_{22}\ (OH)_2$	Orthorhombic
Anthophyllite series	$Ca_2\ (Mg, Fe)_5\ Si_8O_{22}\ (OH)_2$	Monoclinic
Tremolite-Actinolite series	$Na\ Ca_2\ (Mg,Fe,Al)_5\ (Si,Al)_8O_{22}(OH)$	Monoclinic
Hornblende series	$(Mg, Fe)\ SiO_3$	Orthorhombic
Pyroxene Group **		
Enstatite-Hypersthene series	$Ca\ (Mg, Fe)\ Si_2O_6$	Monoclinic
Diopside-Hedenbergite series	$Ca\ (Mg, Fe, Al)\ (Al, Si)_2\ O_6$	Monoclinic
Augite	$(Mg, Fe)_2\ SiO_4$	Orthorhombic
Olivine series **		
Forsterite	Mg_2SiO_4	Orthorhombic
Fayalite	Fe_2SiO_4	Orthorhombic

* Felsic – rich in silicon (Si), aluminium (Al), sodium (Na), potassium (K) and calcium (Ca)

** Mafic – rich in iron (Fe) and magnesium (Mg) or ferromagnesian

2.5 Principle and practice of petrography

The description and classification of rocks basedon mineral identification and texture using a microscope is known as petrography. Petrographic technique is the method used in identifying and quantifying rock minerals with the aid of a polarised microscope. The technique uses the different physical and optical characteristics (such as textures, twining, reflectance, colour, level and type of cleavage) of the rock minerals in mineralogical study (Michael *et al*., 2012; Wase and George,2015). To use the method, there are two main stages involved - thin section preparation and observation of the prepared section under petrographic microscope.

2.5.1 Thin section preparation

A thin section, which is a small portion of the rock,is carefully cut from the parent rock sample. The procedure of preparation involves cutting small chips or billets of about 1 mm thick from the parent rock samples, using a thin-sectioning machine (model Logitech MP2A). One surface of a billet will thereafter be lapped on a glass lapping plate facilitated with a paste of water and carborundum. Similarly, a surface of a glass slide will be lapped until it becomes translucent. The billet and slide will then be rinsed with water and allowed to dry. The billet will thereafter be mounted on the glass slide with the lapped surfaces facing each other, epoxied and dried on a hot plate at about 50^{o}C. The pre-lapping at this stage is to ensure proper bond between the duo (slide and billet). About an hour after, the billet mounted on the slide is taken back to the cutting machine where large part of the sample is reduced to 50 micron on the slide. This is eventually transferred to the jig of the electric Logitech lapping machine (model CL50, shown in Fig. 2.2). The jig has asucking property so that on inversion, the samples cannot fall-off. Two of such prepared billets are put on it at a time. There are three stoppers made of diamond at the edge of the jig preventing the samples from falling out when lapping is on-going. The lapping is done till the required thin level of 30 μm is obtained. The thin section produced as indicated above is viewed using a petrographic microscope where the mineral components are identified and estimated.

Fig. 2.2. Logitech CL 50

2.5.2 Petrographic microscope

Petrographic microscope is a modified compound microscope in order to suit the purpose of magnifying the crystallised rock minerals. A compound microscope consists of an objective lens and an ocular lens (or eyepiece), both made of convex glass. The lenses are placed parallel to each other with a common axis and separated with an adjustable distance.

The object to be magnified is placed a bit outside the focal point of the objective lens. The object position is so close enough to the focal point that the object distance from the lens can be approximated to the focal length of the objective lens. The next step is to adjust the separation between the two lenses to produce an enlarged, inverted and real image of the object, by the objective lens, just inside the focal point of the ocular lens. The ocular lens now serves as a magnifying lens for the produced image, which acts as a new object for the eyepiece. Thus a magnified, virtual and erect image of the new object is produced by the ocular lens viewable by the observer. The product of the lateral magnification produced by the objective lens and angular magnification produced by the ocular lens gives rise to the overall magnification of the instrument. The magnification is expressed as:

$$M = -\frac{l}{f_o} . \frac{25cm}{f_e} \qquad (2.1)$$

where M is the total magnification, l is the tube length of the instrument approximated to the first image distance from the objective lens, f_o is the focal length of the objective lens, f_e is the focal length of the eyepiece lens and 25 cm is the eye near point (Halliday and Resnick, 2007).

For mineralogical analysis, the microscope is modified as a specially designed polarizing microscope for suitability of viewing mineral compositions of the rocks. The microscope is equipped with two polarizing elements and certain other accessories, which make it different from ordinary microscopes. The specimen sample to be viewed is illuminated through an arrangement of a 6V 20W halogen light source emitting light rays on a collector (a lens system). The collector in turn directs the rays through the condenser in-between to the specimen (Michael *et al.*, 2012). On adjustment for petrographic study, a medium of highly refractive index, such as, canada basalm is introduced in-between the position of the specimen and the objective. Its purpose is to check the spherical and chromatic aberration of intermediate image produced by the objective. The correction is possible because the resolution of the

instrument is greatly improved by increasing the angular aperture of the cone of light rays coming from a point on the specimen that strikes the objective. Eye lens and field lens are combined as part of the ocular from where the observer views the final image of the specimen. The microscope used are sometimes fitted with a camera connected to a computer from which photomicrographs could be taken after viewing. An example of a petrographic microscope is shown in Figure 2.3.

Fig. 2.3. A petrographic microscope

2.6 Physical features enabling mineral identification

Rocks are composed of various minerals characterised with different physical and optical properties. These properties go a long way in petrographic identification of the minerals present in a rock sample (Michael *et al*., 2012; Ibrahim*et al*., 2015). The modal volume or compositions of various minerals in such a sample, in percentage, are thus determined through their diagnostic features, which include texture, level and type of cleavage, and or colour of the minerals. Table 2.4 shows the main rock-forming minerals of granitic rocks with their features. After thin section preparation, the slides produced are viewed under a petrological microscope. The optical properties of the minerals, which include colour, twinning, cleavage, relief, extinction angle, pleochroism, birefringence, transparency, refractive index, crystal form or shape, texture and alteration are used for the identification. Some of the common crystal forms of rock-forming minerals expected in granitic rocks are shown in Figure 2.4.

Table 2.4. Identifying the main rock-forming minerals of granitic rocks in hand-specimen

Mineral	Colour	Habit	Cleavage
Quartz	Colourless/grey	Usually anhedral	No cleavage
Alkali feldspar (Microcline)	Pink or white	Lath-shape, tabular	Poor, 2 sets at 90^o
Plagioclase	White (rarely green or black)	Lath-shape, tabular	Poor, 2 sets at $\sim 90^o$
Pyroxene (Apatite)	Black to dark green or brown	4 or 8 sided prisms	Two good sets at $\sim 90^o$
Amphibole (Hornblende)	Black to dark green	Lozenge-shaped	Two good sets at $\sim 120^o$
Biotite	Black to dark brown	Dark shiny flakes (6-sided)	One excellent cleavage
Muscovite	colourless	Silvery flakes (6-sided)	One excellent cleavage
Tourmaline/Opaque	Usually black	Clongate 3-sided prismatic/needles	No cleavage

Source: (Robin, 2010)

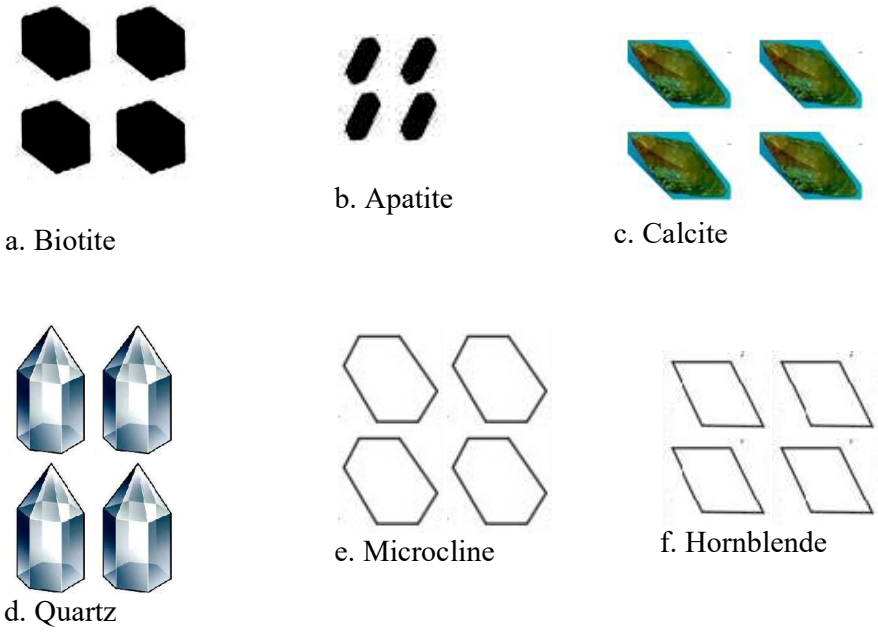

Fig. 2.4. Crystal structures of the rock forming minerals (Henry and Yokuts, 1997)

2.7 Advantage and limitation of the petrographic studies

Mineralogical compositions of the granitic rocks are determined using petrographic method alone. Geochemical analysis based on chemical composition are more expensive and not readily available, though it is not entirely equivalent in the information it conveys with petrographic method (Robin, 2010). Affordability of the petrographic method is another advantage and it is also more accessible.

Fine grained and glassy rocks, such as basalts and rhyolite are difficult to identify with the polarizing microscope alone (Robin, 2010). In that case thin-section examination may be supplemented by geochemical analysis. This constitutes a limitation in this work, which does not really affect the validity because this research involves coarse grained igneous rocks whose minerals are identifiable both qualitatively and quantitatively using petrography.Another limitation is that petrographic method involves point counting and measurement by percentage volume % whereas geochemical analyses is by weight %. Minerals vary in colour from dark to light, dense to less-dense, thereby introducing a bias in geochemical data (Robin, 2010). In this study, however, petrographic method is adequate and requires no comparison with geochemical data.

2.8 Quarry industry and their operational units

Outcrops of granitic rocks (granites, gneisses and migmatites) occur abundantly and widespread in southwestern Nigeria. These crystalline rocks support the establishment and expansion of quarry rock business in the region. They provide dimension stones, hard core boulders, chippings and granite dust, which are called coarse and fine aggregates depending on the grain size. Granitic rocks are used as aggregates in southwestern Nigeria because granite is hard enough to resist most abrasion, strong to bear significant weight, inert to resist weathering and possesses brilliant-polish aesthetic character. Granite and granitic rocks are consumed in building, roads, dams, drainages and bridges construction. They are also used in the provision of table tops in homes, electric poles and sculpture.

Quarrying is a major economic activity in many developing countries including Nigeria (Tauli-Corpuz, 1997; UNEP, 1997). Granite is an igneous rock and also a non-metallic industrial mineral/rock whose aggregate is also used as construction mineral (Osasan, 2009). The socio-economic development of many countries has received a boost from mineral exploration, exploitation and utilization because a vibrant mining

sector tends to generate larger fiscal income than other sectors (Akande and Idris, 2005).

As at 2012, the mining and quarry industries in Nigeria have almost 1.5 million workers (NBS, 2015). With the large number of quarry industries in southwestern Nigeria and the population growth rate of about 2.9 % (NPC, 2006), over half a million people are engaged in quarry activities in southwestern Nigeria. Various protective measures are put in place to ensure safety of the workers from dust and other dangers in the quarries. These include wearing of helmet, industrial coat, hand-glove, nose and mouth cover. The workers also enjoy annual leaves and their service is on shifting basis. However, the measure is only to reduce the hazardous effects associated with ionizing radiation that may be present in the quarried granitic rocks. Assessment of radiological hazard to the workers in the course of performing their duty is therefore necessary.

Quarrying is the multistage process by which rock is blasted from an outcrop, such as, a hill and crushed to produce aggregate, which is then screened into sizes required for immediate use. It may be further processed to produce, for example, asphalt when coated with bitumen for road pavements. A quarry is a place from which dimension stone, rock, construction aggregate, riprap, sand, gravel, or slate is excavated from the ground for various constructions. Every viable quarry industry has the three operational units which are Blasting, Crushing and Depot units.

2.8.1 The granite blasting unit

The granite blasting unit is a place where blasting process is carried out on the granitic rock for the purpose of extraction of its fragmented boulders. This is achievable by drilling holes of about 2 inches in diameter and 20 feet deep at an interval of about 5 to 20 feet depending on the size of the fragments required. The larger the distance between adjacent holes, the larger the fragments. The holes are drilled in columns and rows using rock drills or jet flame drills. A rock drilling machine rotates a rod tipped with a rolling gear-like bit into the rock while a jet flame drill uses a high-velocity flame to create holes in hard rock.

Explosive charges and detonators are placed in the holes with the detonators linked together by wires connected to a source of electricity. An explosive is a chemical compound or mixture of compounds that undergoes a very rapid decomposition when energized by heat, impact, friction or shock. Detonation of high

explosives is accompanied by shock waves and hot gas release. The hot gas produces extremely high pressures within the borehole, which eventually cause the fragmentation of the rock.

The four types of commercial explosives used in the industry are dynamite, slurries, ANFO and two-component explosives. The detonators have different time-delay in fractions of seconds. They are arranged such that those in the front rows have shorter time-delay and will explode before those in the next rows. This is to avoid flying off of the fragments in all directions but to ensure their falling in a particular direction. Hard rocks are broken out of the ground using this technique, while weaker rocks may be excavated directly using a ripper. The objective in both cases is to fragment the rock to a size suitable for loading and transportation to the crushing unit for further processing. In either case, dust emission occurs as stones are being quarried from the earth.

2.8.2 The granite crushing and screening unit

The granite crushing unit is engaged in the production of rock aggregates of different sizes using crushers and screens for size classification. Large capacity haulage vehicles are used to transport broken rock from the blast unit to the crusher which has two steel jaws with which it crushes the large rock fragments into pieces. The pieces, after crushing, are conveyed to the screening section where they are sorted out into different sizes. The size of aggregates produced depends on the request by the end-users. The aggregates are commonly used in the construction of roads, highways, bridges, buildings and canals. The air-borne dust is higher in the crushing and screening units than the depot unit due to the motions to which the fragments are subjected during the crushing and screening process. Dust emissions can cause respiratory diseases to the quarry workers and the neighbouring inhabitants.

2.8.3 The granite depot unit

The crushed and screened rock material has to be transported from the processing plant (crushing and processing unit) to the depot unit where marketing takes place. Aggregates of different sizes are packed separately. Among different sizes available are gravels which are above 4mm in size and quarter-size granite product is called granite dust. Air-borne dust is released into the atmosphere as granite product is loaded and off-loaded. These activities can expose the workers involved to natural radiation from the primordial radionuclides in the granitic rocks.

2.9 Occupational radiological exposure in granite quarry operations

Granite quarry operational activities, such as, blasting, crushing, loading and off-loading of granite products can lead to radiological health hazards. Air-borne dust from the exercise carries finite amount of natural radionuclides, which could be inhaled by the workers. These could constitute a source of internal radiation exposure that can lead to respiratory disease (Jibiri and Okorie, 2006). Accumulation of the radiation dose with time could result in chronic exposure of the quarry workers, which may lead to delayed carcinogenic effect of radiation. Food and water can also be the pathway for the ingestion of radionuclides by the workers when the air-borne dust comes in contact with food and water they consume at work. External radiation is also possible with the dust coming in contact directly with the body. Skin and eye diseases may result from workers exposure to irradiation.

Research work on limestone showed that minor radiological health hazard are recorded during limestone mining operation while such operations on hard rocks, such as, granite may expose workers to very dangerous levels of respiratory dust (Ugbogu *et al*., 2009). This present study is limited to the radiation activities in granitic quarry industries in southwestern Nigeria. Different indices are used to assess radiological hazard to the workers in the environment. The results obtained will be compared to standards including the maximum permissible occupational annual effective dose of3 $mSvy^{-1}$for quarry(mining) workers and 1 $mSvy^{-1}$ for the public (UNSCEAR, 2010; UNEP, 2016; UNSCEAR, 2017). The results were compared to the world average value of absorbed dose rate due to soil samples by UNSCEAR (2000), which is 59 nGy h^{-1} and compared to equivalent of absorbed dose values derivable from UNSCEAR (1993) activity concentrations of natural radionuclides due to granitic rock samples.

2.9.1 Radium equivalent

This is a quantity used to examine the total exposure caused by ^{40}K, ^{226}Ra and ^{232}Th in environmental samples. The combining effect is necessary because equal concentrations of the radionuclides are not causing equal amount of biological effects as a result of differences in gamma energies (UNSCEAR, 1982). Their radioactivity concentrations were combined in terms of radium equivalent, which is defined as:

$$Ra_{eq} = C_{Ra} + \frac{10}{7}C_{Th} + \frac{10}{130}C_K \qquad (2.1)$$

where, C_{Ra}, C_{Th} and C_K are the respective activity concentrations in Bq kg^{-1} (Berekta and Mathew, 1985; Khater, 1997, Xinwei *et al*., 2008). This quantity is useful in setting a safety criterion, with the recommended limit of 370 Bq/kg to keep absorbed dose of the populace below 1 $mSv.y^{-1}$ for safe use of the granitic rocks in building construction (UNSCEAR, 1982).

2.9.2 Absorbed dose rate

The activity concentration of a radionuclide is a measure of the intensity of the radiation obtainable from such a source. It does not directly determine the health effect on the exposed individual. However, the energy an individual receives determines the health effects from the exposure. The absorbed dose is a measure of energy deposition per unit mass in any medium by any type of radiation. The absorbed dose rate, *D* (nGy h^{-1}), at a height of 1 m above the ground surface due to the concentrations of ^{226}Ra, ^{232}Th and ^{40}K in the granite in each of the locations surveyed was calculated using the equation (Beck *et al.,* 1972):

$$D = 0.462C_{Ra} + 0.621C_{Th} + 0.0417C_K \qquad (2.2)$$

where,C_{Ra}, C_{Th} and C_K are the radioactivity concentrations (in Bq kg^{-1}) of ^{226}Ra, ^{232}Th and ^{40}K, respectively.

This could be used to assess the radiological health hazard to gonads of the quarry workers in the study area. The results obtained will be compared with the UNSCEAR reports. UNSCEAR (2000) has reported world average value of 59 $nG.h^{-1}$ for absorbed dose rate in air due to worldsoil samples. World average activity concentration values of ^{40}K (1104 $Bqkg^{-1}$), ^{226}Ra (78 $Bqkg^{-1}$) and ^{232}Th (111 $Bqkg^{-1}$), due to granitic rock, were also reported by UNSCEAR (1993) and cited by Papadopoulos *et al*. (2012).

2.9.3 Annual effective dose

The health effect of an exposure to radiation depends on the magnitude of the absorbed dose as well as the effectiveness of the radiation type in causing tissue damage. Absorbed doses of different types of radiation are weighted for their potential to cause certain types of biological damages. The weighted doses, known as equivalent doses, are also weighted to have effective doses because some parts of the body are more vulnerable than the other. Thus the effective dose gives information about the

likelihood of cancer and genetic effects in the life of an exposed individual to low doses of radiation (UNEP, 2016). The effective dose of ionizing radiation received annually by an individual depends on the time for which the person is exposed to the radiation. The annual effective dose, E (mSv y^{-1}) that can be received by such a person due to the activity of the radionuclides in the granites has been calculated using the following equation (UNSCEAR, 2000) and also used by Rafique*et al*. (2011):

$$E = TxQxDxO_f x10^{-6} \qquad (2.3)$$

Where, T is time in hours in one year (8760h), Q is 0.7 Sv Gy^{-1} h^{-1} for environmental exposure to gamma rays of moderate energy, D is the dose rate given in equation (2.2) and O_f is the occupancy factor (0.8).

Since the focus of this study is the annual occupational effective dose to the quarry workers from the granitic rock in quarry sites, the equation can be modified for this purpose. It is estimated that the quarry workers spend 9 hours each of 6 days in a week. They work for about 46 weeks out of 52 weeks in a year because of annual leave and other public holidays therein. The equation is thus modified as follows:

$$E = Dx\ 1.7388\ x10^{-3} \qquad (2.4)$$

Equation (2.4) was used to calculate the annual occupational effective dose to the quarry workers due to ^{226}Ra, ^{232}Th and ^{40}K in granitic rock samples collected from selected quarry sites in southwestern Nigeria. The values obtained were compared with the UNSCEAR average annual effective dose of 3.0 $mSv.y^{-1}$ for global occupational exposure of monitored workers due to natural sources (UNSCEAR, 2010; UNEP, 2016; UNSCEAR, 2017).

2.9.4 Lifetime cancer risk

Human exposure to gamma radiation, especially over a long time, predisposes the exposed individuals to risks of different health effects. The health effects are said to be stochastic or probabilistic without a causative threshold.

Quarry workers are subjected to low level ionising radiation exposure on regular basis. Accumulation of the dose can result in severe radiological health hazard like induced cancer. Investigation has revealed that with low doses of gamma radiation, through extrapolation, induced cancer is possible (BEIR, 1990: IAEA, 1996). It is therefore of crucial importance to assess the occupational level of cancer

risk among the quarry workers in the study area. On this basis, evaluation of the excess lifetime cancer risk (ELCR) of quarry workers resulting from accumulation of low level radiation dose from granitic quarry sites in southwest was carried out.

The ELCR deals with the probability of developing cancer over a lifetime at a given exposure level (Emelue *et al*., 2014). Thus the following equation was used to calculate the excess lifetime cancer risk in this work (Taskin *et al*., 2009):

$$ELCR = ExDLxRF \qquad (2.5)$$

where, *E* is the annual effective dose in sievert per year, *DL* is the average duration of life which is estimated to be 70 years (Emelue *et al*., 2014) and *RF* is the fatal cancer risks per sievert known as risk factor. The risk factor of 0.05 proposed for public by ICRP (1991; 2005 and 2012) for the stochastic effects was used. This has been used by different researchers (Taskin *et al*., 2009; Emelue *et al*., 2014; Azize*t al*., 2014). The commission has adopted the same cancer risk factor for both the workers and the public because the difference is not large enough to deserve separate protection values (OECD, 2011).Although a number of studies have been conducted on the assessment of ELCR arising from gamma radiation due to various environmental materials, there are scanty data on ELCR assessment due to granitic rocks in particular. The results of the present study will therefore be compared with the available ELCR data from gamma radiation emanating from different environmental sources. The value of ELCR obtained in this study will also be compared with the world average of 1.45 x 10^{-3} (UNSCEAR, 2000; Taskin *et al*., 2009; Davou and Mangset, 2015).The cancer death probability of about 0.1% is tolerated for quarry workers due to their exposure to inevitably low level dose of ionizing radiation arising from operational activities by ICRP 60, OECD (2011). The cancer death probability value derived from ELCR data of this work will as well be compared with that of the ICRP.

2.10 Principle of gamma spectrometry

One of the methods of radiation measurement is by counting number of electrical pulses from detector chamber per unit time.This is a function of the number of photons absorbed in the detector volume per unit time. However, gamma spectrometry is not restricted to count rate alone but the energy of the gamma radiation is equally important. The count rate is used to determine the activity concentration (Bq kg^{-1}) of the different radionuclides in the sample while the identification of the

radionuclides emitting the gamma radiation in the sample is done by the energy of the gamma radiation.

Out of about twelve different processes (Fano, 1953) by which gamma rays can be absorbed or scattered, when it comes to the region of 0.01 – 10 MeV, which is the region of the energy of gamma rays emitted by building materials, such as granite, (Ademola, 2003), most interactions are explainable in terms of just three. They are photoelectric effect, compton effect and pair production. All or part of the energy of gamma radiation absorbed in the medium is transferred through any of the three processes.

In photoelectric effect, all the photon energy is transferred to the ejected electron, called photoelectron in the absorbing medium. It loses the energy to ionization and excitation of absorbing atom resulted in peak termed as photopeak. The number of counts under a photo peak per unit time is proportional to the activity of the sources.

Pair production is obtainable when photon energy is above 1.02 MeV or $2m_0c^2$. Here the photon is absorbed completely in the medium and replaced by a positron and an electron pair under the influence of the columbic field of the nucleus. The total energy is equal to the energy of the initial photon. The positron annihilates with a nearby electron after losing its kinetic energy to excitation in the absorbing crystal to produce two photons of energy 0.511MeV in approximately 180^o to conserve momentum. The annihilation photons may result in light pulses that can contribute in addition to the photopeak due to photoelectric absorption as one of three possibilities. It is also possible that one of the annihilation photon escapes to result in a "single-escape peak'' in the spectrum at energy *hv* - 0.511 MeV. When both annihilation photons escape from the detector volume, it leads to a "double-escape peak" corresponding to energy *hv* - 1.02 MeV.

Compton interaction takes place when the photon has an elastic collision with shell electron of the detector material. In this case, the photon transfers only fractions of its energy to the electron. It is scattered and carries a reduced energy. The scattered photon may leave the detector or can even have further interactions. The measured pulse height thus corresponds to the energy of the produced Compton electron. The maximum energy, according to conservation of momentum and energy that can be transferred to an electron is when the angle between the scattered photon and the recoil electron is 180^o and is given as:

$$E_C = \frac{E_\gamma}{1+\frac{m_0 C^2}{2.E_\gamma}} \quad (2.6)$$

In gamma spectrometry, a material medium (detector) is required in transforming the gamma energy to electrical pulses that are eventually analysed. The materials that demonstrate this property are called transducers. There are two main types of transducers; they are semiconductor and scintillation detectors. The commonest type of semiconductor detector presently is hyper pure germanium detector (HPGe) with a band gap of about 0.7 eV. This type, though has high resolution, is not used in this work because of its liquid nitrogen requirement for cooling (at -196^{o}C or 77K) during operation making it expensive to maintain.

In a scintillation detector, the material exhibits the property of luminescence when excited by radiation. A common example of scintillator used extensively in gamma-ray measurements is sodium iodide crystal activated with thallium [NaI(Tl)] to improve on the conversion of energy absorbed in the crystal to light. The detector crystal is optically coupled to the photocathode of a preamplified photomultiplier tube (PMT). Scintillation photons incident on the photocathode of the PMT and liberate electrons through the photoelectric effect. Since the photons arrive at the photocathode at about the same time, the individual currents combine to produce a single large current pulse. The strong electric field in the PMT multiplies the pulse (10^4) to a measurable size.

Further amplification is always required using an external Amplifier Base to the PMT. A typical example of sodium iodide scintillator is shown in Figure 2.5. Pulses of different sizes are produced due to photoelectric scattering, compton scattering, pair production and scattering in the neigbourhood of the detector. They emerge from the PMT with subsequent amplification. The initial number of photoelectrons liberated at the photocathode, from the pulses due to photoelectric effect, is proportional to the amount of light incident on the photocathode, which, in turn, is proportional to the initial gamma ray energy of the source. For such pulses, the output pulse size is proportional to gamma ray energy. This is a major advantage of gamma spectrometry. A typical example of a single gamma photon spectrum is shown in Figure 2.6.

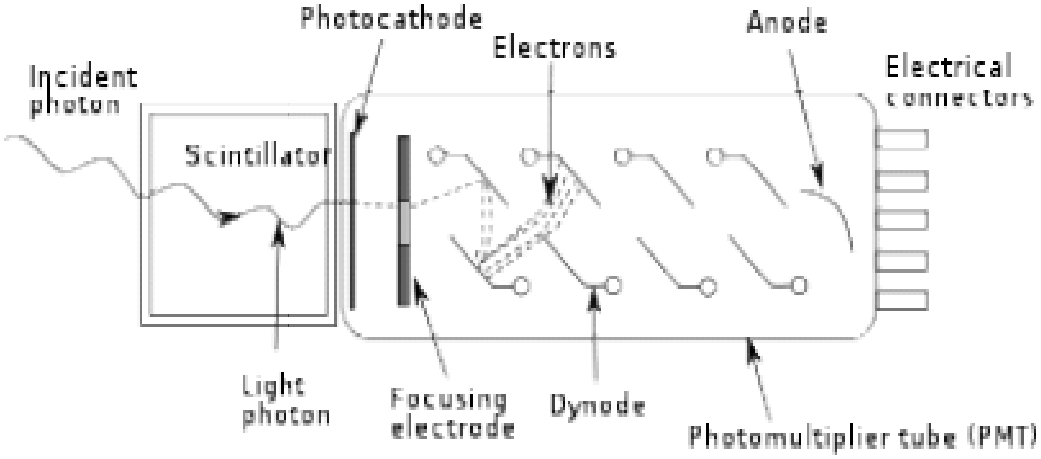

Fig. 2.5. Operation of NaI(Tl) scintillator

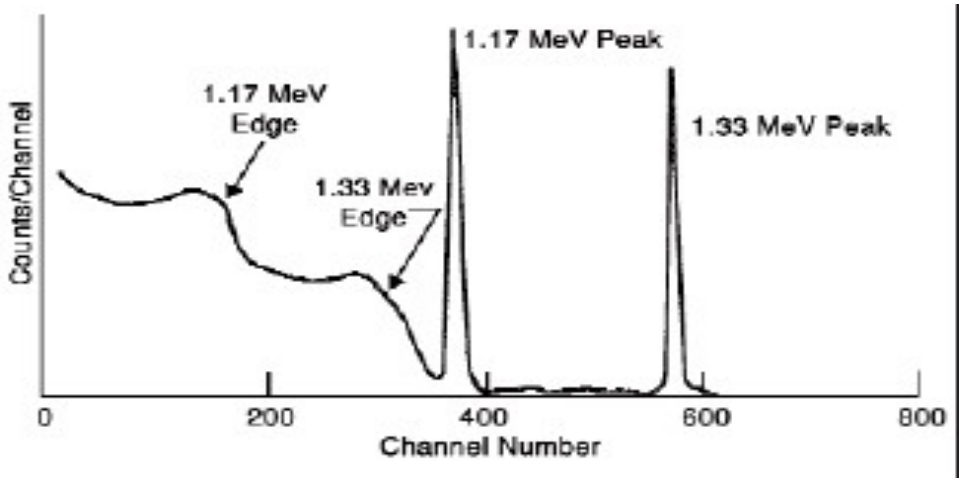

Fig. 2.6. A spectrum of ^{60}Co

The computer based spectrum multichannel analyzer (MCA) sorts out the pulses according to their sizes. The feature of the MCA allows automated data-processing operations, such as, background subtraction and spectrum stripping. This feature was employed in this work. The digital signal (due to one gamma photon in the photoelectric interaction) is then added as one unit into the memory word or channel corresponding to the size of the digital signal. There are typically up to 4096 channels. A display of the number of pulse units (number of counts) in each channel against the channel number represents the gamma spectrum. The collection of pulses due to photoelectric interactions gives rise to a peak around the channel corresponding to the gamma energy. This peak is called the photopeak, which is the peak of interest in gamma spectrometry.

The peak resulted from the pulse output from the photomultiplier tube is subjected to statistical fluctuations due to the processes leading to the distribution around the photopeak. As a result of this, two pulses produced by gamma photons of the same energy may be slightly different in height and sorted into two different but close channels. Thus the photopeaks due to monoenergetic gamma rays form a distribution which spreads over some neighbouring channels and the width of the distribution is a measure of the resolution of the spectrornetric system. A spectrometric system of good resolution will clearly distinguish between two photopeaks that are close together.

In scintillation spectrometry, quantitative evaluation of Resolution (R) is done by measuring the Full Width at Half Maximum (FWHM) at a photopeak of interest. It is defined as:

$$R = \frac{FWHM}{Peak}\ x\ 100\% \qquad (2.7)$$

The resolution of the system used in this study is about 8% at 662 keV of ^{137}Cs. Though the resolution is low when compared with the resolution of a gamma spectrometer due to a semiconductor detector, the system is capable of distinguishing the photopeaks due to the three primordial radionuclides of interest in this work and cost effective.

Energy calibration of the system was carried out before being used in this work. This is achieved using standard radioisotopes with known gamma energies, the

straight line graph relating channel number *N* with gamma energy *E* was obtained as illustrated in the straight line equation below:

$$E\ (MeV) = kN + c \qquad (2.8)$$

where k is a constant and c is the channel number of zero gamma energy. This is usually stored as an algorithm in the memory of the MCA so that gamma energies (in keV or MeV) are displayed directly. With the energy calibration equation stored in the memory of the system, the photopeaks of an acquired spectrum can be read in the units of gamma energy (keV or MeV).

2.10.1 Principle of radiation detection by a NaI(Tl) crystal

A gamma radiation incident on the crystal loses its energy in the scintillating material to produce a number of light photons through photoelectric interaction with the atoms of the crystal. The number of light photon is given by:

$N = (E/W_o)q$ (2.9)

where *E* is the gamma energy (*hv*) of the photon, *Wo* is the average energy required to produce a single photon whose value is about 3 eV for NaI(Tl) and q is the probability of a photoelectric interaction of the incident photon called luminescence quantum efficiency. A fraction of these photons impinge on the photocathode and a fraction of them reaching the photocathode is converted into photoelectrons. The number, N_c of electrons from the cathode is given by:

$$N_c = \left(\frac{E}{W_0}\right) qmC_{pe}G \qquad (2.10)$$

where G is a fraction of the photons impinges on the photocathode and is called light collection efficiency, C_{pe} is the photoquantum efficiency of the window-cathode system and *m* is a factor between 0 and 1 depending on the spectral matching between scintillation spectrum and the response of the photocathode. Thereafter, the total number of electrons N_d arriving at the first dynode is given by:

$$N_d = q\left(\frac{E}{W_0}\right) mC_{pe}g_cG \qquad (2.11)$$

where g_c is the efficiency with which the electrons are collected by the first dynode. A lot of factors are affecting the above efficiencies. *G* depends on self-absorption, reflection losses, light trapping, optical flaws and the geometry of the photocathode. In order to significantly reduce self-absorption in NaI(Tl) crystal, the detector is coated

with a reflector like MgO and G, as a result, can be nearly made unity. The term $mC_{pe}g_c$, depends in a complex manner on the wavelength of the light emitted. The factor C_{pe} depends on the cathode material and its thickness while g_c depends on the structure of the first dynode and the applied voltage.

A factor of n successive dynodes multiplies the N_d electrons shown in the above equation to give an overall gain M, given as:

$$M = \pi_{i=1}^{n} m_i \qquad (2.12)$$

where m_i is the multiplication at the *ith* dynode and is roughly proportional to the voltage between the dynodes. The total number of electrons Q, collected at the anode after the last dynode is thus given as:

$$Q = N_d M \qquad (2.13)$$

Equations 2.12 and 2.13, as can be observed, show that Q is a linear function of the energy E of the initial incident photon.

Apart from the number of electrons given by equation 2.13, there are a number of electrons produced due to thermionic emission in the photomultiplier tube. According to Birks (1964), the number of electrons with thermal energy greater than the work function of the photo cathode which are emitted as thermionic electrons is a function of temperature as given in the equation:

$$n_T = ATe^{(-Qe/kT)} \qquad (2.14)$$

where T is the absolute temperature, e is the electronic charge, k is the Boltzman constant, A and Q are characteristics of the cathode material. The thermionic electrons are multiplied in the PM tube. They therefore constitute the dark current, which is the current produced in the PM tube in the absence of incident radiation. The pulses arising from these thermionic electrons form part of the background of the energy spectrum, which may pose a significant problem when low energy radiation or weak sources of radiation are being measured.

2.10.2 Pulse shaping and height analysis

The number of electrons that are collected at the anode (or collector) decays according to the equation:

$$N = Qe^{-(\frac{t}{\tau})} \qquad (2.15)$$

where $\boldsymbol{\tau}$ is the modified decay time of the scintillant, which is about 0.25 μsec for NaI(Tl). A pile up may await the pulses because of their short lifetime. Therefore it is required to collect information about a pulse as quickly as possible. In order to achieve this, a pulse shaping *RC* circuit is usually placed after the amplifier as shown in Figure 2.7. Its function is to preserve maximum information while the pulse duration is reduced. According to Birk (1964) and cited by Ademola (2003) and Obed (2004), the number of the shaped output electrons *N(t)* is given as:

$$N(t) = Q\left[\frac{RC}{RC - \boldsymbol{\tau}}\right][e^{-\frac{t}{RC}} - e^{-\frac{t}{\tau}}] \qquad (2.16)$$

The voltage is, thus, given by:

$$V(t) = \frac{Qe}{C_s}\left[\frac{RC}{RC - \boldsymbol{\tau}}\right][e^{-\frac{t}{RC}} - e^{-\frac{t}{\tau}}] \qquad (2.17)$$

Equation 2.17 shows that the amplitude of the pulse depends on C, $\boldsymbol{\tau}$ and *RC* (time constant) of the circuit. In order to ensure that *V(t)* peak is proportional to the energy dissipated by the primary radiation in the scintillator, the *RC* must be greater than $\boldsymbol{\tau}$. In essence, the purse height is maximized and subsequent noise will have minimum degrading effect. This therefore ensures the amplitude distribution *V(t)* and the energy spectrum relation.

2.10.3 Pulse selection

Owing to different types of interaction in the detector crystal, the pulse amplitude given in equation 2.17 is of random occurrence in size and in spacing. The fluctuation of the pulses is illustrated by a typical PMT output shown in Figure 2.8 (Martin and Harbison, 1979). The analogue information in *V(t)* is first converted into a digital information before the acquisition of the final spectrum for convenient process. The illustrated output is obtained after using a discriminator, such as, Schmitt-trigger or an analogue comparator to filter off noise or other background pulses. The discriminator will only allow the pulses whose amplitude exceeds the discriminator's bias voltage level such as D in the Figure 2.8 and the pulses below the level are rejected as noise signals. The counted pulses are then analyzed according to their heights.

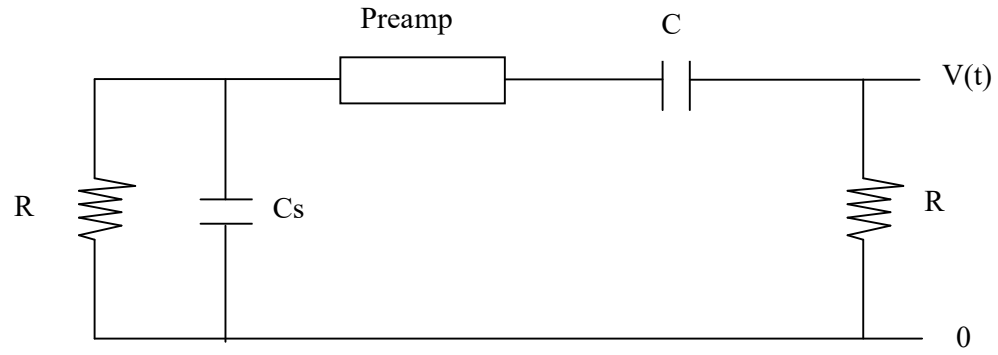

Fig. 2.7. A schematic representation of a pulse shaping circuit (Martin and Harbison, 1979)

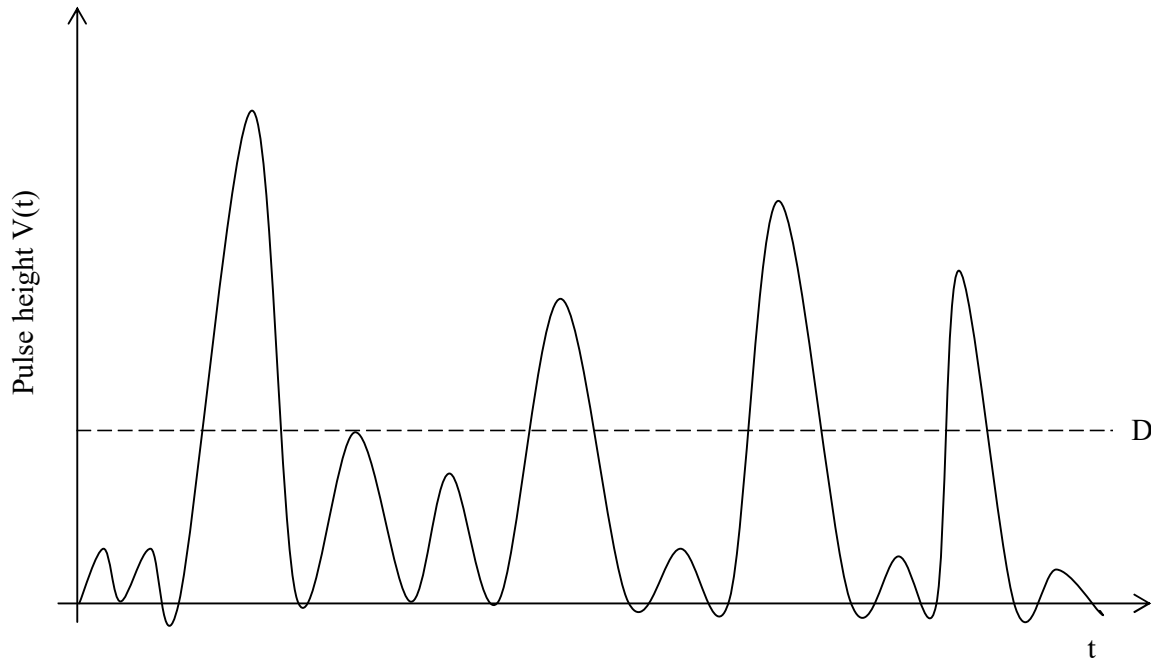

Fig. 2.8. Pulse height distribution and their selection (Martin and Harbison, 1979)

Multichannel analyzer (MCA) used in most modern scintillation systems works on the principle of pulse to time conversion which is illustrated in Figure 2.9. After amplification and shaping, the input pulse (A) is fed into the analyzer. The pulse is then stretched at its maximum height *V(t)* which is maintained constant at B. At time t_0, when the input pulse is at its maximum height, two pulses are simultaneously fed in. They are a linearly increasing sweep pulse (S) and a series of clock pulses (C). When S reaches the height *V(t)* of the stretched pulse at time t_1, the clock pulses stop. The number of clock pulses in the time $t_1 - t_0$ is proportional to pulse height *V(t)* and hence the energy of the Υ- radiation. The digital signal is then added as one unit into the memory word or channel, which corresponds, to the size of the digital information. The memory can thereafter provide information about the radiation in the form of channel number and the number of pulses in each channel. The gamma radiation intensity and other parameters thus become possible to assess. The Canberra MCA used in the present study based on this principle of operation.

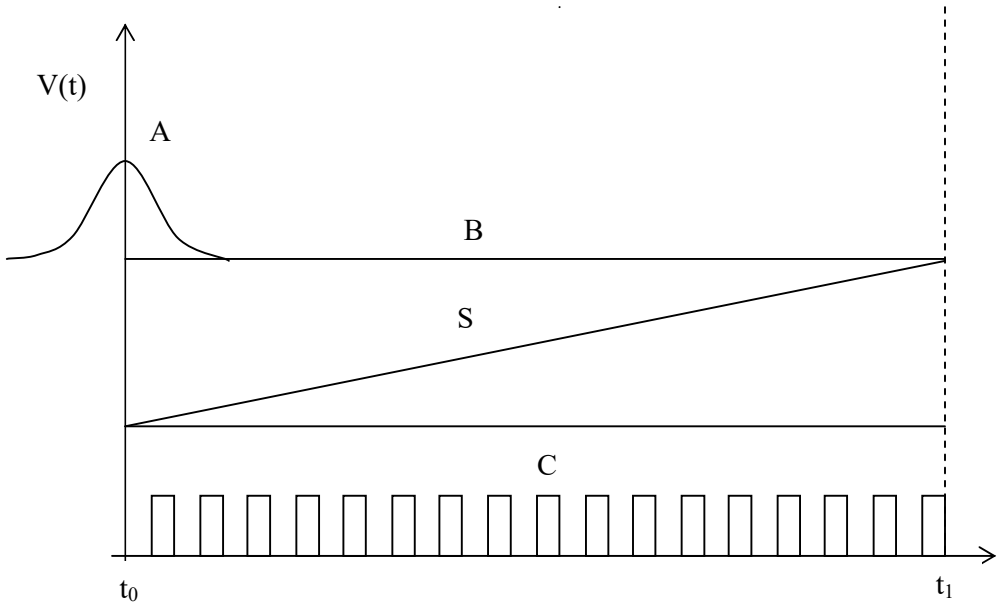

Fig. 2.9. Principle of pulse to time conversion (Kowalski, 1970)

2.10.4 The evaluation of net area under a photopeak

Events such as dark current, electronic noise of the system, compton plateaux of higher peaks contribute to the counts under a photopeaks from a particular gamma energy. This always makes accurate determination of the area under a photopeak due to such Y-energy difficult. The actual count due to photoelectric absorption of the Y-energy is equal to the integral count in the region of the photopeak after the deduction of the total background count in that region. The method adopted in this work for the computation of the net area is programmed in the memory of the analyser system as illustrated in Figure 2.10.

A region of interest (ROI) is defined around a photopeak, which is symmetrically bounded by channels q and t on either side of the photopeak. The average count B due to background radiations in each channel of this region has been estimated by considering 3 channels at the tail of the Gaussain curve on either side. Well defined photopeaks of the three natural radionuclides of interest involved in this study which are also with very low continuum enables the applicability of only 3 channels considered in determining the peaks. Usually, up to 5 channels are required for low energy peaks because the peaks are not well defined and usually sit on a very large continuum due to the poor resolution of NaI(Tl) detector.

In Canberra MCA operational manual, the average count B is given as:

$$B = \frac{B_1+B_2}{2(k)} \qquad (2.18)$$

where $k = 3$ for the well-defined radionuclides, $B_1 = \sum_q^r X_a$, $B_2 = \sum_s^t X_a$; and X_a is a constant of each channel. The integral count I in a region of interest (ROI) is given by:

$$I = I_P + B_1 + B_2 \qquad (2.19)$$

Where I_p is the sum of the contents of N channels actually under the photopeak and not in B_1 and B_2, I_p is given by:

$$I_P = \sum_m^n X_a \qquad (2.20)$$

The net area, A, which is the area due to actual photoelectric absorption is equal to the total count I_p minus the total background, NB in all the N channels. That is:

$$A = I_P - NB \qquad (2.21)$$

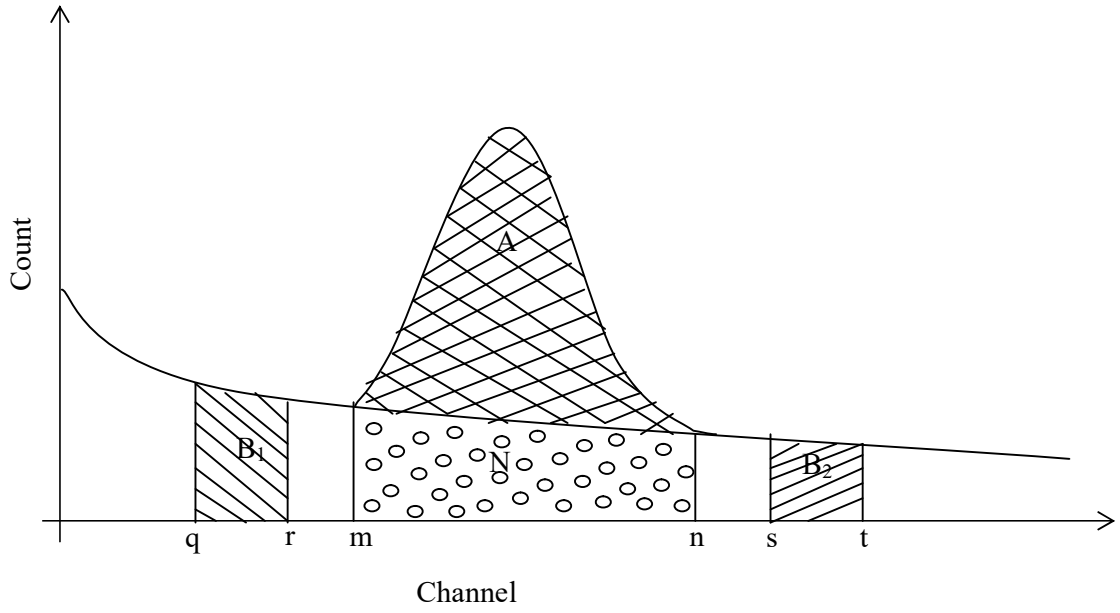

Fig: 2.10. Evaluation of net area under a photopeak

Equations 2.20 and 2.21 are stored as computation algorithms in the memory of the MCA system used in this work. They are processed and the results are displayed whenever the region of interest is judiciously created around the photopeak due to a particular Υ-ray energy of a radionuclide. From equation 2.21, the accurate reproduction of the net count A depends on the statistical errors in the actual photoelectric and background events. That is, the standard deviation, σ_A, in the net count *A* is given by (Canberra, MCA operational manual) as:

$$\sigma_A^2 = \sigma_P^2 + \sigma_B^2 \left(\frac{N}{6}\right)^2 \qquad (2.22)$$

Also, the percentage standard deviation error, *E*, in *A* is given by:

$$E = \frac{F}{A}\sigma_A \, x \, 100\% \qquad (2.23)$$

These algorithms have also been stored in the memory of the system with F =1 .645 implying that the error statement is at 90% confidence limit. The error statement is always displayed along with the net count *A* whenever analysis is made in the various regions of interest (Ademola, 2003).

2.11 Advantages and limitations of gamma spectrometry

Radiation effect measurement involves using a Geiger counter to determine the count rates due to the radiation without identifying the emitting sources. The advantage of gamma spectrometry lies in its ability to identify the sources of the radiation, through their energy spectra, and the measurement of activity concentration, quantitatively through calibration of the instrument.

One of the limitations is that some of the radionuclides (^{226}Ra and ^{232}Th) depend on the gamma-radiation produced by their daughter products for detection. Since the method relies on the assumption of radioactive equilibrium between the parent and daughter, such equilibrium may be disrupted by the removal of one of the intermediate radionuclides in the series probably due to loss of a gaseous member of the decay series (Killeen *et al*,. 1994). Another limitation is that gamma spectrometry is not suitable at low energy line. This is because the efficiency of sodium iodide detector is high; the consequence noise from the detector is so much that the output signal from low energy line may not be measurable. In this study, the samples are hermetically

sealed to avoid escape of gaseous product like radon gas and kept for up to 4 weeks to ensure equilibrium between the parent nuclides and their progenies.

CHAPTER THREE

METHODOLOGY

3.1 Granitic rock sample collection

Granitic rock samples were collected from selected quarry sites in Oyo, Osun, Ekiti, Ondo and Ogun states in southwestern Nigeria. The sampling locations within the respective states is as shown in Figure 3.1. Granitic rocks can vary greatly in radionuclide content depending on their percentage mineral compositions which may be due to their geological locations.

A total of two hundred and thirteen (213) granitic samples were collected with three samples from blasting, crushing and depot locations of each quarry site ranging between 21 and 69 samples per state. The sample plan was based on the density of quarries in the states and accessibility to the quarries. The number of granitic rock samples collected from each state is shown in Table 3.1. Each sample was split into two, with one half used for petrographic and the other for gamma spectrometry radioactivity concentration studies.

3.1.1 Oyo state

The major quarry locations in Oyo State are along Ibadan - Lagos express road Figure 3.1). Other locations include those of Lanlate owned by Quarry construction company (QCC), Iresapa, Nigerian Construction Company (NCC quarry) and Oyo town (Lad &Sons quarry). Available records showed that thousands of workers are engaged in the quarries. It is therefore expedient in this work to assess the radiological hazard associated with the production and handling of the granite products.

3.1.2 Osun state

Quarries are located around Awo (Wetipp Construction Company and Awo Stone Quarry), Iwo (Iwo Construction Company), Ijabe (TJ Construction Company) and Ila-Orangun (Bristo Construction Company) towns in Osun State. Most of the granite samples collected are the felsic type. The quarries are located in the outskirts of

the towns. According to available records from the management of the quarries, over one hundred thousand workers are engaged across the state.

3.1.3 Ekiti state

The granite quarries in Ekiti State are located all over the state. However, some of the quarries sites visited for sample collection include those in Igbemo (Quarry Construction Company), Igede (Brico Construction Company in Nigeria) and Ikere (Dekit Construction Company) (Figure 3.1). Many of the quarries are located away from residential and official buildings. Records from the quarries showed over two hundred thousand workers are engaged. The large population of the work force necessitated evaluation of radiological hazard in the quarries.

3.1.4 Ondo state

The highest number of granitic rock samples collected was from Ondo State (Table 3.1, Figure 3.1). They are a mixture of quartzofeldspathic and mafic types. Some of the quarries are located very close to the main road. Examples of such quarries include those of Ebenezer Construction Company and Focus Construction Company in Akure. Others are at Ifon (Hispanic Nigeria Limited), Idanre (Levant Construction Limited), Ore (Raycon & Co. Nigeria Limited), and Elegbaka (Silver Construction Company), Akure (Japaul Nigeria Limited). The workers' population, according to the various managements, is estimated to be over two hundred thousand.

3.1.5 Ogun state

Several prominent outcrops of granite and gneisses occur as hills, ridges and inselbergs in Ogun State. Most of the granite quarry locations in Ogun State are located at Abeokuta (De Crown Quarry, FW SAN He Concept Limited and Casagrande Construction Company, Odeda (Kepxing Nigeria Limited), Ogbere (Milatex Quarry) and Ago-Iwoye (China Civil Engineering Construction Coporation Nigeria Limited) (Figure 3.1). Granitic rock samples collected from Ogun State are similar in colour to those of Ondo State. They are mainly the felsic type though some are mafic. Over two hundred thousand workers are reported to be working in the quarries. Most of the products from Ogun State are used in Lagos State for construction.

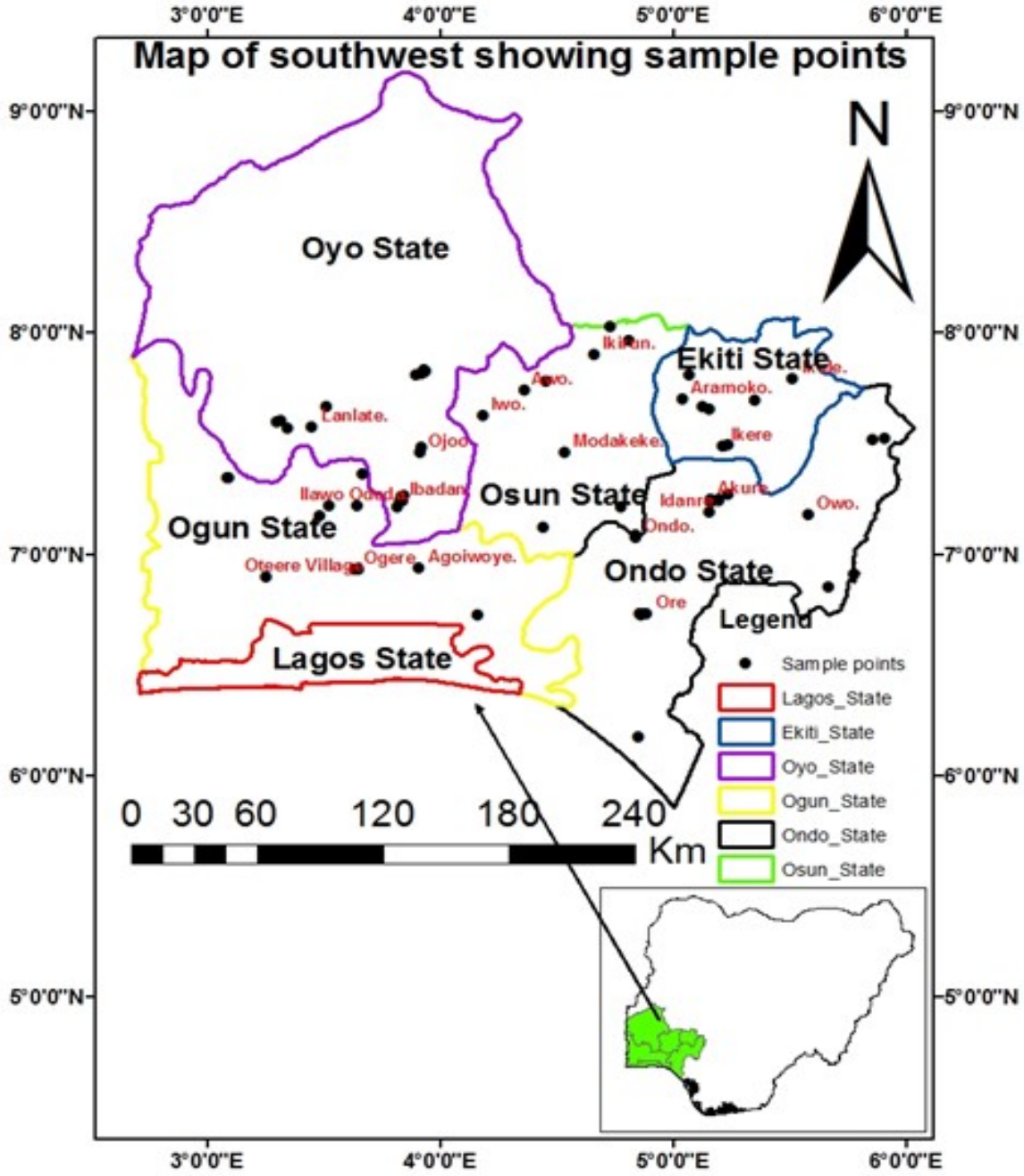

Fig. 3.1. Map of southwestern Nigeria showing sample collection places

Table 3.1. Number of samples from each state in southwest

State	Number of samples collected
Oyo	36
Osun	21
Ekiti	27
Ondo	69
Ogun	60

3.2 Thin section preparation

Thin section of the granitic rock samples collected were prepared and observed under a petrographic microscope for mineral identification described in sections 2.5 and 2.6. The procedure involved cutting achip or billet of 1 mm thick from the parent rock sample, using a thin-sectioning machine (model Logitech MP2A) of the Department of Geology, University of Ibadan. One surface of the billet was lapped on a glass lapping plate using water and carborundum. Also one surface of a glass slide on which to mount the billet was equally lapped until the slide becomes translucent. The billet and slide were then rinsed with water and dried on a hot plate at 50^{o}C after which the two lapped surfaces of the slide and billet were epoxied.

About an hour after, the billet on the slide was taken back to the cutting machine where the sample was reduced to 50 micron. This was eventually transferred to the jig of the electric Logitech lapping machine of model LP50. The sucking property of the jig, discussed in section 2.5.1, would not allow the samples to fall-off. Two of the prepared billets were put on it at a time. The samples were prevented from falling out during the lapping by the three stoppers made of diamond at the edge of the jig. The lapping attained the required thickness of30 μm as soon as the stoppers began to rub the lapping plate. The next stage was the identification of the mineral compositions under a petrographic microscope discussed in section 2.5.2.

3.3 Petrographic studies

Granitic rock samples collected from quarries in Oyo, Osun, Ekiti, Ondo and Ogun States in southwestern Nigeria (Table 3.1, Figure 3.1) were identified in hand specimen and subjected to petrographic studies using a transmited-light petrographic microscope described in sections 2.5, 2.51 and 2.52. The modal compositions of the minerals in the rocks were determined through visual estimation of the identified minerals. The relevant optical properties just as described in section 2.6 were used to identify the minerals present and consequently the rocks.

Each thin section produced was placed under the microscope for observation. The physical feature, such as, cleavage, colour and crystal structure of the minerals were used to identify the minerals. The structures and number of cleavages or the inclination angles of the cleavages of these minerals were used in the identification. These identification and determination of modal composition were carried out on thin sections produced from one half of the rock samples obtained from the quarries.Quartz

was identified with its colourless or white to light yellow and conchoidal fracture without pleochroism and alteration. Identification of microcline was possible with its pink andpale green or white colour, lath-shape, simple twins and poor set of cleavage. Under the polarised light, the plagioclase was detected through its white albite twining and cleavage characteristics. Brown colour, strong pleochroism and pleochroic haloes, cleavage and moderate relief revealed the presence and concentration of biotite in the study. Muscovite was colourless or silvery white flake with one perfect cleavage. Black and brown coloured apatite possesses eight-sided prismatic shape and cleavage which was used to identify it. Hornblende was also identified with its greenish-brown colour, strong pleochroism and characteristic cleavage intersection while opaque minerals were identified through their black colour and lack of cleavage.

Each identified mineral was visually estimated under the microscope and weighted upon the whole minerals counted. The fraction was multiplied by 100 expressing it in modal percentageby volume or percentage composition of the minerals.The modal percentage (volume %) concentrations of each mineral from the three samples obtained from each quarry represents the percentage concentrations of the minerals in the sampled quarry location.The identified major minerals and their influence on the activity concentrations of the natural radionuclides in the rock samples are presented and discussed in chapter four.

3.4 Gamma spectroscopic system

The method used in this work involves a gamma spectroscopic system consisting of a scintillation detector which is optically coupled to a photomultiplier tube and, connected through a preamplifier base to a Canberra multichannel analyzer. The detector is a 7.6 cm x 7.6 cm thallium activatedsodium iodide, NaI(Tl) manufactured by Bicorn (Model No 802 series) and shielded with 5 cm thick lead castle. The multichannel analyser, which is a Canberra series 10 plus is a complete gamma spectroscopic system having all functions needed for spectrometric analysis. The block diagram of the measuring system is presented in Figure 3.2. The detector, D, is a 7.6 cm x 7.6 cm NaI(T1) crystal located inside a lead castle C. It is interfaced with the MCA through a 50 Ω coaxial cable and has a positive signal output. The MCA system consists of an internal preamplifier (AMP), a 100 MHz Wilkinson type Analogue to Digital Converter (ADC), Control Logic (CL) with input and output

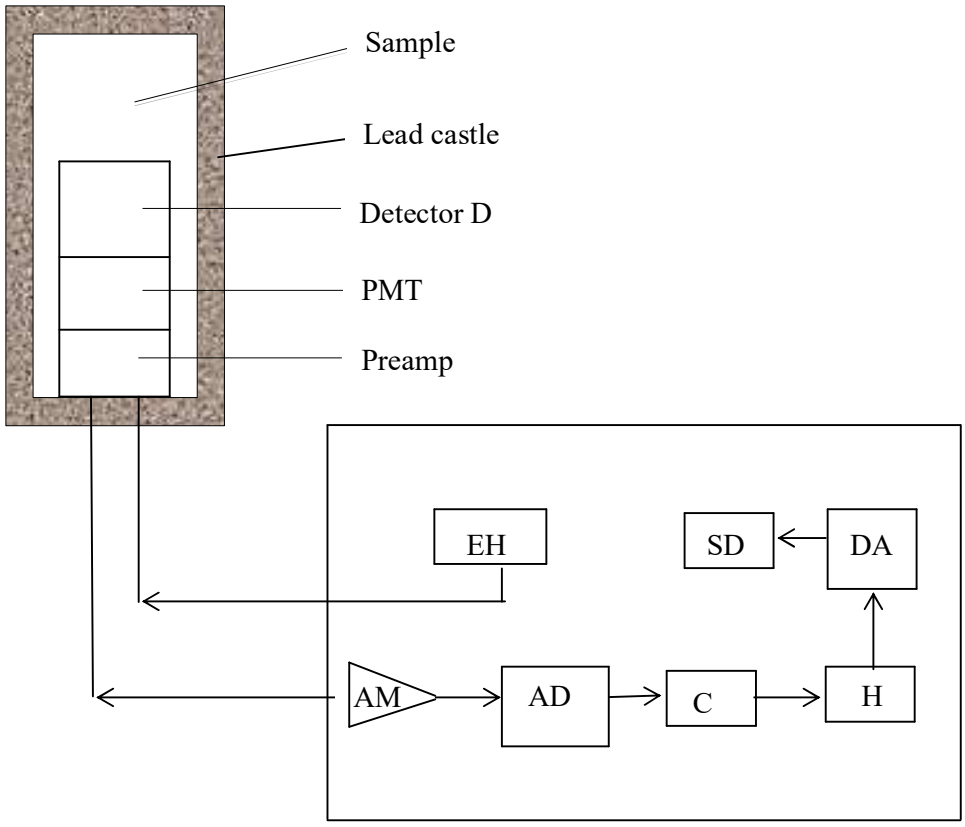

Fig. 3.2. A functional block diagram of the measuring system

devices and multichannel scaling input, 4K Memory (M), Display and Analysis Logic (DAL) and Screen Display (SD).

The system can be operated with batteries which can last up to 8 hours after being fully charged. This is a unique advantage because there is no fear of power interruption when main source is cut off and counting will not be interrupted. Apart from the preamplification of the PMT to receive measurable output voltage signal, the MCA has facilities to supply a stabilized extra high voltage (EHT) bias to the detector. Table 3.2 displays the settings used for all the measurements in this work.

3.5 Measurement of spectral characteristics

Spectral analysis was aimed at counting the number of pulses under each peak within a preset time. The counting involved the determination of the number of events occurring in the detector within the time, which was related to the radioactivity concentration of the source. Some preliminary measurements, such as, resolution, dependence of energy on channel number and efficiencies of the system at various gamma energies, were carried out. The investigations were carried out so as to evaluate the performance of the system and to calibrate it for the measurement of the radioactivity concentration of the rock samples.

Table 3.2. Setting of the equipment

	Setting		
AMP	INPUT – Positive,	SHAPING – Fast,	GAIN -3.50
SCA	Lower Level Discriminator L.L.D. – 0%,		Upper Level
	Discriminator (U.L.D. – 110%)		
ADC	GAIN – 1024, OFFSET – 0, ZERO – 0%,		PHA – ADD
HVPS	1000 V,	STABILIZER – OFF	

3.5.1 Resolution

The degree to which a photopeak approaches a line spectrum is termed the energy resolution of the system. It therefore shows the ability of the detection system to distinguish between two gamma ray energies that are close. To investigate this property qualitatively, a Co-60 source was counted for 300 s and the example of the spectrum obtainedis as shown in Figure 3.3 with clear separation of its two relatively close peaks of 1.17 and 1.33 MeV (ie 0.16 MeV difference). This demonstrates that the system has a good resolution under the defined settings.

A number of standard sources were used to measure quantitatively the resolution of the system. The following relation (3.1) was used to determine each resolution:

$$\text{Resolution, } R = \frac{FWHM}{Peak}\, x\ 100\% \qquad (3.1)$$

The different values of R obtained, due to different energies, are shown in Table 3.3. They conform with the values of R obtained by EI-Assaly (1981); Farai (1989) and Ademola (2003) for a 7.6 cm x 7.6 cm NaI(T1) detector. This indicates that the detector is in a good condition to carry out the measurements in this study. The graph of square of resolution, R^2 (in square of percentage, $\%^2$) versus inverse of gamma energy, E^{-1} (in MeV^{-1}) is shown in Figure 3.4. It is in conformity with the results of Farai (1989), confirming the reliability of the detector system for use in this work. The R^2 is inversely proportional to the gamma energy, E, as reflected in the Figure 3.4.

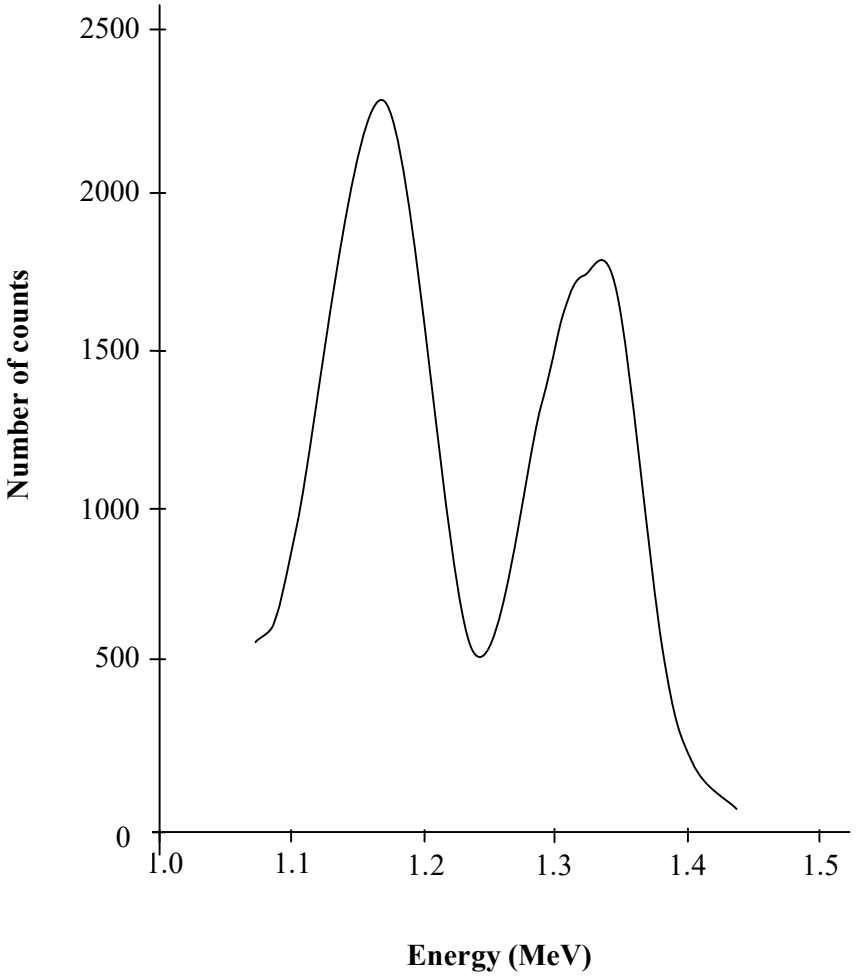

Fig. 3.3. A drawn resolution of two close peaks resulted from ^{60}Co

Table 3.3. Resolution of the detector at different gamma energies

Nuclides	Energy (E) (MeV)	Peak Location	Resolution R (%)		E^{-1} $(MeV)^{-1}$	R^2 $(\%)^2$
			Present work	Ademola (2003)		
^{22}Na	0.511	111	9.08	9.03	1.96	82.45
^{137}Cs	0.662	143	8.04	8.16	1.51	64.64
^{60}Co	1.173	25	6.18	6.33	0.85	38.19
^{22}Na	1.275	274	5.92	6.13	0.78	35.05
^{60}Co	1.332	288	5.57	5.55	0.75	31.02

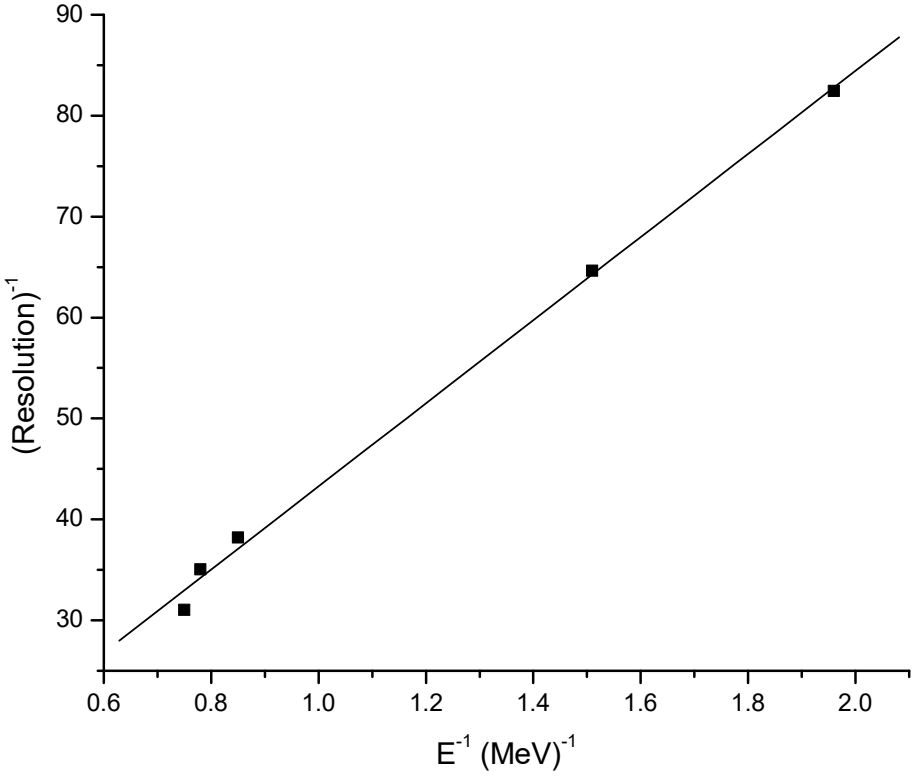

Fig. 3.4. Plot showing resolution-gamma energy dependence

3.5.2 Energy calibration

The size of a pulse output displayed and hence the channel number corresponding to it is directly proportional to the initial gamma energy producing the pulse through photoelectric interaction. This implies that it is possible to have a linear equation connecting the gamma energy with the corresponding channel number for a fixed spectrometric system setting. Such a linear equation, referred to as energy calibration equation, is determined for use in this work. This was achieved by determining the channel numbers for known gamma energies of some standard radionuclides from Nucleus Inc., Oak Ridge TN USA. The channel numbers with the corresponding gamma energies obtained from the treatment of the standard source are given in Table 3.4. The line of best fit involving energy, E in MeV and channel number, N was thereafter plotted to get the calibration line and hence to obtain a linear equation relating together gamma energy, E and channel number, N (Figure 3.5). This is as shown in equation 3.2.

$$E\ (MeV) = 0.004N - 0.023 \qquad (3.2)$$

It is possible, with this equation stored as an algorithm in the memory of the MCA of the system, to identify radionuclides in a field of mixed radionuclides of different gamma energies through their emitted gamma energies. With the channel number, N for any peak, the energy was known and in turn was traced to the radionuclide that emitted such energy for identification. This is because the detector system used does not have a library of its own.

Table 3.4. Energy with corresponding channel number

Radionuclides	Energy (MeV)	Channel number
^{22}Na	0.511	110
^{137}Cs	0.662	145
^{60}Co	1.173	257
^{22}Na	1.275	270
^{60}Co	1.332	286
^{40}K	1.46	310
^{214}Bi (^{226}Ra)	1.75	375
^{208}Tl (^{232}Th)	2.615	554

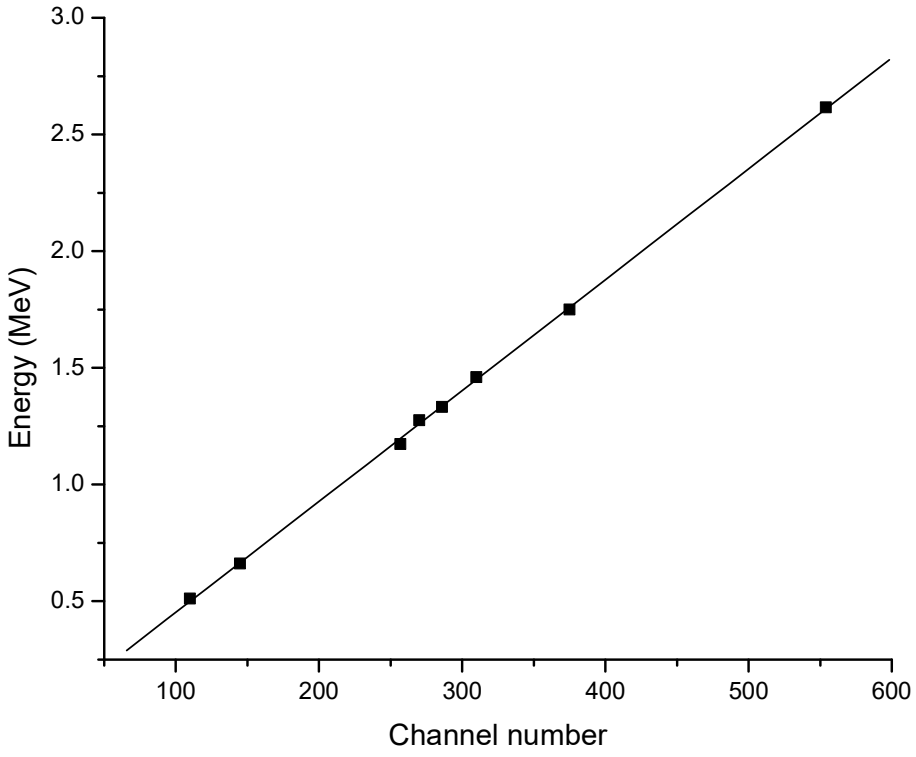

Fig. 3.5. Plot of energy dependence on channel number

3.5.3 Detection efficiency of the detector

The number of counts under a photopeak after a specified counting time is proportional to the activity of the source. The constant of proportionality is what is called detection efficiency of the detector. It is the ratio of total number of gamma emitted from the radiation source to the number of counts under the photopeak and proportional to source-detector geometry, intrinsic detector efficiency of the crystal and emission probability of the detected radiation. The detection efficiency of a gamma spectrometer is a direct relation between the count-rate under the photopeak and the intensity of the gamma photons of known activity at a constant geometry. The high density of a NaI(Tl) crystal, together with its high effective atomic number, results in a high detection efficiency.

In order to determine the detection efficiency, and hence, the activity of the source, a pulverized standard sample, prepared from Rocketdyne Laboratories, California, USA, which is traceable to a mixed standard gamma source (No 48722 – 356) by Analytics inc., Atlanta, Georgia was counted for 36,000 seconds at the suitable geometry for granite samples. The counted reference source was certified to have activity concentrations for ^{137}Cs, ^{40}K, ^{226}Ra and ^{232}Th and are presented in row 2 of Table 3.5. The detection efficiency ϵ_p for each of the four gamma energies also given in the Table 3.5, row 6, were determined by computing the net count C_r under each photopeak resulted from the reference source and relating it to the activity concentration A_r of the source using the relation (Luigi *et al*., 2000):

$$\epsilon_p = \frac{C_r}{tA_rYm} \quad (3.3)$$

where C_r is the net count above the background after counting a reference sample of known activity A_r (Bq/kg) and mass m (kg) for a time t(s) and Y is the gamma ray emission probability also known as gamma yield. Standard sources with gamma-ray energies in range 0.66 to 2.62 MeV were counted for the efficiency determination Figure 3.6 shows the plot of the detection efficiency as a function of the γ-ray energy thus obtained. The curve was used to interpolate the detection efficiency at any particular gamma energy within the limit.

Table 3.5. Efficiency at different gamma energies

Radionuclides	Activity, A_r (Bq/kg)	Energy (MeV)	Yield, Y	Counts	Efficiency, ϵ_p (x 10^{-2})
^{137}Cs	5.10	0.662	0.852	1943	6.21
^{40}K	578.40	1.460	0.107	9268	2.08
^{226}Ra	20.90	1.760	0.159	414	1.73
^{232}Th	10.47	2.614	0.358	291	1.08

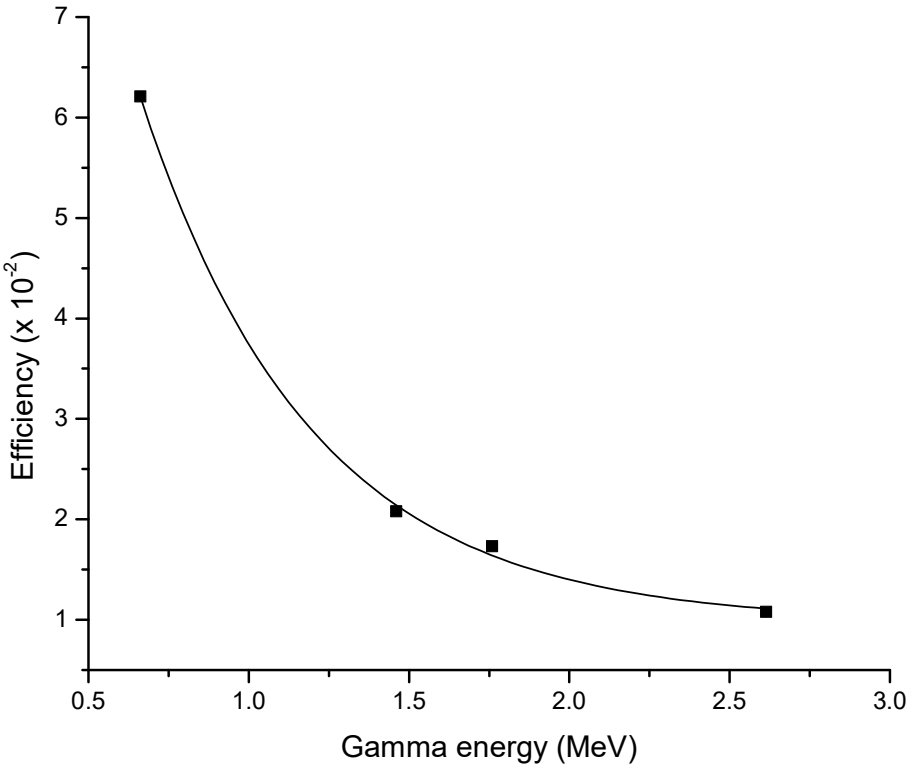

Fig. 3.6. Detection efficiency against energy

3.5.4 Lowest limit of detection

There is a limit to the value of activity of a sample that a gamma counter can measure. The minimum amount of sample activity concentration that can produce a large enough net-count to suggest the presence of the activity is referred to as lowest limit of detection (LLD) for the gamma detector. The limit is of a decisive activity point-value defined as the smallest count which can be interpreted that activity has been measured. The possibility of concluding falsely about the presence of the sample activity is a preselected statistical risk, governing the size of the quantity. (Pasternack and Harley, 1971; Ademola, 2003).

The lowest limit of detection(LLD) at 95% confidence level is given by equation 3.4 (USDOE, 2007):

$$LLD = 4.65\left(\frac{C_b}{t_b}\right)^{0.5} f \qquad (3.4)$$

where C_b is the background count under the full-energy peak due to the particular radionuclide, t_b is the time for the background count (36,000 seconds) and f is the factor used to convert count rate to activity which includes consideration of mass, counting efficiency, time of counting and gamma yield. The LLDs for the radionuclides in this work were calculated and the results are presented in Table 3.6. Any radionuclide content in the samples with activity below the LLD is regarded as being Below Detectable Limit of the system.

Table 3.6. Lowest limit of detection (LLD) for full-energy peaks of the radionuclides

Nuclide	Count (C_b)	f (Count/(Bq kg^{-1}))	LLD (Bq kg^{-1})
^{40}K	1894.77	16.02	17.09
^{226}Ra	70.28	19.81	4.07
^{232}Th	44.86	27.84	4.57

3.6 Sample preparation for gamma spectrometry

The same samples used for the gamma spectrometry were also used for the petrography in order to correlate the results from the two methods. The rock samples were divided into two, with each half prepared separately for the petrographic and gamma spectrometer investigations.

Two hundred grams (200 g) of the samples were packed and sealed in plastic containers of dimensions 7 cm in diameter and 8 cm in height verified to be non-radioactive. The sealed samples were left for 28 days for ^{226}Ra and ^{232}Th to attain secular radioactive equilibrium with their gamma emitting daughters. The weighted mean count of the three samples from each quarry location was determined.

3.6.1 Gamma spectrometry measurement

Because of the low radioactivity levels in the samples, the geometry of the counting assembly was maximized by placing the sample container directly on the NaI(Tl) detector and the counting time was set at 10 hours (360,000 s). The three primordial radionuclides were observed under photopeaks given in Table 3.5.

3.6.2 Background count

A large error can be introduced if environmental background radiation is not taken care of. Although the 5 cm thick lead castle has effectively reduced environmental radiation, electronic noise (dark current) within counting system can introduce significant error. The spurious counts due to dark current is unavoidable and hence, must be evaluated and taken care of in all the net counts. The count with an empty container was first obtained to evaluate contribution from background radiations.

3.7 Determination of activity concentration

The activity concentration A_s of each sample was obtained from a rearrangement of equation 3.3 as follows:

$$A_s = \frac{C_n}{t\epsilon_p Ym} \qquad (3.5)$$

where C_n is the net count above the background under each photopeak after a counting time t (360,000 s). The values of other quantities used in the computation are as given in Table 3.5. The weighted activity concentration of each radionuclide obtained from the three samples in each quarry represents the activity concentration of the

radionuclide in the sampling quarry location. The results are presented and discussed in chapter four.

The dataobtained in this section and that of section section 3.3, which are also presented and discussed in chapter four, form the basis for correlation between the activity concentration of the radionuclides and the mineral percentage composition of the rock samples.The evaluation of the data was carried out using a statistical package.

3.8 Statistical treatment of data

The analysis of data from gamma counting and data from petrographic microscope of the samples from selected quarries in southwest was carried out using Statistical Package for Social Sciences (SPSS), version 23.0,at 0.05 confidence level. The strength of correlation between the activity concentrations and the mineral concentrations of the rocks were examined for possible modeling. The observed and the predicted results from the analysis were obtained using general linear model to examine the reliability of the model. The principle component analysis was also carried out to identify the specific minerals contributing to the radioactivity concentrations of the radionuclides in the rocks. The use of the statistical analysis was also extended to radiological hazard evaluation from the data of activity concentrations obtained from the granitic rock samples collected from the selected quarries in southwestern Nigeria. All the results are presented and discussed in chapter four.

CHAPTER FOUR

RESULTS AND DISCUSSION

4.1 Mineral concentrations of quarry rocksamples

Example of the photomicrograph showing the pictures of the minerals under microscope is presented in Figure4.1.The minerals identified are Quartz, Microcline, Plagioclase, Biotite, Muscovite, Apatite, Hornblende and Opaque.

The weighted mean value from the quarry samples representing the percentage mineral composition of the granitic rock sample in each quarry are tabulated for each state with the range shown in Table 4.1. The represented values of the percentage compositions of the samples collected from various selected quarries in southwestern Nigeria are displayed in Appendix A(1) – A(5).The relationship between the mineral composition of the rock samples and the activity concentrations of the natural radionuclides in the rock samples was discussed in section 4.3.

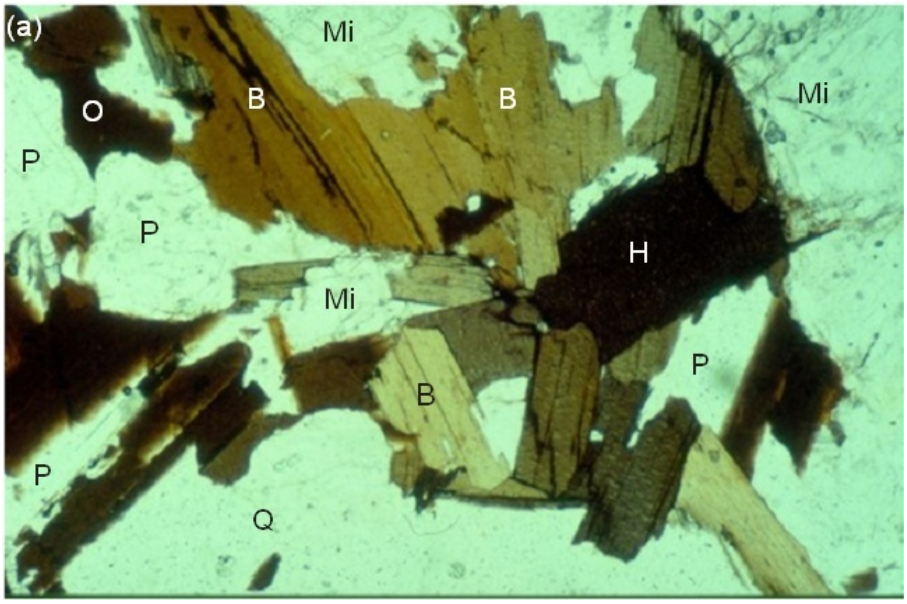

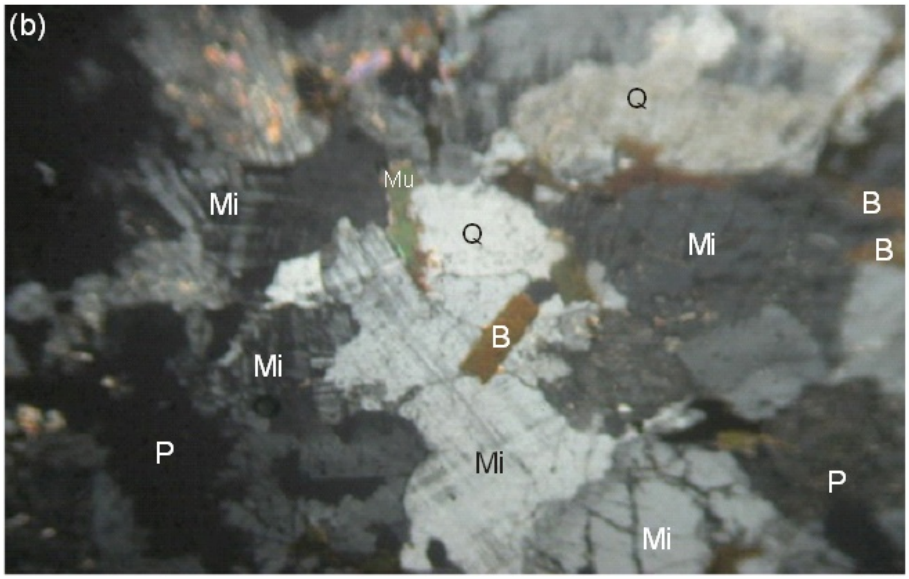

Fig. 4.1. Photomicrograph of granite from a quarry in (a) Ogun State and (b) Oyo State. (a) under plane polarized light (Mag. x 10); (b) under cross polarized light (Mag. x 10). Mi – Microcline, B – Biotite, O – Opaque, Q – Quartz, P – Plagioclase, Mu – Muscovite, H – Hornblende

Table 4.1. Percentage mineral compositions in the 213 rock samples

State	No of samples	Range of percentage mineral concentration			
		Quartz	Microcline	Plagioclase	Biotite
Oyo	36	10.75 - 19.11	6.56 - 14.53	21.37 - 36.67	18.94 - 25.31
Osun	21	11.56 - 18.86	5.15 -22.59	23.95 - 34.05	19.95 - 26.53
Ekiti	27	9.96 - 18.38	5.50 - 28.28	22.05 - 37.37	20.67 - 26.97
Ondo	69	8.31 - 19.24	4.68 - 17.6	25.58 - 37.82	19.27 - 35.85
Ogun	60	7.68 - 18.14	6.86 - 29.28	19.65 - 34.82	18.21 - 36.95

Table 4.1 (Contd.)

State	No of samples	Range of percentage mineral concentration			
		Muscovite	Apatite	Hornblende	Opaque
Oyo	36	1.06 - 4.96	0.85 - 4.02	3.54 - 14.86	1.22 - 5.18
Osun	21	0.81 - 4.93	0.85 - 4.05	0.13 - 14.34	1.12 - 5.18
Ekiti	27	0.89 - 4.14	1.01 - 3.85	0.02 - 14.15	2.04 - 5.17
Ondo	69	0.93 - 4.96	0.74 - 4.05	3.17 - 14.82	0.86 - 5.28
Ogun	60	0.89 - 5.14	0.77 - 4.05	0.25 - 15.20	0.80 - 5.22

4.2 Activity concentration

The rock samples in this study are not contaminated because of the absence of artificial radionuclide. This is discernible because no source of artificial radionuclide was detected in any of the rock samples considered in this study.

The values of activity concentration with the range in each state are presented in Table 4.2. The associated standard errors displayed in the Table signify the degree of spatial distribution of the radionuclides in each state. The activity concentrations of rock samples from each state is shown in Appendix B(1) – B(5).

The state mean values of the activity concentrations varied from 323.44 ± 146.95 to 450.81 ± 231.47, 12.70 ± 5.91 to 19.15 ± 16.47 and 64.02 ± 41.86 to 105.06 ± 57.03 $Bq.kg^{-1}$ for ^{40}K, ^{226}Ra and ^{232}Th respectively. All the mean values of the activity concentrations for the state were observed lower than the world average activity concentration values of ^{40}K (1104 $Bqkg^{-1}$), ^{226}Ra (78 $Bqkg^{-1}$) and ^{232}Th (111 $Bqkg^{-1}$) on granitic rock (UNSCEAR, 1993; Papadopoulos *et al*., 2012).Part of the factors causing variations in activity concentrations of the radionuclides in the granitic rock samples may be attributed to the radioactive mineral composition of the samples and also to the geological and geographical origins of the rocks (Kobeissi *et al*., 2013, Asaduzzaman *et al*., 2015). The concentration of ^{40}K was found highest in all the samples signifying its abundance in the granitic rock in southwest. The abundant nature of ^{40}K was also reported on soil and sediment samples by different researchers in the time past (Berekta and Mathew, 1985; Khater 1997; Roy *et al*., 2000; Xinwei *et al*., 2008; Farai and Isinkaye, 2009). The values of activity concentrations of ^{226}Ra were generally observed to be lower than those of ^{232}Th; this is in line with the report of Ramasamy *et al*. (2005) where they observed thorium/radium ratio to be approximately 1.5 in the earth's crust. The levels of concentration of ^{40}K, ^{226}Ra and ^{232}Th were all found highest in samples collected from Ogun state. High content of the radionuclides in Ogun state is supported by earlier report of high activity concentration of soil of Abeokuta, Ogun state by Farai and Jibiri (2000). Also, the lowest concentration level of ^{226}Ra was in samples from Ogun state while the lowest levels of ^{40}K and ^{232}Th were in samples from Oyo and Osun state respectively.

Table 4.2. Activity concentrations of ^{40}K, ^{226}Ra and ^{232}Th in all rocksamples

State	No of samples	Activity concentration (Bq kg^{-1})					
		^{40}K		^{226}Ra		^{232}Th	
		Range	Mean ± σ	Range	Mean ± σ	Range	Mean ± σ
Oyo	36	79.26 - 454.22	328.75±120.63	5.96 - 33.66	13.43±7.75	28.86 - 188.16	66.86±41.72
Osun	21	120.39 - 893.31	394.29±246.57	8.05 - 25.41	12.70±5.91	25.72 - 150.69	64.02±41.86
Ekiti	27	116.07 - 1115.08	426.29±291.40	6.79 - 33.02	17.59±8.30	47.74 - 156.42	83.54±31.29
Ondo	69	80.21 - 608.26	323.44±146.95	6.07 - 62.15	16.13±11.91	54.87 - 261.19	87.56±42.18
Ogun	60	134.07 - 1187.38	450.81±231.47	4.45 - 67.31	19.15±16.47	64.60 - 271.03	105.06±57.03

Note: σ = standard deviation

4.3 Correlation between percentage mineral composition and activity concentration

Using statistical package - SPSS 23.0 version, the strength of correlations existing between the activity concentrations and the mineral concentrations of the rocks were analysed. Regression lines of activity concentrations of the radionuclides against the mineral concentrations of the rock were obtained for each of the radionuclides of interest and the identified rock minerals. The plotting was carried out on data arising from samples collected from each state and southwest as a whole. Twenty-four scatter plots were obtained showing various patterns, ranging from null correlation to fairly negative and fairly positive correlations. Quite interestingly, scatter plots of Microcline and ^{40}K, Biotite and ^{226}Ra and Biotite and ^{232}Th, show strong positive correlation, indicating their good potential for use for the rapid evaluation of natural radionuclides in granitic rock. These plots are shown with their trend lines in Figures 4.2 – 4.4. Their respective correlation coefficients R, using SPSS package, 23.0 version, were estimated as 0.92, 0.86 and 0.87. The correlation coefficients of all the scatter plots are summarized in Tables 4.3 – 4.8.

The significant association of microcline and ^{40}K is confirmed by the reports of El-Arabii *et al*. (2007) and Gbadebo (2011). Non-uniformity in the variation of microcline with other radionuclides (^{232}Th and ^{226}Ra) as observed in the plots and Tables, suggests that only ^{40}K has affinity for K- rich feldspathic rocks, such as microcline and orthoclase ($KAlSi_3O_8$). However, orthoclase is crystallised at a higher temperature than microcline (Elueze and Bolarinwa, 2004). The temperature barrier therefore precludes the presence of orthoclase in the granitic samples collected in this study.The plagioclase, does not show good relationship with ^{40}K as shown in Table 4.3 – 4.8, because they are Na – Ca feldspars.

The positive relationship demonstrated by biotite with ^{226}Ra and ^{232}Th, is in agreement with the work of Nash (1979) who reported significant influence of biotite on the level of thorium and radium concentration in granitic rocks. The biotite and ^{232}Th correlation is a bit stronger than the one between biotite and ^{226}Ra. This could be due to the higher mobility of ^{226}Ra over ^{232}Th, which is capable of shifting radium position (El-Arabi *et al*., 2007). Also, the relationship between biotites and ^{40}K is weak and not useful in evaluation of the natural radionuclides.

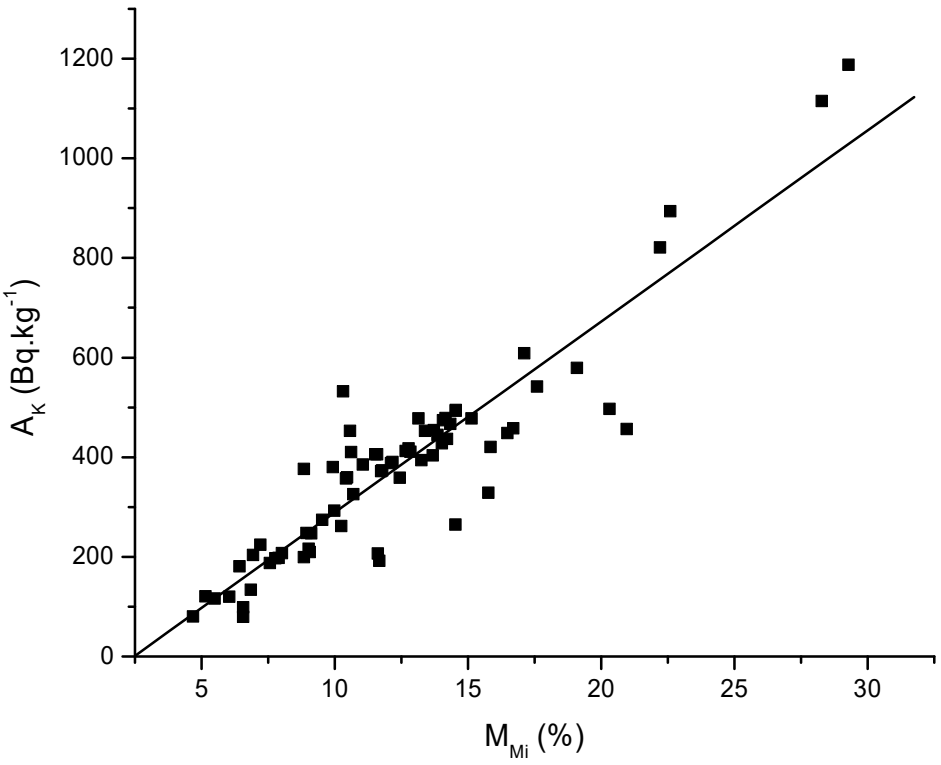

Fig. 4.2. Scatter plot of Concentration of ^{40}K and Microcline Composition

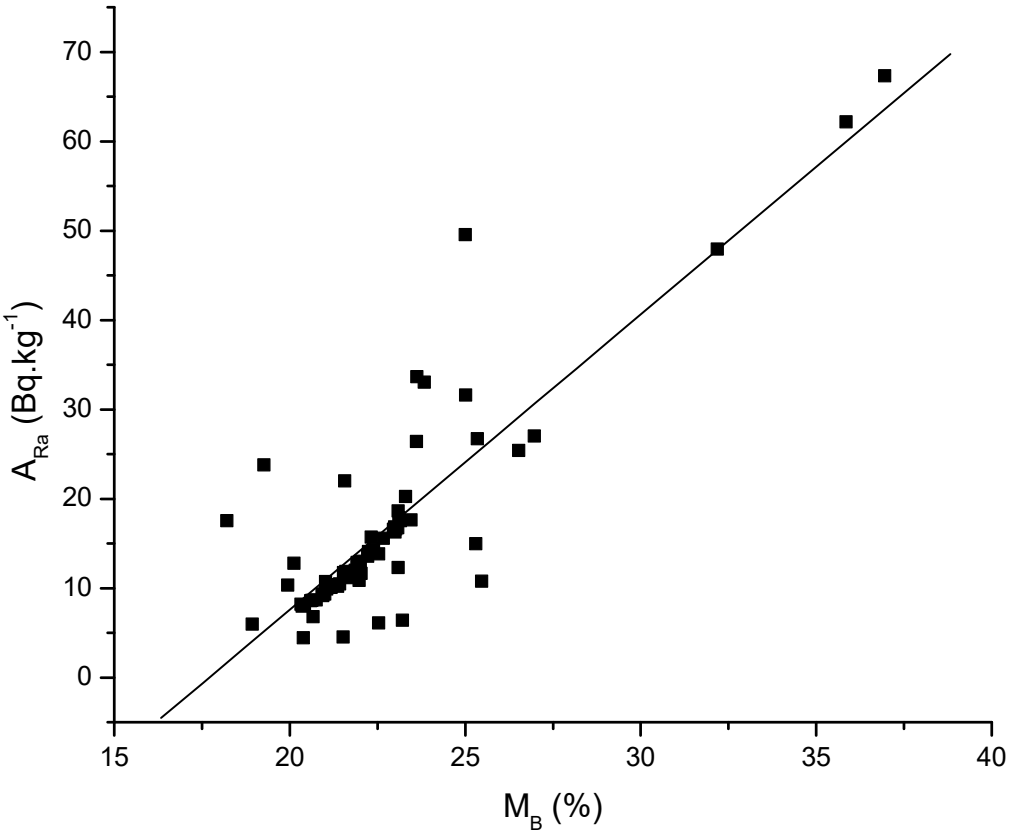

Fig. 4.3. Scatter plot of Concentration of ^{266}Ra and Biotite Composition

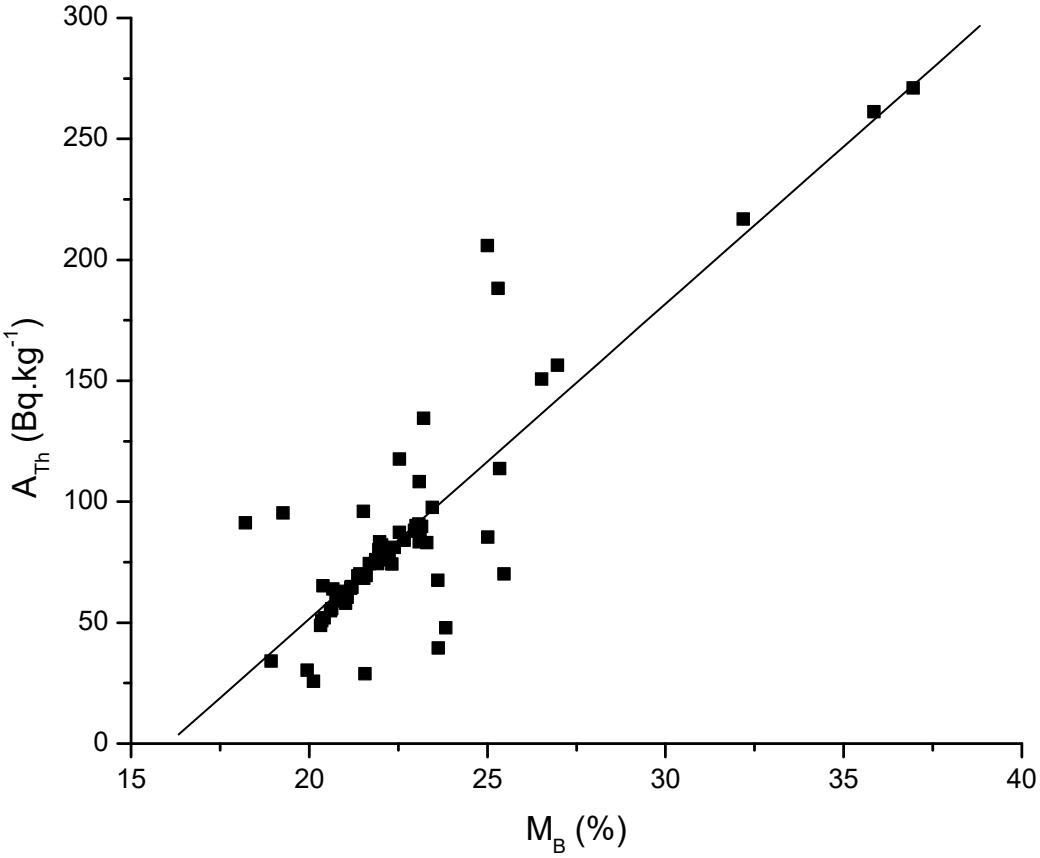

Fig. 4.4. Scatter plot of Concentration of ^{232}Th and Biotite Composition

Table 4.3. Correlation coefficients between mineral compositions and activity concentrations – Oyo State

Mineral	Correlation coefficients, R		
	^{40}K	^{226}Ra	^{232}Th
Quartz	-0.138	-0.474	-0.167
Microcline	+0.778*	-0.045	+0.130
Plagioclase	-0.329	-0.032	-0.807
Biotite	-0.190	+0.637*	+0.731*
Muscovite	-0.110	+0.527	+0.550
Apatite	+0.182	+0.176	+0.641
Hornblende	+0.141	-0.274	+0.498
Opaque	-0.352	+0.202	-0.663

*Useful relationships

Table 4.4. Correlation coefficients between mineral composition and activity concentrations – Osun State

Mineral	Correlation coefficients, R		
	^{40}K	^{226}Ra	^{232}Th
Quartz	-0.761	-0.709	-0.639
Microcline	+0.944*	+0.699	+0.567
Plagioclase	+0.480	+0.576	+0.566
Biotite	-0.765	+0.943*	+0.983*
Muscovite	-0.469	-0.295	-0.345
Apatite	-0.383	-0.212	+0.000
Hornblende	-0.867	-0.924	-0.857
Opaque	-0.359	-0.298	-0.387

*Useful relationships

Table 4.5. Correlation coefficients between mineral composition and activity concentrations – Ekiti State

Mineral	Correlation coefficients, R		
	^{40}K	^{40}K	^{40}K
Quartz	-0.663	-0.801	-0.480
Microcline	+0.925*	+0.598	+0.470
Plagioclase	-0.414	-0.202	-0.896
Biotite	+0.675	+0.808*	+0.793*
Muscovite	+0.055	+0.292	+0.652
Apatite	-0.288	-0.158	+0.335
Hornblende	-0.511	-0.326	+0.114
Opaque	-0.469	-0.387	-0.624

*Useful relationships

Table 4.6. Correlation coefficients between mineral composition and activity concentrations – Ondo State

Mineral	Correlation coefficients, R		
	^{40}K	^{226}Ra	^{232}Th
Quartz	-0.138	-0.032	-0.456
Microcline	+0.922*	-0.318	-0.200
Plagioclase	-0.235	-0.148	-0.184
Biotite	-0.355	+0.876*	+0.897*
Muscovite	-0.110	+0.071	+0.381
Apatite	-0.045	+0.272	+0.411
Hornblende	-0.077	-0.249	-0.071
Opaque	-0.308	-0.190	-0.257

*Useful relationships

Table 4.7. Correlation coefficients between mineral composition and activity concentrations – Ogun State

Mineral	Correlation coefficients, R		
	R	R	R
Quartz	-0.481	-0.483	-0.477
Microcline	+0.904*	+0.653	+0.604
Plagioclase	-0.341	-0.718	-0.719
Biotite	+0.464	+0.867*	+0.876*
Muscovite	-0.345	+0.000	+0.000
Apatite	-0.239	-0.055	-0.089
Hornblende	-0.517	-0.333	-0.286
Opaque	-0.367	-0.332	-0.326

*Useful relationships

Table 4.8. Correlation coefficients between mineral composition and activity concentrations – Southwest

Mineral	Correlation coefficients, R		
	^{40}K	^{226}Ra	^{232}Th
Quartz	-0.425	-0.352	-0.449
Microcline	+0.916*	+0.327	+0.329
Plagioclase	-0.290	-0.369	-0.497
Biotite	+0.268	+0.858*	+0.865*
Muscovite	-0.134	+0.130	+0.265
Apatite	-0.126	+0.100	+0.277
Hornblende	-0.420	-0.336	-0.176
Opaque	-0.359	-0.245	-0.414

*Useful relationships

Quartz, in most of the correlation coefficients, show negative relationship with the radionuclides. This might be a consequence of the presence of accessory minerals with quartz in the samples.

The modal composition (volume %) of muscovite and apatite in the granitic rocks are very low, that is, they occur as accessory minerals. Therefore, their contribution to radionuclide concentrations is low and as such indicated weak relationship with the radionuclides. Similarly, hornblende did not exhibit any noticeable link to the trend of radionuclides distributions as revealed by the values of correlation coefficients in Tables 4.3 – 4.8.

Opaque minerals in the granitic rocks are mainly oxides of iron (magnetite and ilmenite), which occur as accessory minerals in low percentage. They remained significantly constant, indicating little or no level of influence on the radionuclides. According to Bolarinwa (2005), opaque mineral is a component, comprising elements (Fe_3O_4 and $FeTiO_3$) and has no attachment to any of the radionuclides of interest in this study. This informed its passive contribution to the distributions of the radionuclides.

The microcline and biotite have been observed from Table 4.3 – 4.8 to have consistently demonstrated strong and positive correlation capable of predicting activity concentrations of the radionuclides. Hence the following equations relating activity concentrations and mineral concentrations were derived:

$$A_K = 38.04M_{Mi} - 90.58 \quad (4.1)$$

$$A_{Ra} = 3.30M_B - 58.50 \quad (4.2)$$

$$A_{Th} = 13.02M_B - 208.9 \quad (4.3)$$

where A_K,A_{Ra} and A_{Th} are activity concentrations (Bqkg^{-1}) of ^{40}K, ^{226}Ra and ^{232}Th respectively; M_{Mi} and M_B are percentage compositions of microcline and biotite. With the equations thus obtained, other radiological indices can be calculated.

To demonstrate the reliability of the above three equations in predicting the activity concentrations from the mineral composition, a sample was selected randomly from each of the 71 quarry sites. Scatter plots with measured and predicted values of activity concentrations against microcline and biotite contents are presented in Figures 4.6 - 4.7. The plots reflect strong and positive correlation between the measured and predicted values of the activity concentrations, confirming the dependability of the model in rapid evaluation of natural radionuclides in granitic rock.

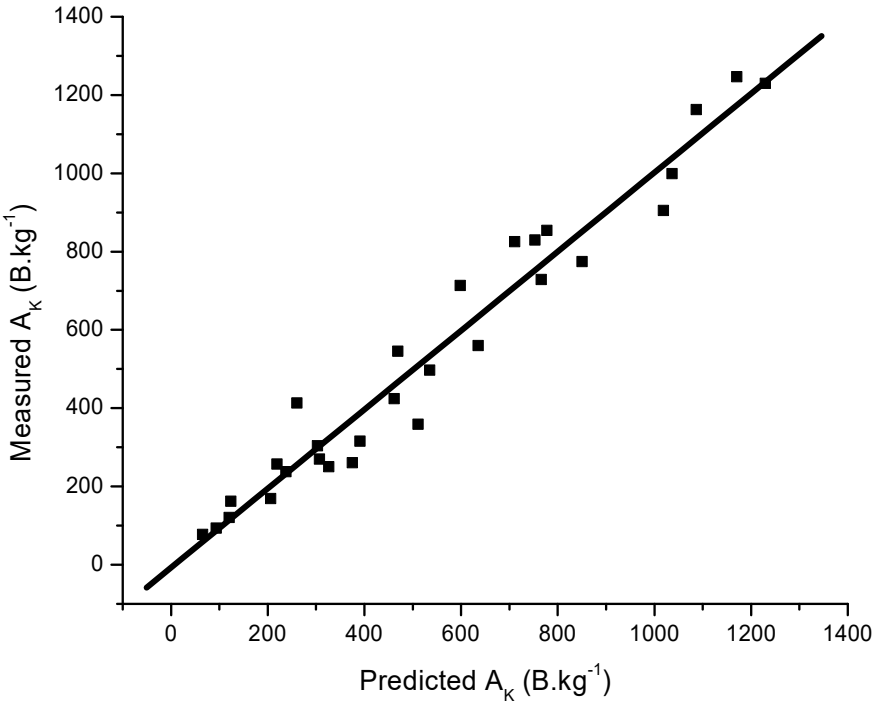

Fig. 4.5. Measured and predicted activity concentration values of ^{40}K

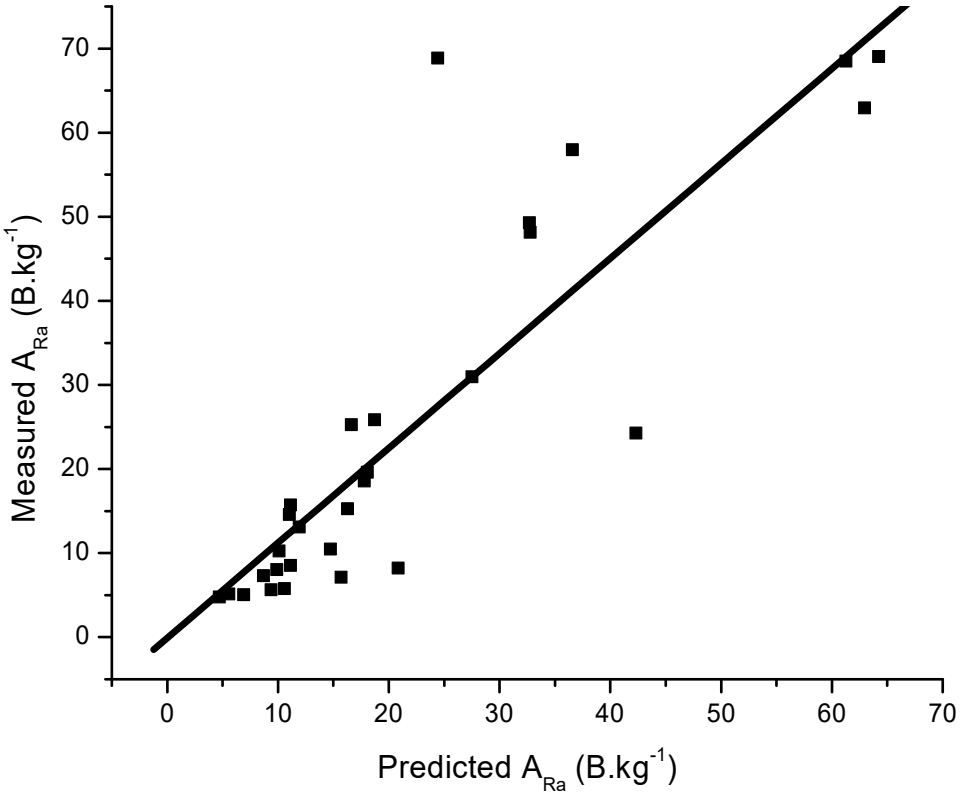

Fig. 4.6. Measured and predicted activity concentration values of ^{226}Ra

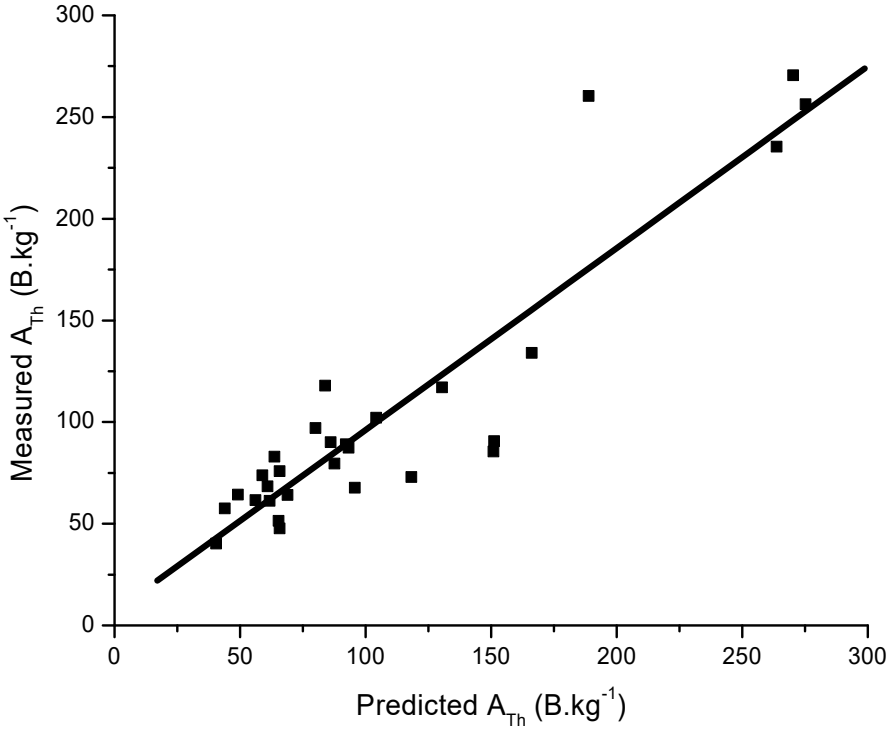

Fig. 4.7. Measured and predicted activity concentration values of ^{232}Th

4.4 Radium equivalent activities

Radiological effects caused by activity concentrations ^{40}K, ^{226}Ra and ^{232}Th in environmental samples are combined in terms of radium equivalent. This is expressed in equation 2.1 and was used to calculate the radium equivalent for all the granitic samples in this study. The range of values of radium equivalent for each State with their corresponding average values (and standard deviations expressing the spatial distribution of the values) are presented in Table 4.9, while details of the values are shown in Appendix C(1) to C(5) (column 1) for the five States considered in southwest. The average values of the radium equivalent activity of all the granitic rock samples (for all the States) are less than the recommended permissible limit of 370 $Bq.kg^{-1}$. They ranged between 134.23 $Bq.kg^{-1}$ for Oyo state and 203.91 $Bq.kg^{-1}$ for Ogun state. The highest mean value of radium equivalent for the states constitutes about 55 % of the limit. The variation of the mean values of the radium equivalent within the states in the study areain the granite samples is shown on the bar chart in Figure 4.8.

As discussed earlier (section 4.2), level of activity concentrations of ^{40}K is generally the highest among the three radionuclides followed by the concentrations of ^{232}Th and ^{226}Ra. However, it is worthy of note that only 17.34 % of radium equivalent level (Ra_{eq}) are contributed by ^{40}K while ^{232}Th contributed 72.96% and ^{226}Ra just 9.70 %. The contribution of ^{40}K to Ra_{eq} is lower than that of ^{232}Th because the effectiveness of the activity of ^{40}K on biological tissue is lower than that of ^{232}Th. Most of the values of the radium equivalent activity were found lower than the recommended maximum limit of 370 Bq kg^{-1}. However, the values of one sample (454.25 Bq kg^{-1}) and three samples (381.68, 449.00 and 499.02 Bq kg^{-1}) collected from Ondo and Ogun states, respectively exceeded the recommended maximum limit. The observed high values of radium equivalent in the samples could be attributed to high concentration of biotite, which was responsible for high activity concentration of ^{232}Th. The average values of radium equivalent on granites from different countries are compared with results from the present. The values of Ra_{eq} in this study area are comparable with the results from Taiwan, Greece, India and Ibadan as observed in Table 4.10.

Table 4.9. Ranges and mean values of radium equivalent (Ra_{eq})

State	No of samples	Ra_{eq} ($Bq.kg^{-1}$)		
		Lowest	Highest	Mean ± σ
Oyo	36	69.30	318.7	134.23±62.49
Osun	21	80.57	309.40	134.49±79.54
Ekiti	27	129.67	336.22	169.73±65.62
Ondo	69	129.23	454.25	166.10±67.24
Ogun	60	138.50	499.02	203.91±106.68

Note: σ = Standard deviation

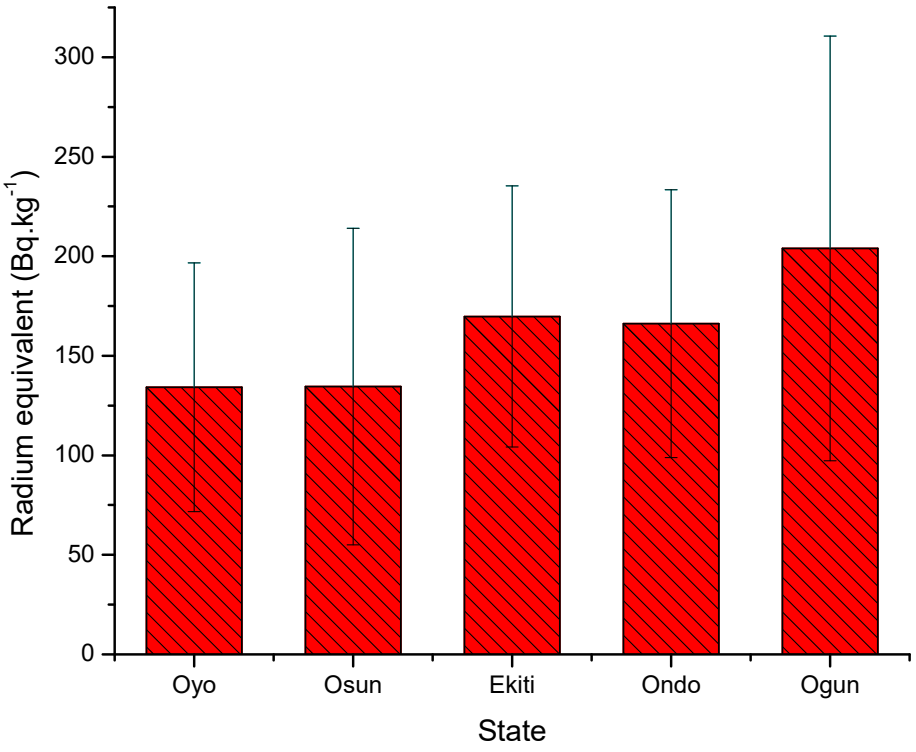

Fig. 4.8. Variation of mean radium equivalent for all rock samples

Table 4.10. Comparison between the mean activity concentrations and Ra_{eq} (Bq kg^{-1}) obtained and that of other works on granite from different countries

Countries	Radioactivity concentration (Bq/ kg)				References
	^{226}Ra	^{232}Th	^{40}K	Ra_{eq}	
SW, Nigeria	16.37	86.16	380.24	168.71	Present work
Ibadan, Nigeria	18.1	41.8	775.5	137.47	Jibiri and Okorie (2006)
India	82	11	1908	244.48	Sonkawade *et al*. (2008)
Hong Kong	202	140	1030	481.23	Yu *et al*. (1992)
Brazil	48.6	288.2	1335	563.01	Malanca *et al*. (1993)
France	90	80	1200	296.59	NEA-OECD (1989)
Egypt	556.76	73.36	1151.64	752.80	Arafa (2004)
Saudi Arabia	23±1.6	30.0±0.4	340±6.7	92.01	El-Taher (2012)
Taiwan	42	73	1055	227.44	Chen and Lin (1996)
Greece	67	95	1200	295.02	Stoulos *et al*. (2003)

4.5 Gamma absorbed dose rate in air in quarries

The activity concentration values shown in Appendix B(1) to B(5) and Table 4.2 do not directly translate to the predisposition of quarry workers in the environment to health risks. The health effects of radiation exposure is determined by radiation energy or dose absorbed by the individual. The dose in air at gonadal level of the quarry workers was discussed in section 2.6.2. Equation 2.2 was used to determine the absorbed gamma dose rates in air due to the activity concentration of each radionuclide in granitic samples from the selected quarries. This is necessary for assessment of radiological health hazard of the quarry workers due to exposure to ionizing radiation in the study area.

Because of large number of data involved, the range of absorbed dose values, with their respective mean values, due to the radionuclides concentration at different quarries in each of the states is presented in Table 4.11 with bar chart of mean values of absorbed dose rate for the states in Figure 4.9. However, all the values of the absorbed gamma dose rate in air obtained for all the granitic samples are presented in Appendix C1 – C5, column 2. The mean absorbed dose values for the states are: Oyo (61.43 ± 27.53 $nGy.h^{-1}$), Osun (62.07 ± 36.41 $nGy.h^{-1}$), Ekiti (77.78 ± 30.73 $nGy.h^{-1}$), Ondo (75.31 ± 29.33 $nGy.h^{-1}$) and Ogun (92.89 ± 47.94 $nGy.h^{-1}$) with that in Oyo state the least and Ogun state the highest. Though significantly lower than these values, earlier report of Farai and Jibiri (2000) on radioactivity level of the soil of Abeokuta, Ogun state showed support for high radionuclide concentration in the samples collected from the state. The significantly higher values in this work could be due to the reality that granites usually have relatively higher contents of natural radionuclides (UNSCEAR, 2000; Tzortzis *et al*., 2003). The absorbed dose rate levels in most of the granitic samples at the various quarries in each of the states in southwest, were higher than the world average external dose value of 59 $nGy.h^{-1}$ (UNSCEAR, 2000). These results are in line with the results obtained on selected granitic quarry sites in Ibadan, Nigeria by Jibiri and Okorie (2006). Also, relating the average activity concentrations of ^{40}K (1104 $Bqkg^{-1}$), ^{226}Ra (78 $Bqkg^{-1}$) and ^{232}Th (111 $Bqkg^{-1}$) in granitic rock samples reported by UNSCEAR (1993) and referenced by Papadopoulos *et al*. (2012) to absorbed dose, the world average absorbed dose rate value in air due to granitic rock samples was found to be 151.00 $nGy.h^{-1}$. The absorbed dose rate levels in granitic samples from Oyo (31.38 - 142.70) $nGy.h^{-1}$, Osun (38.71 - 142.57) $nGy.h^{-1}$, Ekiti

Table 4.11. Ranges and mean values of absorbed dose rate in air (D)

State	No of samples	Ra_{eq} ($nGy.h^{-1}$)		
		Lowest	Highest	Mean ± σ
Oyo	36	31.38	142.70	61.43 ± 27.53
Osun	21	38.71	142.57	62.07 ± 36.41
Ekiti	27	59.96	156.11	77.78 ± 30.73
Ondo	69	57.42	201.20	75.31 ± 29.33
Ogun	60	64.72	223.55	92.89 ± 47.94

Note: σ = Standard deviation

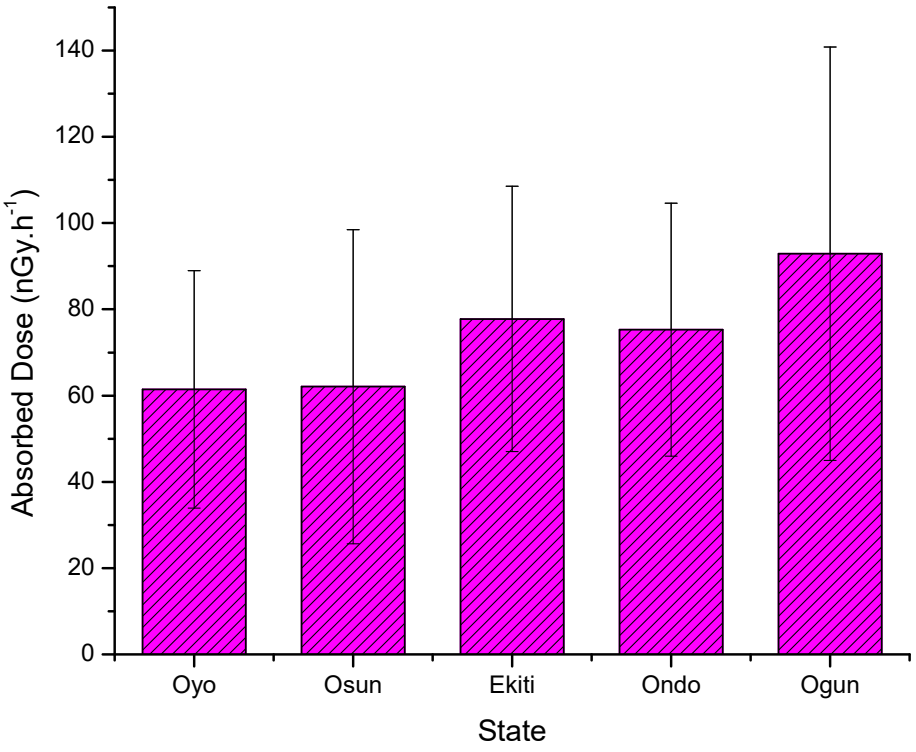

Fig. 4.9. Variation of mean absorbed gamma dose rate in air for all rock samples

(59.96 - 156.11) nGy.h-1, Ondo (57.42 - 201.20) nGy.h-1 and Ogun (64.72 - 223.55) nGy.h-1 are approximately within the average external dose limit of 151.00 nGy.h^{-1}estimated. It is observed that all of the state mean values of the absorbed dose were lower than the limit of 151.00 nGy.h^{-1} with only seven samples (Ekiti state – 1, Ondo state – 2 and Ogun state – 4) were found higher than the limit and constitute about 10 % of the granitic samples. However, the percentage of the exposed workers is significantly less than the estimated 10 % in this work because of some protective measures (discussed in section 2.5), which include shifting work arrangement, periodic public holidays and annual leaves granted to the workers. These values are, therefore seem not to pose any serious external and internal radiological health hazards to the workers.

4.6 Assessment of outdoor effective dose in quarries

Assessment of radiological hazard to man in the quarry industry is possible by relating absorbed gamma dose rates in air to human absorbed gamma dose. In assessing the effective dose to the quarry workers, the modified converting factor (involving conversion of absorbed dose rates (nGy.h^{-1}) in air to human dose (Sv.y^{-1}) and average time spent by the workers per year) discussed in section 2.6.3 was considered. The values of the annual effective dose were calculated for each granitic sample using equation 2.4 in the section 2.6.3 with range and weighted state mean values presented in Table 4.12. The values ranged between (Oyo – 0.05 and 0.25 mS y^{-1}), (Osun – 0.07 and 0.25 mS y^{-1}), (Ekiti – 0.10 and 0.27 mS y^{-1}), (Ondo – 0.10 and 0.35 mS y^{-1}) and (Ogun – 0.11 and 0.39 mS y^{-1}). These values are low when compared to those from earlier report of Jibiri and Okorie, (2006) on granite samples from some selected quarries in Ibadan.
The highest state mean value of 0.16 ± 0.08 mSv.y^{-1} was found with Ogun state. This is in agreement with high level of radioactivity of soil of the state (Abeokuta township) reported by Farai and Jibiri (2000). Oyo and Osun states have the least; 0.11 ± 0.05 mSv.y^{-1} and 0.11 ± 0.06 mSv.y^{-1}, respectively. High annual effective dose in Ogun state was due to the high content of biotite, rich in ^{232}Th, found with the granitic samples collected from Ogun state. High content of ^{232}Th in this work is expected because of earlier report of high level of ^{232}Th in Ogun state (Abeokuta township) (Ademola, 2003). The annual effective dose for samples collected from all the selected quarry locations are presented in Appendix C(1) to C(5), column 3. These values are considered to be low in comparison with natural external radiation of about 2000 μSv.y^{-}

[1] (2 $mSv.y^{-1}$) to which no harmful effects will occur directly (Wollenberg and Smith, 1990 and UNSCEAR, 2000). Furthermore, they are hazardously inconsequential when compared to the UNSCEAR global occupational maximum permissible level of 3000 $\mu Sv.y^{-1}$ (3 $mSv.y^{-1}$) for workers (UNEP, 2016; UNSCEAR, 2017).

Table 4.12. State ranges and means of annual effective dose (E) due to the rock samples

State	No of samples	E ($mSv.y^{-1}$)		
		Lowest	**Highest**	**Mean ± σ**
Oyo	36	0.05	0.25	0.11 ± 0.05
Osun	21	0.07	0.25	0.11 ± 0.06
Ekiti	27	0.10	0.27	0.14 ± 0.05
Ondo	69	0.10	0.35	0.13 ± 0.05
Ogun	60	0.11	0.39	0.16 ± 0.08

4.7 Assessment of occupational life-time cancer risk

It was assumed that long-term exposure of people to radiation have some risks of causing cancer. It is therefore pertinent to assess excess life time cancer risk associated with radionuclides in granitic samples collected from selected quarries in southwest. This will provide information regarding the statistics of possible cancer incidence among over half a million quarry workers in the study area. As a result, equation 2.5 in section 2.6.4 was used to estimate the excess life time cancer risk among the workers. Table 4.13 shows the range and mean of the values of excess life time cancer risk for each state while the values for samples collected from all the quarries are presented in Appendix C(1) – C(5), column 4.

All the values obtained for ELCR due to gamma radiation in the study area are below the UNSCEAR world average value of 1.45 x 10^{-3} (UNSCEAR, 2000; Aziz *et al*., 2014). The overall mean value of ELCR estimated for the granitic samples collected from the selected quarries is 0.47 x 10^{-3}, constituting about 32% of the UNSCEAR world average value. The highest mean value of ELCR (0.57 ± 0.29 x 10^{-3}) was observed in the granitic rock samples from Ogun state (Table 4.13), while Oyo state recorded the lowest mean value of 0.38 ± 0.17 x 10^{-3}. The highest risk values obtained from Ogun state is due to relatively high composition of microcline and biotite minerals which are closely associated with ^{40}K, ^{226}Ra and ^{232}Th.

The value of mean probability of cancer for each state shown in Table 4.13, Column 5, was translated to the cancer death probability (CDP) and presented in Column 6 of the same Table 4.13. For comparison between the cancer death probability values obtained in this study and 0.1% cancer death probability toleranceof ICRP discussed in section 2.9.4, a bar chart of the mean values of the cancer death probability for the states in the study area and the tolerable value by ICRP was plotted and exhibited in Figure 4.10. Ogun state has the highest mean value of the cancer death probability within the states under consideration with 0.057%, while Oyo and Osun states have the same value of 0.038% as the lowest. It can be observed from the plot that all of the CDP mean values are low when compared to ICRP tolerance value, suggesting no appreciable health hazard is attached to working with the granitic rocks in the study area.

Because of the scanty information available on ELCR assessment of granitic rock samples in particular, the value obtained in this study is therefore compared to the available ELCR data from gamma radiation emanating from different environmental

Table 4.13. Ranges and mean values of excess lifetime cancer risks (ELCR) and cancer death probability (CDP) for workers

State	No of samples	ELCR x 10^{-3}			CDP %
		Lowest	Highest	Mean ± σ	
Oyo	36	0.19	0.87	0.38 ± 0.17	0.038
Osun	21	0.24	0.87	0.38 ± 0.22	0.038
Ekiti	27	0.36	0.95	0.47 ± 0.19	0.047
Ondo	69	0.35	1.22	0.46 ± 0.18	0.046
Ogun	60	0.39	1.36	0.57 ± 0.29	0.057
ICRP	-	-	-	-	0.10

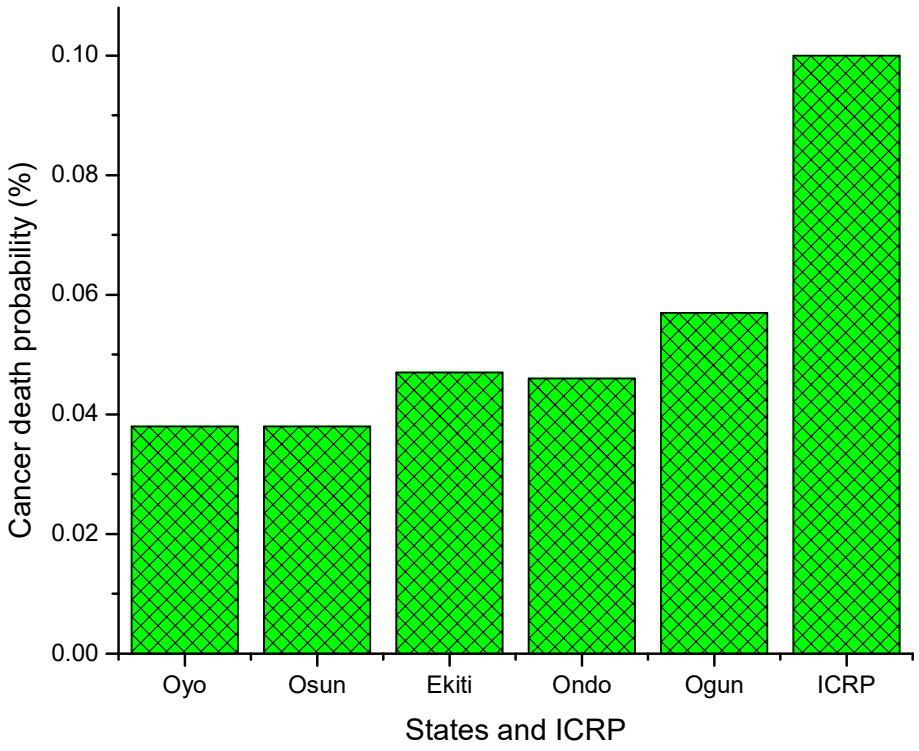

Fig. 4.10. Comparison of cancer death probability (CDP) (%) for workers in selected quarries in southwest with that of ICRP

sources (Table 4.14). Comparing with the report of Thabayneh and Jazzar (2012) in the same Table 4.14, where insignificant carcinogenic risk to the population were reported despite the seemingly high value observed, the value of ELCR obtained in this work is inconsequential to both the workers and the populace. Summarily, the values of excess lifetime cancer risk due to natural radionuclides in granitic rock samples from the selected quarry sites in southwestern Nigeria indicated that the risk of people developing cancer due to the granites in the study area is within the tolerable level.

Table 4.14. Comparison of excess lifetime cancer risk determined in various studies

Study area	Sample medium	ELCR x 10^{-3}	References
Southwest, Nigeria	Granite	0.47	Present study
Egypt	Granite	0.65	Fares *et al*. (2012)
Pakistan	Sediment	3.21	Aziz *et al*.(2014)
South Africa	Soil	0.77	Raymond and Victor(2016)
Akwa Ibom, Nigeria	Dumpsite	0.63	Essien and Essiett(2016)
Niger Delta, Nigeria	Soil	0.07	Emelue *et al*.(2014)
Yalova, Turkey	Soil	0.42	Kapdan, *et al*. (2011)
Tulkarem Province-Palestine	Soil	0.95	Thabayneh and Jazzar(2012)
East Coast, Tamilnadu, India	Sediment	0.37	Chandramohan *et al*. (2015)

CHAPTER FIVE

CONCLUSIONS AND RECOMMENDATIONS

5.1 Conclusions

Granite samples from selected quarry sites in Oyo, Osun, Ekiti, Ondo and Ogun states in southwestern Nigeria were assessed for activity concentrations of primordial radionuclides ^{40}K, ^{226}Ra and ^{232}Th using gamma ray spectrometer. The granite samples were also analysed for identification of mineral compositions of the rock by using petrographic method. The activity concentrations of the radionuclides were correlated with the percentage mineral compositions of the rock samples using SPSS package, 23.0 version, to evaluate the strength of correlation between activity concentrations of the radionuclides and mineral concentrations of the rock. The activity concentrations determined were used to assess the radiological parameters of the granite samples from southwestern Nigeria. The following conclusions were drawn from the results obtained:

1. Eight mineral compositions were identified and their modal percentage composition ranged between 19.65 and 37.82 for plagioclase, 4.68 and 29.28 for microcline, 18.21 and 36.95 for biotite, 7.68 and 19.24 for quartz, 0.81 and 5.14 for muscovite, 0.02 and 15.20 for hornblende, 0.74 and 4.05 for apatite; and 0.80 and 5.28 for opaque.
2. The weighted mean of activity concentrations of ^{40}K, ^{226}Ra and ^{232}Th of the granite samples in the study areas varied from 323.44±146.95 to 450.81±231.47, 12.70±5.91 to 19.15±16.47 $Bq.kg^{-1}$ and 64.02±41.86 to105.06±57.03 $Bq.kg^{-1}$for ^{40}K, ^{226}Ra and ^{232}Th, respectively.
3. Significant correlations were observed between microcline and ^{40}K (R = 0.92), between biotite and ^{226}Ra (R = 0.86); and between biotite and ^{232}Th (R = 0.87). Regression equations indicate good feasibility for the use of mineral compositions of microcline and biotite for a quick estimation of radioactivity concentrations of the primordial radionuclides in quarry rocks.

4. The estimated Ra_{eq} for the states exhibited upper limit value of 203.91 ± 106.68 $Bq.kg^{-1}$ in Ogun state and lower limit of 134.23 ± 62.49 $Bq.kg^{-1}$ in Oyo state. There was no mean value that exceeded the recommended limit of 370 $Bq.kg^{-1}$ indicating that the radiological health hazard associatedwith using the granitic rocks in building construction can be regarded insignificant.
5. The lowest mean absorbed dose rate value was observed in Oyo state result, with a value of 61.43 ± 27.53 $nGy.h^{-1}$, while the highest was from Ogun state with 92.89 ± 47.94 $nGy.h^{-1}$. All the state mean values of the absorbed dose were lower than the limit of 151.00 $nGy.h^{-1}$, based on the UNSCEAR average activity concentration data arising from world granitic samples, while only about 10 % of the whole samples exceeded the limit. The percentage of the exposed workers, however, is significantly less than the estimated 10 % because of the protective measures put in place. From radiological point of view, these levels are seen to be low to have any serious health implications.
6. The computed mean annual effective dose values ranged from 0.11 ± 0.05 $mSv.y^{-1}$ to 0.16 ± 0.08 $mSv.y^{-1}$ for Oyo and Ogun states respectively. No sample from the study area showed annual effective dose exceeding the occupational limit of 3 $mSv.y^{-1}$ and no state mean value of annual effective dose exceeded public limit value of 1 $mSv.y^{-1}$.
7. The maximum mean ELCR ($0.57 \pm 0.29 \times 10^{-3}$) value was recorded in granitic rock from Ogun State, while the minimum value ($0.38 \pm 0.17 \times 10^{-3}$) was recorded in Oyo State. All the values of ELCR were below the UNSCEAR total average value of 1.45×10^{-3}.
8. The associated occupational death probability was determined to be about 0.05%, which is lower than the deduced ICRP limit of 0.1%. The radiation doses and its effects therefore may not preclude the workings and usage of the granitic rocks in southwestern Nigeria, which is considered invaluable to the socio-economic development of the various states in the region.

5.2 Recommendations

Whole-rock geochemistry and micro-chemical studies of the granitic rocks can be used alongside petrographic studies employed in the present study to shed more light on the source of the radionuclide activity. This would also enable comparative study between petrographic and chemical methods. The degree of reliability on the

estimated results in this study could be established from the outcome of such comparative study. Adequate funding would be required to carry out these expensive geochemical analyses outside Nigeria.

Similar study could be extended to other regions where granite quarry workers could be exposed to gamma radiation beyond the recommended limit as a consequence of their occupational activities.

REFERENCES

Ademola, J. A. 2003. Radiation dose from concrete building blocks in eight cities of southwestern Nigeria. PhD. Thesis, Dept. of Physics. University of Ibadan. Xiv + 159pp.

Akande, J. M. and Idris, M. A. 2005. Environmental effects of gemstone exploitation in Ofiki, Oyo state, Nigeria. *Journal of Science and Engineering Technology* 12.1: 5858-5869.

Arafa, W. 2004. Specific activity and hazards of granite samples collected from the Eastern Desert of Egypt. *Journal of Environmental Radioactivity*, 75: 315-327.

Asaduzzaman, K., Mannan, F., Khandaker, M. U., Farook, M. S., Elkezza, A., Amin, Y. B. M., Sharma, S. and Kassim, H. B. A. 2015. Assessment of natural radioactivity levels and potential radiological risks of common building materials used in Bangladeshi dwellings. *PLoS ONE 10(10): e0140667. doi:10.1371/journal.pone.0140667*.

Aziz, A. Q., Shahina, T., Kamal, U. D., Shahid, M., Chiara, C. and Abdul, W. 2014. Evaluation of excessive lifetime cancer risk due to natural radioactivity in the rivers sediments of northern Pakistan. *Journal of Radiation Research and Applied Sciences*,7: 438-447.

Beck, H. L. Decompo, J. and Gologak, J. 1972. *In-situ* Ge(Li) and NaI(Tl) gamma ray spectrometry. *Report 258 health and safety laboratory, US Atomic Energy Commission: Washington, DC*.

BEIR, 1990. Health effects of exposure to low levels of ionizing radiation.*National Research Council, Committee on the Biological Effects of Ionizing Radiations Natl Acad. Press, Washington, DC*.

Beretka, J. and Mathew, P. J. 1985. Natural radioactivity of Australian building materials, industrial wastes and by- products. *Health Physics*, 48: 87-95.

Birks, J. B. 1964. *The Theory and Practice of Scintillation Counting*. Oxford, Pergamon press.

Bolarinwa, A. T. 2005. Geology and Mineral Resources Development. In Okonjo, K. O. and Bolarinwa, A. T. (Eds.) *Science, Industry and Mankind.* Ibadan: General Studies Programme, University of Ibadan. 143-160pp. ISBN 978-068-745-9.

Bruce, W. H. 2009. Natural Radioactivity in the Geologic Environment. *National Nuclear Security Administration Nevada Site Office CEMP* 28 July.

Cetin, E., Altinsoy, N. and Orgun, Y. 2012. Natural radioactivity levels of granites used in Turkey. *Radiation Protection Dosimetry*, 151.2: 299–305.

Chandramohan, J., Tholkappian, M., Harikrishnan, N. and Ravisankar, R. 2015. Assessment of Activity Concentrations of Radionuclides from Pattipulam to Devanampattinam of East Coast of Tamilnadu, India using Gamma Ray Spectrometry. *International Journal of Frontiers in Science and Technology* 3.3: 59-68.

Chen, C. J. and Lin, Y. M. 1996. Assessment of building materials for compliance with regulations of radar operation centre.. *Environment International*,22. 221-226.

Davou, L. C. and Mangset, W. E. 2015. Evaluation of radiation hazard indices and excess lifetime cancer risk due to natural radioactivity in mined tailings in some locations in Jos Plateau state Nigeria. *Journal of Applied Physics* 7.1: 67-72.

Ekwueme, B. N. 1994. Structural features of Obudu Plateau, Bamenda Massif, eastern Nigeria: preliminary interpretation. *Journal of Mining and Geology*, 30.1: 45-59.

Ekwueme, B. N., 1987. Structural orientation and Precambrian deformational episode of Uwet area, Oban Massif, southeast, Nigeria. *Precambrian Research* 34: 269-289.

El Mezayen, A. M., El-Balakssy, S. S., Abdel Ghani, I. M. and El-Setouhy, M. S. 2017. Radioactive mineralization of granitic rocks and their surrounding stream sediments at Gabal Rei El-Garrah area, Central Eastern Desert, Egypt. *Nature and Science*, 15.12: 61-78.

El-Arabi, A. M., Abbady, A. G. E. and Khalifa, I. H. 2007. Radioactive and geochemistry characteristics of the garnetiferous granite of Um Sleimat erea, Egypt. *Online Journal of Earth Sciences* 1.1: 9-20.

El-Assaly, F. M. 1981. Methods of calibrating a gamma spectrometer for a qualitative and quantitative analysis of low-level radioactivity in geological and environmental samples. *Proceedings of a Symposium, Berlin (West), IAEA, Vienna*.

El-Taher, A. 2012. Assessment of natural radioactivity levels and radiation hazards for building materials used in qassim area, saudi Arabia. *Environmental Physics* 57.3: 726-735.

Elueze, A. A. and Bolarinwa, A. T. 2004. Petrochemistry and petrogenesis of granitic gneisses of Abeokuta area, southwestern Nigeria. *Journal of Mining and Geology,* 40.1: 1-8.

Emelue, H. U., Jibiri, N. N. and Eke, B. C. 2014. Excess lifetime cancer risk due to gamma radiation in and around Warri refining and petrochemical company in Niger Delta. *Nigeria British Journal of Medicine & Medical Research* 4.13: 2590-2598.

Essien, I. E. and Essiett, A. A. 2016. Investigation of radiological hazards within Uyo metropolis central dumpsite, Akwa Ibom state, Nigeria. *International Journal of Scientific and Research Publications* 6.5: 687–691.

Fano, U. 1953. Geometrical characterization of nuclear state and the theory of angular correlations. *Physical Review* 90: 577-579.

Farai, I. P. 1989. Radon-222 survey in groundwater and its assessment for radiological hazards and seismic monitoring in Nigeria. PhD. Thesis. Dept. of Physics. University of Ibadan.

Farai, I. P. and Isinkaye, M. O. 2009. Radiological safety assessment of surface-water dam sediments used as building material in southwestern Nigeria. *Journal of Radiological Protection* 29: 85-93.

Farai, I. P. and Jibiri, N. N. 2000. Baseline studies of terrestrial outdoor gamma dose rate levels in Nigeria. *Radiation Protection Dosimetry* 88: 247-254.

Farai, I. P., Okwunakwe, C. E. and Makinde, O. S. 2007. Gamma spectroscopic assay of soil samples from waste dump sites in PortHarcourt, Nigeria. *Journal of Applied Radiation and Isotopes*. 66.6-7: 850-854.

Fares, S., Ashour, A., El-Ashry, M. and Abd El-Rahma, M. 2012. Gamma radiation hazards and risks associated with wastes from granite rock cutting and polishing industries in Egypt. *Ядерна та радіаційна безпека* 1.53: 64–73.

Florou, H. and Kritidis, P. 1992. Gamma radiation measurements and dose rate in the coastal areas of a volcanic island, Aegean Sea, Greece. *Radiation Protection Dosimetry* 45.1: 277-279.

Gbadebo, A. M., 2011. Natural Radionuclides Distribution in the Granitic Rocks and Soils of Abandoned Quarry Sites, Abeokuta, Southwestern Nigeria. *Asian Journal of Applied Sciences* 4: 176-185.

Halliday, D. and Resnick, R. 2007. *Fundamentals of Physics*. 8th Edition, United State of America, John Wiley & Sons, 943 – 947.

Harb, S., Abbady, A., El-Kamel, A., Saleh, I. I. and Abd El-Mageed, A. I. 2012. Natural radioactivity and their radiological effects for different types of rocks from Egypt. *Radiation Physics and Chemistry* 81: 221–225.

Henry, D.T. and Yokuts, I.P. 1997. *Rocks and minerals*. 1-37. Available at http://www.kean.edu

IAEA, 1996. Methods for estimating the probability of cancer from occupational radiation exposure. *International Atomic Energy Agency, IAEA-TECDOC*870.

Ibrahim, A., Toyin, A. and Sanni, Z. J. 2015. Geological Characteristics and Petrographic Analysis of Rocks of Ado-Awaiye and its Environs, Southwestern Nigeria. *International Journal of Applied Science and Mathematical Theory* 1.8: 28-47.

ICRP, 1991. Recommendations of the International Commission on Radiological Protection in 1990. *ICRP Publication 60. Annals of ICRP* 21: 1-3.

ICRP, 2005. Dose limits and risks (Chapter 4). *Based onPublication 60 - Radiation protection*.

ICRP, 2012. Compendium of dose coefficients based on ICRP Publication 60. *ICRP Publication 119. Annals of ICRP 41* (Supplement).

Jibiri, N. N. and Okorie, R. O. 2006. Radionuclide concentrations and gamma radiation dose rate levels in selected granite quarry sites in Ibadan, Southwestern Nigeria. *Nigerian Journal of Science* 40: 19-28.

Kapdan, E., Varinlioglu, A. and Karahan, G. 2011. Radioactivity levels and health risks due to radionuclides in the soil of Yalova, northwestern Turkey. *International Journal of Environmental Research* 5.4: 837-846.

Kerur, B. R., Rajeshwari, T., Sharanabasappa, Kumar, S. A., Narayani, K., Rekkha, A. K. and Hanumaiah, B. 2010. Radioactivity levels in rocks of north Karnataka, India. *Indian Journal of Pure & Applied Physics* 48: 809–812.

Khater, A. E. M. 1997. Radiological study on the environmental behavior of some radionuclides in the aquatic ecosystem. PhD. Thesis. Cairo University. Egypt.

Killeen, P. G., Pflug, K. A., Zelmer, R. L. and McCallum, B. A. 1994. Advantages and disadvantages of gamma-ray spectral logging for site characterization of low-level radioactive waste.

Kobeissi, M. A., El-Samad, O. and Rachidi, I. 2013. Health assessment of natural radioactivity and radon exhalation rate in granites used as building materials in Lebanon. *Radiation Protection Dosimetry* 153: 342-351.

Kowalski, E. 1970. *Nuclear electronics*. 1st ed. Heidberg, New York. Springer-Varlay, Berlin.

Lilley, J. S. 2001. *Nuclear Physics: principles and applications*. 1st ed. England: John Wiley and Sons Ltd. 1-393.

Luigi, B., M. Aurizio, B., Giorgio, M., Renato, M. and Serena, R. 2000. Radioactivity in raw materials and end products in the Italian ceramic industries. *Journal of Environmental Radioactivity* 47: 171-181.

Makanjuola, A. A. 1982. A review of the petrology of the Nigerian syenites. *Journal of Mining and Geology* 19.2: 1-14.

Malanca, A., Pessina, V., Dallara, G., Luce, C. N. and Gaidol, L. 1993. Natural radioactivity in building materials from the Brazilian state of Espirito Santo. *Applied Radiation and Isotopes* 46: 1387–1392.

Martin, A. and Harbison, S. A. 1979. *An introduction to radiation protection*. 2nd ed. London. Chapman and Hall limited.

Mason, B., and Moore, C. B. 1982. *Principles of geochemistry*, 4th ed. New York, Wiley.

Michael, M. R., Peter, R. and Jurgen, R. 2012. *Guide to thin section microscopy*. http://www.minsocam.org/msa/openaccess_publications/Thin_Section_Microscopy_2_rdcd_eng.pdf. 1-127.

Nash, J. T. 1979. Uranium and thorium in granitic rocks of northeastern Washington and northern Idaho, with comments on uranium resource potential. *United states department of the interior Geological survey* 1-39.

NBS, 2015. National Bureau of Statistics: *Nigerian Mining and Quarrying Sector* 1-20

NEA-OECD, 1989. Nuclear Energy Agency. Exposure to radiation from natural radioactivity in building materials. *Report by NEA Group of Experts, Organisation for Economic Coperation and Development (OECD), Paris*.

NGSA, 2004. Revised Geological Map of Nigeria. *Nigeria Geological Survey Agency* (NGSA).

NPC, 2006. National Population Commission. 2006 Population and housing census of the federal republic of Nigeria. *Pirority Table* 1: 1-326.

Obed, R. I. 2004. Soil radioactivity concentration and cancer incidence in eighteen cities in Nigeria. PhD. Thesis. Dept. of Physics. University of Ibadan.Xiv + 171pp.

Obiora, S. C., 2005. *Field Descriptions of Hard Rocks, with examples from the Nigerian Basement Complex*. Enugu. SNAAP Press (Nigeria) Limited.

Obiora, S. C., 2006. Petrology and geotectonic setting of basement complex rocks around Ogoja, southeastern Nigeria. *Ghana Journal of Science* 46: 13-25.

OECD, 2011. Organisation for Economic Co-operation and Development, Evolution of ICRP Recommendations 1977, 1990 and 2007.*NEA 6920*. https://www.oecd-nea.org/rp/pubs/2011/6920-icrp-recommendations.pdf.

Olarewaju, V. O. 1987. Charnockite granite association in SW Nigeria: rapakivi granite type and charnockite plutonism in Nigeria. *Journal of African Earth Sciences* 6.1: 67-77.

Onyeagocha, A. C., 1984. Petrology and geologic history of northwestern Akwanga in Northern Nigeria. *Journal of African Earth Sciences* 2.1: 41-50.

Osasan, S. K. 2009. Economic assessment of granite quarrying in Oyo state, Nigeria. *Journal of Engineering and Applied Sciences* 4.2: 135-140.

Oyawoye, M. O., 1964. The geology of the Nigerian basement complex: A survey of our present knowledge of them. *Nigerian Mining, Geological and Metallurgical Society* 1: 87-102.

Oyawoye, M. O., 1972. The basement complex of Nigeria in Dessauvagie, T. F. J. and Whiteman, A. J. eds. *African Geology*. Ibadan University Press, Ibadan, 67-99.

Papadopoulos, A. Christofides, G. Koroneos, A. Stoulos, S. and Papastefanou, C. 2012. Natural radioactivity and dose assessment of granitic rocks from the Atticocycladic Zone (Greece).*An International Journal of Mineralogy*, 81.3: 301-311.

Pasternack, B. S. and Harley, N. H. 1971. Detection limits for radionuclides in the analysis of multicomponent gamma ray spectrometer data. *Nuclear Instruments and Methods* 91: 533-540.

Paulo, E. O. L. 2015. Thorium and its future importance for nuclear energy generation. *International Nuclear Atlantic Conference*, Brazil, October 4-9.

Pourimani, R., Ghahri, R. and Zare, M. R. 2014. Natural radioactivity concentrations in Alvand granitic rocks in Hamadan, Iran. *Radiation Protection and Environment* 37: 132-142.

Rafique, M., Rehman, H., Matiullah, Malik, F., Rajput, M. U., Rahman, S. U. and Rathore, M. H. 2011. Assessment of radiological hazards due to soil and

building materials used in Mirpur Azad Kashmir; Pakistan. Iran. *Journal of Radiation Researches* 9.2: 77-87.

Rahaman, M. A. 1976. Review of basement geology of southwestern Nigeria in Kogbe, C. A., ed., *Geology of Nigeria. Elizabethan Press, Lagos*, pp. 41-57.

Ramasamy, V., Ponnusamy, V., Hemalatha, J., Meenakshisundaram, V., and Gajendiran, V. 2005. Evaluation of natural radioactivity and radiological hazards caused by different marbles of India. *Indian Journal of Pure and Applied Physics* 43: 815-820.

Raymond, L. N. and Victor, M. T. 2016. Lifetime cancer risk due to gamma radioactivity in soils from Tudor Shaft mine environs, South Africa. *Journal of Radiation Research and Applied Sciences* 9: 310-315.

Read, H. H. (2004). *Rutley's elements of mineralogy*. 27th ed. London, Thomas Murby & Co.

Robin, G. 2010. *Igneous Rocks and Processes: A Practical Guide*. London, John Wiley & Sons, Ltd., 1-477.

Rodrigo, O. B. and Carlos, R. A. 2009. Radioactivity of rocks from the geological formations belonging to the Tibagi River hydrographic basin. *International Nuclear Atlantic Conference Brazil, September 27 to October 2*.

Roy, S., Alam, M. S., Miah, F. K. and Alam, B. 2000. Concentrations of naturally occurring radionuclides and fission products in brick samples fabricated and used in and around greater Dhaka city. *Radiation Protection Dosimetry* 88: 255-260.

Shams, A. M. I, Uosif, M. A. M. and Abd El-Salam, L. M. 2012. Natural radionuclide concentrations in granite rocks in Aswan and central-southern eastern desert, Egypt and their radiological implications. *Radiation Protection Dosimetry*, 150.4: 488 – 495.

Sonkawade, R. G., Kant, K., Muralithar, S., Kumar, R. and Ramola, R. C. 2008. Natural radioactivity in common building construction and radiation shielding materials. *Atmospheric Environment* 42.9: 2254-2259.

Stoulos, S., Manolopoulou, M. and Papastefanou, C. 2003. Assessment of natural radiation exposure and radon exhalation from building materials in Greece. *Journal of Environmental Radioactivity* 69.3: 225-240.

Taskin, H., Karavus, M., Ay, P., Topuzoglu, A., Hidiroglu, S. and Karahan, G. 2009. Radionuclide concentrations in soil and lifetime cancer risk due to gamma

radioactivity in Kirklareli, Turkey. *Journal of Environmental Radiation* 100.1: 49-53.

Tauli-Corpuz, V., 1997. The globalization of mining and its impact and challenges for women. *A paper presented at conference on 'Women and Mining', Baguio city, 20-28 January*.

Thabayneh, K. M. and Jazzar, M. M. 2012. Natural Radioactivity Levels and Estimation of Radiation Exposure in Environmental Soil Samples from Tulkarem Province-Palestine. *Open Journal of Soil Science* 2: 7-16.

Tzortzis, M., Tsertos, H., Christofides, S. and Christodoulides, G. 2003. Gamma radiation measurements and dose rates in commercially-used natural tiling rocks (granites). *Journal of Environmental Radioactivity* 70: 223-235.

Ugbogu, O. C., Ohakwe, J. and Foltescu, V. 2009. Occurrence of Respiratory and Skin problems among manual stone quarrying workers. Mera. *African Journal of Respiratory Medicine* 23–26.

UNEP, 1997. United Nations Environment Programme. Governing Council of the United Nations Environment Programme. Available at https://wedocs.unep.org/bitstream.

UNEP, 2016. United Nations Environment Programme. Radiation effects and sources. *A report based on findings of the United Nations Scientific Committee on the Effects of Atomic Radiation and on the United Nations Environment Programme, Austria*.

UNSCEAR, 1982. United Nations Scientific Committee on the Effects of Atomic Radiation. Ionizing Radiation: Sources and Biological Effects. *Report to the General Assembly, with Annexes. United Nations, New York*.

UNSCEAR, 1988. United Nations Scientific Committee on the effects of Atomic Radiation. Sources, effects and risks of ionizing radiation. *Report to the general assembly with annexes, United Nations, NewYork*.

UNSCEAR, 1993. United Nations Scientific Committee on the Effects of Atomic Radiation Sources and Effects of Ionising Radiation *Vol. I. United Nations, New York.*

UNSCEAR, 2000. United Nations Scientific Committee on the Effects of Atomic Radiation. Sources, Effects and Risks of Ionizing Radiation. *Report to the General Assembly with annex B*, *United Nations, New*

York.http://www.unscear.org/docs/publications/2000/UNSCEAR_2000_Annex-B.pdf

UNSCEAR, 2010. United Nations Scientific Committee on the Effects of Atomic Radiation. Sources and Effects of Ionizing Radiation. *UNSCEAR 2008 Report to the General Assembly with Scientific Annexes*, Volume I, New York.

UNSCEAR, 2017. United Nations Scientific Committee on the Effects of Atomic Radiation. Sources, Effects and Risk of Ionizing Radiation. *UNSCEAR 2016 Report to the General Assembly with Scientific Annexes A,B, C and D*, New York.

Uosif, M. A. M. and Abdel-Salam, L. M. 2011. An assessment of the external radiological impact in granites and pegmatite in central eastern desert in Egypt with elevated natural radioactivity. *Radion Protection Dosimetry*, 147.3: 467-473.

Uosif, M. A. M. Shams, A.M. I. and Abd El-Salam M. 2015. Measurement of natural radioactivity in granites and its quartz-bearing gold at El-Fawakhir area (Central Eastern Desert), Egypt.*Journal of Radiation Research and Applied Sciences*, 8.3: 393-398.

USDOE,1992. Procedure Manual Environmental. Measurement Laboratory. *United State Department of Energy* HASL-300, P4, 5. 29,27th ed.

Wase, A. and George, V. V.2015. *Petrographic Examination Methods*.U.S.A. BUEHLER, a division of Illinois Tool Works.

Wollenberg, H. A. and Smith, R. A. 1990. A geochemical assessment of terrestrial gamma-ray absorbed dose rates. *Health Physics*, 58: 183-189.

Xinwei, Xiaolan, Z. and Fengling, W. 2008. Natural radioactivity in sediment of Wei River, China. *Environ. Geol*. 53: 1483-1489.

Yu, K. N., Guan, Z. J., Stokes, M. J. and Young, E. C. M. 1992. The assessment of the natural radiation dose committed to the Hong Kong people. *Journal of Environmental Radioactivity* 17: 31-48.

APPENDIX A

Table A1. Mineral concentrations of the granite samples from Oyo State

Quarry location	Mineral concentrations (%)							
	Q	**Mi**	**P**	**B**	**Mu**	**A**	**H**	**O**
EQNL, Ibadan	17.24	11.59	36.67	21.07	4.67	3.05	3.54	2.17
ECC, Ibadan.	16.24	14.22	34.75	18.94	1.06	0.93	9.25	4.61
NCCQ, Iresapa	18.25	7.57	28.72	22.67	4.83	3.89	12.85	1.22
RATCON, Ibadan.	19.11	6.56	34.62	21.57	1.93	0.85	10.18	5.18
NSCE, Ibadan.	16.25	12.78	29.72	20.36	1.83	2.89	13.08	3.09
ICC, Ibadan.	12.46	9.02	33.32	22.25	3.78	3.05	11.15	4.97
BSAPQ, Ibadan	17.25	10.62	30.72	20.92	2.83	1.89	12.68	3.09
CC, Ojoo	16.26	11.52	27.27	21.42	3.12	2.87	14.15	3.39
LADSON, Oyo	10.75	14.53	31.93	23.63	4.93	3.19	5.95	5.09
QCC, Lanlate.	18.26	9.53	33.82	20.76	2.12	1.87	8.78	4.86
WCC, Ibadan.	15.24	13.25	31.75	20.32	1.06	2.93	10.65	4.8
DCC, Ibadan.	14.48	13.72	21.37	25.31	4.96	4.02	14.86	1.28

NB: Q = Quartz; Mi = Microcline; P = Plagioclase; B = Biotite; Mu = Muscovite; A = Apatite; H = Hornblende and O = Opaque

Table A2. Mineral concentrations of the granite samples from Osun State

Quarry location	Mineral concentrations (%)							
	Q	**Mi**	**P**	**B**	**Mu**	**A**	**H**	**O**
ICC, Iwo.	18.14	11.62	27.52	20.42	1.93	0.85	14.34	5.18
AQC, Modakeke.	11.56	22.59	34.05	26.53	0.81	1.09	0.13	3.24
BCC, Otan.	12.21	15.85	26.92	21.02	4.92	3.9	14.06	1.12
TJ CC, Ijabe.	17.25	12.17	33.43	19.95	0.83	0.89	10.39	5.09
WCC, Awo	18.86	10.7	25.35	20.64	2.81	3.05	13.62	4.97
ICC, Ikirun.	17.32	5.15	29.64	22.01	4.90	4.05	12.71	4.22
ACC, Awo.	16.75	13.68	23.95	20.13	4.93	1.26	14.22	5.08

NB: Q = Quartz; Mi = Microcline; P = Plagioclase; B = Biotite; Mu = Muscovite; A = Apatite; H = Hornblende and O = Opaque

Table A3. Mineral concentrations of the granite samples from Ekiti State

Quarry location	Mineral concentrations (%)							
	Q	**Mi**	**P**	**B**	**Mu**	**A**	**H**	**O**
QCC, Igbemo	18.02	16.7	34.7	21.54	3.14	2.84	0.02	3.04
ACC, Ikole.	17.21	5.50	29.30	22.39	3.52	2.90	14.06	5.12
MSTCC, Ikere.	18.38	12.67	34.58	20.67	0.89	1.28	7.16	4.37
RQI, Ijero,	9.96	28.28	22.05	26.97	4.14	2.44	4.12	2.04
GEOVERTRAG, Iyin.	11.21	14.54	27.82	23.46	3.12	1.87	14.15	3.83
BCCN Igede	15.82	7.78	31.05	23.16	4.14	3.85	11.98	2.22
DCC, Ikere	16.31	9.93	32.55	21.17	1.96	2.05	10.86	5.17
KCC, Ikere	17.21	9.07	26.22	23.3	4.12	2.9	13.84	3.34
FQ, Aramoko.	10.68	20.96	37.37	23.84	1.79	1.01	0.25	4.1

NB: Q = Quartz; Mi = Microcline; P = Plagioclase; B = Biotite; Mu = Muscovite; A = Apatite; H = Hornblende and O = Opaque

Table A4. Mineral concentrations of the granite samples from Ondo State

Quarry location	Mineral concentrations (%)							
	Q	**Mi**	**P**	**B**	**Mu**	**A**	**H**	**O**
PQL, Ifon	18.57	11.75	34.33	21.87	2.85	3.74	5.67	1.22
RAVCON, Ore	19.14	6.56	37.82	22.33	0.93	0.85	7.53	4.84
ATLOR, Akure	19.24	4.68	30.25	25.02	3.12	2.93	10.21	4.55
FCC, Akure.	18.96	17.6	28.05	20.96	2.14	2.86	8.39	1.04
SNL, Ore.	16.6	6.04	28.36	23	3.85	3.74	13.19	5.22
NDECL, Ise Akoko	18.38	7.9	35.58	22.99	2.89	1.77	9.26	1.23
ZFM, Akure	8.96	12.45	31.73	22.54	4.14	3.84	13.3	3.04
DNL, Akure	18.38	13.15	25.58	21.06	2.92	4.05	9.66	5.2
SC, Iboropa Akoko	14.75	8.84	28.77	22.96	4.93	2.19	12.47	5.09
SW, Akure	18.24	6.94	31.16	21.96	3.06	1.93	11.91	4.8
SETRACO, Ore.	18.86	8.85	36.35	21.18	4.54	2.08	3.17	4.97
Hispanic, Ifon	10.31	8.02	32.67	23.11	2.85	3.05	14.82	5.17
GENC, Ondo.	18.88	10.47	26.35	23.09	2.81	2.06	14.18	2.16
MOL Ltd., Ore	16.21	17.11	32.83	20.6	1.94	0.9	7.29	3.12
NC, Ifon	12.25	9.12	29.39	35.85	3.83	3.89	3.58	2.09
SCC, Elegbeka-Ifon.	16.68	14.16	35.01	20.95	1.96	1.01	4.95	5.28
BALLESTER, Ifon	14.03	15.77	27.93	19.27	4.12	3.87	14.15	0.86
LCL, Idanre.	8.31	12.12	29.56	23.21	4.96	4.05	14.62	3.17
DCC, Ose-Owo	18.38	6.43	36.58	21.98	3.45	2.84	5.14	5.2
OSAC, Akure	18.28	9.98	34.13	23.61	1.85	3.74	4.19	4.22
SQL, Owo.	15.57	11.79	31.33	21.19	2.27	0.74	11.89	5.22
ECC, Akure	16.24	14.07	30.65	21	1.77	2.87	9.24	4.16
Japaul, Elegbaka.	9.86	15.14	28.97	21.6	4.81	3.08	14.57	1.97

NB: Q = Quartz; Mi = Microcline; P = Plagioclase; B = Biotite; Mu = Muscovite; A = Apatite; H = Hornblende and O = Opaque

Table A5. Mineral concentrations of the granite samples from Ogun State

Quarry location	Mineral concentrations (%)							
	Q	Mi	P	B	Mu	A	H	O
CCECC, Agoiwoye.	14.26	11.06	25.46	22.22	4.83	3.89	14.19	4.09
MRL, Alagutan.	12.21	14.02	28.82	25.47	2.92	2.9	8.54	5.12
DCQ, Eye Village.	18.14	13.86	33.82	18.21	3.93	3.85	6.01	2.18
CHEC, Agbede Village.	15.85	10.58	29.65	21.92	2.77	3.87	14.2	1.16
MRC, Oloparun.	15.18	16.48	33.87	21.93	4.96	3.05	0.25	4.28
RATCON, Ogere	17.24	7.21	29.65	22.04	4.77	3.57	11.36	4.16
PGC, Iwaye.	10.54	14.34	34.37	23.08	4.83	3.01	6.55	3.28
PQL, Akenu Village	11.65	22.21	30.68	21.37	4.93	3.19	3.88	2.09
MILATEX, Ogbere.	15.68	13.39	26.58	21.96	3.89	3.77	12.53	2.2
QNL, Eriola Village	14.24	11.67	23.45	23.03	5.06	3.93	14.82	3.8
SQ, Ibare Orile.	17.43	20.32	19.65	25.01	4.94	4.05	4.42	4.18
ABL, Agbede Village.	10.24	29.28	20.30	32.18	1.77	2.21	2.86	1.16
CGL, Oteere Village.	12.97	10.25	29.65	23.09	4.77	2.92	15.2	1.15
SSQ, Iyanju Village.	15.05	8.94	32.75	22.54	5.06	2.94	11.92	0.8
SVPC, Arege Village.	17.38	12.84	33.58	25.35	0.89	0.77	7.99	1.2
CCC, Ayoyo Village.	15.74	14.54	34.82	21.2	4.12	3.87	1.85	3.86
CNC, Orile Ilugun.	18.14	10.31	31.87	20.39	1.52	0.95	14.64	2.18
KNL, Ilawo Odeda.	15.57	10.42	26.33	21.69	3.85	2.74	14.18	5.22
FW SAN HE, Sowemimo	7.68	19.09	19.70	36.95	5.14	2.84	7.56	1.04
VMC. Agba Village.	17.75	6.86	33.44	21.53	3.93	3.19	8.21	5.09

NB: Q = Quartz; Mi = Microcline; P = Plagioclase; B = Biotite; Mu = Muscovite; A = Apatite; H = Hornblende and O = Opaque

APPENDIX B

Table B1. Activity concentrations of ^{40}K, ^{226}Ra and ^{232}Th in granite samples from Oyo State

Quarry location	Activity concentration (Bq kg^{-1})		
	^{40}K	^{226}Ra	^{232}Th
EQNL, Ibadan	405.95±20.97	10.38±2.09	60.47±9.79
ECC, Ibadan.	436.49±22.54	5.96±1.20	33.98±5.50
NCCQ, Iresapa	187.45±9.68	15.58±3.14	83.99±13.60
RATCON, Ibadan.	79.26±4.09	21.97±4.43	28.86±4.67
NSCE, Ibadan.	417.27±21.55	7.96±1.61	50.69±8.21
ICC, Ibadan.	215.85±11.15	14.10±2.84	78.10±12.64
BSAPQ, Ibadan	410.13±21.18	9.30±1.88	60.78±9.84
CC, Ojoo	405.85±20.96	10.44±2.11	70.03±11.34
LADSON, Oyo	264.60±13.67	33.66±6.79	39.54±6.40
QCC, Lanlate.	273.79±14.14	8.66±1.75	58.96±9.55
WCC, Ibadan.	394.08±20.35	8.18±1.65	48.76±7.89
DCC, Ibadan.	454.22±23.46	14.96±3.02	188.16±30.46

Table B2. Activity concentrations of ^{40}K, ^{226}Ra and ^{232}Th in granite samples from Osun State

Quarry location	Activity concentration (Bq kg^{-1})		
	^{40}K	^{226}Ra	^{232}Th
ICC, Iwo.	206.73±16.62	8.05±1.62	51.87±8.40
AQC, Modakeke.	893.31±46.14	25.41±5.13	150.69±24.40
BCC, Otan.	420.38±21.71	10.74±2.17	57.93±9.38
TJ CC, Ijabe.	390.19±20.15	10.31±2.08	30.34±4.91
WCC, Awo	325.25±18.80	8.64±1.74	55.60±9.00
ICC, Ikirun.	120.39±11.85	12.99±2.62	76.01±12.31
ACC, Awo.	403.80±20.86	12.77±2.58	25.72±4.16

Table B3. Activity concentrations of ^{40}K, ^{226}Ra and ^{232}Th in granite samples from Ekiti State

Quarry location	Activity concentration (Bq kg^{-1})		
	^{40}K	^{226}Ra	^{232}Th
QCC, Igbemo	458.05±23.66	11.71±2.36	68.21±11.04
ACC, Ikole.	116.07±10.02	14.34±2.89	81.11±13.13
MSTCC, Ikere.	412.58±21.31	6.79±1.37	63.80±10.33
RQI, Ijero,	1115.08±51.17	26.99±5.44	156.42±25.32
GEOVERTRAG, Iyin.	493.19±25.47	17.61±3.55	97.60±15.80
BCCN Igede	196.60±10.15	17.52±3.53	89.66±14.52
DCC, Ikere	379.76±19.61	10.14±2.05	64.27±10.41
KCC, Ikere	209.13±10.80	20.22±4.08	83.04±13.44
FQ, Aramoko.	456.12±23.56	33.02±6.66	47.74±7.73

Table B4. Activity concentrations of ^{40}K, ^{226}Ra and ^{232}Th in granite samples from Ondo State

Quarry location	Activity concentration (Bq kg^{-1})		
	^{40}K	^{226}Ra	^{232}Th
PQL, Ifon	371.73±19.20	12.00±2.42	76.05±12.31
RAVCON, Ore	98.56±5.09	15.71±3.17	74.16±12.01
ATLOR, Akure	80.21±4.14	31.60±6.37	85.36±13.82
FCC, Akure.	541.70±27.98	9.32±1.88	61.76±10.00
SNL, Ore.	119.58±6.18	16.28±3.28	90.11±14.59
NDECL, Ise Akoko	197.34±10.19	16.83±3.39	87.84±14.22
ZFM, Akure	358.66±18.52	6.07±1.22	117.57±19.03
DNL, Akure	477.86±24.68	9.89±1.99	62.12±10.06
SC, Iboropa Akoko	199.06±10.28	16.56±3.34	88.08±14.26
SW, Akure	203.48±10.51	11.62±2.34	80.09±12.97
SETRACO, Ore.	376.14±19.43	10.08±2.03	64.64±10.46
Hispanic, Ifon	207.06±10.69	17.89±3.61	86.77±14.05
GENC, Ondo.	359.27±18.56	18.64±3.76	83.35±13.49
MOL Ltd., Ore	608.26±31.42	8.59±1.73	54.87±8.88
NC, Ifon	246.67±12.74	62.15±12.54	261.19±42.29
SCC, Elegbeka-Ifon.	478.05±24.69	9.15±1.85	62.14±10.06
BALLESTER, Ifon	328.49±16.97	23.79±4.80	95.33±15.43
LCL, Idanre.	388.30±20.06	6.39±1.29	134.44±21.77
DCC, Ose-Owo	180.96±9.35	10.85±2.19	83.43±13.51
OSAC, Akure	292.53±15.11	26.39±5.32	67.40±10.91
SQL, Owo.	373.58±19.30	10.14±2.05	64.84±10.50
ECC, Akure	474.24±24.49	9.31±1.88	62.83±10.17
Japaul, Elegbaka.	477.34±24.65	11.85±2.39	69.43±11.24

Table B5. Activity concentrations of ^{40}K, ^{226}Ra and ^{232}Th in granite samples from Ogun State

Quarry location	Activity concentration (Bq kg^{-1})		
	^{40}K	^{226}Ra	^{232}Th
CCECC, Agoiwoye.	385.28±19.90	13.56±2.74	79.39±12.85
MRL., Alagutan.	427.75±22.09	10.76±2.17	70.05±11.34
DCQ, Eye Village.	444.91±26.00	17.53±3.54	91.13±14.75
CHEC, Agbede Village.	452.75±23.38	12.46±2.51	75.63±12.24
MRC, Oloparun.	448.04±23.14	12.87±2.60	74.30±12.03
RATCON, Ogere	224.18±11.58	11.64±2.35	82.08±13.29
PGC, Iwaye.	466.34±26.10	16.73±3.37	90.64±14.67
PQL, Akenu Village	821.11±52.43	10.21±2.06	69.35±11.23
MILATEX, Ogbere.	453.04±23.40	12.55±2.53	76.32±12.36
QNL, Eriola Village	191.77±9.90	16.62±3.35	89.58±14.50
SQ, Ibare Orile.	496.57±18.22	49.53±9.99	205.77±33.31
ABL, Agbede Village.	1187.38±61.33	47.92±9.67	216.82±35.10
CGL, Oteere Village.	261.25±13.49	12.29±2.48	108.31±17.53
SSQ, Iyanju Village.	247.80±12.80	13.80±2.78	87.25±14.13
SVPC, Arege Village.	411.03±21.23	26.71±5.39	113.58±18.39
CCC, Ayoyo Village.	494.74±25.55	10.28±2.07	64.60±10.46
CNC, Orile Ilugun.	531.83±27.47	4.45±1.56	65.20±10.56
KNL, Ilawo Odeda.	357.42±18.46	11.16±2.25	74.34±12.04
FW SAN HE, Sowemimo	578.88±29.90	67.31±13.58	271.03±43.88
VMC. Agba Village.	134.07±6.92	4.52±1.49	95.91±15.53

APPENDIX C

Table C1. Radium equivalent activity (Ra_{eq}), absorbed dose in air (D), annual effective dose rate (E) and excess lifetime cancer risk (ELCR) due to natural radionuclides in granite samples- Oyo State

Location	Ra_{eq} (Bq/kg)	D ($nGy.h^{-1}$)	E ($mSv.y^{-1}$)	ELCR x 10^{-3}
EQNL, Ibadan	127.99	59.28	0.10	0.36
ECC, Ibadan.	88.08	42.06	0.07	0.26
NCCQ, Iresapa	149.98	67.17	0.12	0.41
RATCON, Ibadan.	69.30	31.38	0.05	0.19
NSCE, Ibadan.	112.47	52.56	0.09	0.32
ICC, Ibadan.	142.28	64.02	0.11	0.39
BSAPQ, Ibadan	127.68	59.14	0.10	0.36
CC, Ojoo	141.70	65.24	0.11	0.40
LADSON, Oyo	110.50	51.14	0.09	0.31
QCC, Lanlate.	113.95	52.03	0.09	0.32
WCC, Ibadan.	108.15	50.49	0.09	0.31
DCC, Ibadan.	318.70	142.70	0.25	0.87

Table C2. Radium equivalent activity (Ra_{eq}), absorbed dose in air (D), annual effective dose rate (E) and excess lifetime cancer risk (ELCR) due to natural radionuclides in granite samples- Osun State

Location	Ra_{eq} (Bq/kg)	D ($nGy.h^{-1}$)	E ($mSv.y^{-1}$)	ELCR x 10^{-3}
ICC, Iwo.	98.05	44.55	0.08	0.27
AQC, Modakeke	309.40	142.57	0.25	0.87
BCC, Otan.	125.83	58.47	0.10	0.36
TJ CC, Ijabe.	83.67	39.88	0.07	0.24
WCC, Awo	113.09	52.08	0.09	0.32
ICC, Ikirun.	130.84	58.22	0.10	0.35
ACC, Awo.	80.57	38.71	0.07	0.24

Table C3. Radium equivalent activity (Ra_{eq}), absorbed dose in air (D), annual effective dose rate (E) and excess lifetime cancer risk (ELCR) due to natural radionuclides in granite samples- Ekiti State

Location	Ra_{eq} (Bq/kg)	D ($nGy.h^{-1}$)	E ($mSv.y^{-1}$)	ELCR x 10^{-3}
QCC, Igbemo	144.39	66.87	0.12	0.41
ACC, Ikole.	139.14	61.83	0.11	0.38
MSTCC, Ikere.	129.67	59.96	0.10	0.36
RQI, Ijero,	336.22	156.11	0.27	0.95
GEOVERTRAG, Iyin.	194.98	89.31	0.16	0.54
BCCN Igede	160.73	71.97	0.13	0.44
DCC, Ikere	131.17	60.43	0.11	0.37
KCC, Ikere	154.94	69.63	0.12	0.42
FQ, Aramoko.	136.31	63.92	0.11	0.39

Table C4. Radium equivalent activity (Ra_{eq}), absorbed dose in air (D), annual effective dose rate (E) and excess lifetime cancer risk (ELCR) due to natural radionuclides in granite samples- Ondo State

Location	Ra_{eq} (Bq/kg)	D ($nGy.h^{-1}$)	E ($mSv.y^{-1}$)	ELCR x 10^{-3}
PQL, Ifon	149.24	68.27	0.12	0.42
RAVCON, Ore	129.23	57.42	0.10	0.35
ATLOR, Akure	159.71	70.95	0.12	0.43
FCC, Akure.	139.22	65.25	0.11	0.40
SNL, Ore.	154.21	68.47	0.12	0.42
NDECL, Ise Akoko	157.50	70.55	0.12	0.43
ZFM, Akure	201.62	90.77	0.16	0.55
DNL, Akure	135.39	63.07	0.11	0.38
SC, Iboropa Akoko	157.70	70.65	0.12	0.43
SW, Akure	141.69	63.59	0.11	0.39
SETRACO, Ore.	131.36	60.48	0.11	0.37
Hispanic, Ifon	157.77	70.78	0.12	0.43
GENC, Ondo.	165.35	75.35	0.13	0.46
MOL Ltd., Ore	133.76	63.41	0.11	0.39
NC, Ifon	454.25	201.20	0.35	1.22
SCC, Elegbeka-Ifon.	134.69	62.75	0.11	0.38
BALLESTER, Ifon	185.24	83.89	0.15	0.51
LCL, Idanre.	228.32	102.63	0.18	0.62
DCC, Ose-Owo	143.96	64.37	0.11	0.39
OSAC, Akure	145.18	66.25	0.12	0.40
SQL, Owo.	131.51	60.53	0.11	0.37
ECC, Akure	135.55	63.09	0.11	0.38
Japaul, Elegbaka.	147.75	68.50	0.12	0.42

Table C5. Radium equivalent activity (Ra_{eq}), absorbed dose in air (D), annual effective dose rate (E) and excess lifetime cancer risk (ELCR) due to natural radionuclides in granite samples- Ogun State

Location	Ra_{eq} (Bq/kg)	D ($nGy.h^{-1}$)	E ($mSv.y^{-1}$)	ELCR x 10^{-3}
CCECC, Agoiwoye.	156.61	71.63	0.12	0.44
MRL, Alagutan.	143.74	66.31	0.12	0.40
DCQ, Eye Village.	181.94	83.24	0.14	0.51
CHEC, Agbede Village.	155.33	71.60	0.12	0.44
MRC, Oloparun.	153.48	70.77	0.12	0.43
RATCON, Ogere	146.14	65.70	0.11	0.40
PGC, Iwaye.	182.09	83.46	0.15	0.51
PQL, Akenu Village	172.44	82.02	0.14	0.50
MILATEX, Ogbere.	156.43	72.08	0.13	0.44
QNL, Eriola Village	159.34	71.30	0.12	0.43
SQ, Ibare Orile.	381.68	171.37	0.30	1.04
ABL, Agbede Village.	449.00	206.30	0.36	1.26
CGL, Oteere Village.	187.11	83.83	0.15	0.51
SSQ, Iyanju Village.	157.50	70.89	0.12	0.43
SVPC, Arege Village.	220.58	100.01	0.17	0.61
CCC, Ayoyo Village.	140.62	65.50	0.11	0.40
CNC, Orile Ilugun.	138.50	64.72	0.11	0.39
KNL, Ilawo Odeda.	144.85	66.23	0.12	0.40
FW SAN HE, Sowemimo	499.02	223.55	0.39	1.36
VMC. Agba Village.	151.85	67.24	0.12	0.41